

4

AD-A203 864

DTIC FILE COPY

LUMINOSITY VARIATIONS OF STARS SIMILAR TO THE SUN

G. W. Lockwood and B. A. Skiff  
Lowell Observatory  
1400 West Mars Hill Road  
Flagstaff, Arizona 86001

1 September 1988

FINAL REPORT

1 January 1984-31 December 1987

Approved for public release; distribution unlimited.

Air Force Geophysics Laboratory  
Air Force Systems Command  
United States Air Force  
Hanscom AFB  
Massachusetts 01731


DTIC  
ELECTE  
JAN 19 1989  
S D  
cb H

89

1 17 3 71

This technical report has been reviewed and is approved for publication.

  
RICHARD R. RADICK  
Contract Manager

  
STEPHEN L. KEIL, Chief  
Solar Research Branch

FOR THE COMMANDER

  
RITA C. SAGALYN, Director  
Space Physics Division

This report has been reviewed by the ESD Public Affairs Office (PA), and is releasable to the National Technical Information Service (NTIS).

Qualified requestors may obtain additional copies from the Defense Technical Information Center. All others should apply to the National Technical Information Service.

If your address has changed, or if you wish to be removed from the mailing list, or if the addressee is no longer employed by your organization, please notify AFGL/DAA, Hanscom AFB, MA 01731. This will assist us in maintaining a current mailing list.

Do not return copies of this report unless contractual obligations or notices on a specific document requires that it be returned.

unclassified

SECURITY CLASSIFICATION OF THIS PAGE

## REPORT DOCUMENTATION PAGE

1a REPORT SECURITY CLASSIFICATION Unclassified		1b. RESTRICTIVE MARKINGS	
2a SECURITY CLASSIFICATION AUTHORITY		3 DISTRIBUTION/AVAILABILITY OF REPORT approved for public release; distribution unlimited	
2b DECLASSIFICATION/DOWNGRADING SCHEDULE			
4. PERFORMING ORGANIZATION REPORT NUMBER(S)		5. MONITORING ORGANIZATION REPORT NUMBER(S) AFGL-TR-88-0221	
6a. NAME OF PERFORMING ORGANIZATION Lowell Observatory	6b. OFFICE SYMBOL (If applicable)	7a. NAME OF MONITORING ORGANIZATION Air Force Geophysics Laboratory	
6c. ADDRESS (City, State, and ZIP Code) 1400 West Mars Hill Road Flagstaff, Arizona 86001		7b. ADDRESS (City, State, and ZIP Code) Hanscom Air Force Base Massachusetts 01731	
8a. NAME OF FUNDING/SPONSORING ORGANIZATION	8b. OFFICE SYMBOL (If applicable)	9 PROCUREMENT INSTRUMENT IDENTIFICATION NUMBER F19628-84-K-0013	
8c. ADDRESS (City, State, and ZIP Code)		10. SOURCE OF FUNDING NUMBERS	
		PROGRAM ELEMENT NO 61102F	PROJECT NO. 2311
		TASK NO. G3	WORK UNIT ACCESSION NO. CZ
11 TITLE (Include Security Classification) Luminosity Variations of Stars Similar to the Sun			
12 PERSONAL AUTHOR(S) G. W. Lockwood and B. A. Skiff			
13a TYPE OF REPORT Final	13b TIME COVERED FROM 84Jan01 TO 87Dec31	14. DATE OF REPORT (Year, Month, Day) 88Sep01	15 PAGE COUNT 110
16. SUPPLEMENTARY NOTATION			
17 COSATI CODES		18 SUBJECT TERMS (Continue on reverse if necessary and identify by block number)	
FIELD	GROUP	SUB-GROUP	
		stellar photometry, solar type stars	
19 ABSTRACT (Continue on reverse if necessary and identify by block number) Using precision differential photoelectric photometry at 472 and 551 nm, the variability characteristics of 36 solar-type stars (spectral types F, G, and K) and their 65 comparison stars were determined from nearly 2000 measurements made on more than 350 nights between March 1984 and December 1987. Each observation consists of four cycles (two at each wave-length) of intercomparison of the brightnesses of a trio (or quartet) of stars, thus producing 12 (or 24) pairwise differential magnitudes. Program stars and comparison stars within each trio or quartet group are measured identically. The precision of nightly measurement cycles is typically 0.2% rms, and the median range of annual mean brightness over four seasons is 0.2% for stars whose output appears to be intrinsically constant. →  Nightly and annual mean light curves, annual mean differential magnitudes, interseason ranges, and intraseason root mean square dispersions are given for each differential pair, (continued reverse)			
20 DISTRIBUTION/AVAILABILITY OF ABSTRACT <input type="checkbox"/> UNCLASSIFIED/UNLIMITED <input type="checkbox"/> SAME AS RPT <input type="checkbox"/> DTIC USERS		21 ABSTRACT SECURITY CLASSIFICATION Unclassified	
22a NAME OF RESPONSIBLE INDIVIDUAL Richard Radick		22b TELEPHONE (Include Area Code)	22c OFFICE SYMBOL AFGL/PHS

19. ABSTRACT (continued).

Individual stars are designated as variable, probably variable, or constant within each season and over the duration of the program. A complete statistical profile of the observations is included along with a discussion of the observational and analytical methodology.

The principal conclusions of this study are (1) about one-half the program stars and one-fourth the comparison stars are demonstrably variable on short-time scales at levels typically 0.3% and greater, (2) variability is about twice as common among K stars as among F- and G-type stars, (3) rotational modulation was measurable in nine stars, (4) sixteen program stars and eight comparison stars varied by more than 0.5% over four seasons, (5) twenty-six pairs of exceptionally stable stars varied by less than 0.3% over four years, (6) variability of the program stars is strongly correlated with independently determined chromospheric activity levels, and (7) interseason variability is more consistent with long-term cyclic variation than with stochastic fluctuations.

Accession For	
NTIS GRA&I	<input checked="checked" type="checkbox"/>
DTIC TAB	<input type="checkbox"/>
Unannounced	<input type="checkbox"/>
Justification	
By	
Distribution/	
Availability Codes	
Dist	
A-1	

## TABLE OF CONTENTS

	Page
1. INTRODUCTION . . . . .	1
1.1 Solar luminosity variation . . . . .	1
1.2 Activity cycles in Sun-like stars . . . . .	2
1.3 Photometric variability of Sun-like stars. . . . .	2
2. EXPERIMENTAL DESIGN . . . . .	3
2.1 Selection of stars . . . . .	3
2.1.1 Program stars . . . . .	3
2.1.2 Comparison stars . . . . .	14
2.1.3 Distribution of color and apparent magnitude . . . . .	15
2.2 The observational facility . . . . .	15
2.3 The basic observation sequence . . . . .	17
2.4 Expected precision levels . . . . .	17
2.4.1 Photon-counting errors . . . . .	18
2.4.2 Sky background . . . . .	18
2.4.3 Extinction and airmass . . . . .	19
2.4.4 Temporal atmospheric transparency changes . . . . .	19
2.4.5 Temporal changes in photometer sensitivity . . . . .	19
2.4.6 Scintillation error . . . . .	20
2.4.7 Errors caused by seeing and image motion . . . . .	20
2.4.8 A hypothetical error budget . . . . .	29
3. THE DATA . . . . .	20
3.1 Observations obtained . . . . .	20
3.2 Observational procedures . . . . .	22
3.3 Data rejection criteria . . . . .	22
3.4 Reductions . . . . .	23
3.5 Seasonal mean differential magnitudes . . . . .	23
3.6 Light curves . . . . .	23
3.7 Observed precision levels . . . . .	23
3.7.1 Cycle-to-cycle differences . . . . .	62
3.7.2 Errors arising from differential extinction . . . . .	63
3.8 Possible instrumental effects . . . . .	65
3.8.1 Color effects . . . . .	65
3.8.2 Brightness and brightness difference effects . . . . .	65
4. INTRINSIC STELLAR VARIABILITY ON INTRASEASON	
TIME SCALES . . . . .	65
4.1 Intraseason standard deviations . . . . .	65
4.2 The relation between $s_b$ and $s_y$ . . . . .	67
4.3 Correlations of light curves . . . . .	73
4.4 Frequency histograms of intraseason variability . . . . .	73
4.5 Consistently variable stars . . . . .	75
4.6 Photometrically derived rotation periods . . . . .	76

**TABLE OF CONTENTS** continued.

	<b>Page</b>
5. INTRINSIC STELLAR VARIABILITY ON INTERSEASON	
TIME SCALES . . . . .	76
5.1. The least-variable stars . . . . .	78
5.2. Possible long-term systematic effects . . . . .	80
5.3. The large-range variable stars: incipient cycles? . . . . .	80
6. PHOTOMETRIC VARIABILITY AND CHROMOSPHERIC	
ACTIVITY . . . . .	84
7. SUMMARY AND CONCLUSIONS . . . . .	86
REFERENCES . . . . .	88
APPENDIX: . . . . .	93

## List of Figures

	Page
Figure 1. Chromospheric emission ratio as a function of $B - V$ color . . . . .	14
Figure 2. Location of trio and quartet groups on the sky . . . . .	15
Figure 3. Apparent $V$ magnitudes and $B - V$ colors . . . . .	16
Figure 4.1. Light curves of the HD1835 group . . . . .	32
Figure 4.2. Light curves of the HD10476 group . . . . .	33
Figure 4.3. Light curves of the HD13421 group . . . . .	34
Figure 4.4. Light curves of the HD18256 group . . . . .	35
Figure 4.5. Light curves of the HD23140 group . . . . .	36
Figure 4.6. Light curves of the HD25998 group . . . . .	37
Figure 4.7. Light curves of the HD35296/HD39587 group . . . . .	38
Figure 4.8. Light curves of the HD76572/HD75332 group . . . . .	39
Figure 4.9. Light curves of the HD81809 group . . . . .	40
Figure 4.10. Light curves of the HD82885/HD82635 group . . . . .	41
Figure 4.11. Light curves of the HD103095 group . . . . .	42
Figure 4.12. Light curves of the HD114710 group . . . . .	43
Figure 4.13. Light curves of the HD115383/HD117176 group . . . . .	44
Figure 4.14. Light curves of the HD115404 group . . . . .	45
Figure 4.15. Light curves of the HD120136 group . . . . .	46
Figure 4.16. Light curves of the HD124570 group . . . . .	47
Figure 4.17. Light curves of the HD129333 group . . . . .	48
Figure 4.18. Light curves of the HD131156 group . . . . .	49
Figure 4.19. Light curves of the HD143761 group . . . . .	50
Figure 4.20. Light curves of the HD149661/HD152391 group . . . . .	51
Figure 4.21. Light curves of the HD157856/HD158614 group . . . . .	52
Figure 4.22. Light curves of the HD160346 group . . . . .	53
Figure 4.23. Light curves of the HD161239 group . . . . .	54

# List of Figures continued.

	Page
Figure 4.24. Light curves of the HD176095 group . . . . .	55
Figure 4.25. Light curves of the HD182572 group . . . . .	56
Figure 4.26. Light curves of the HD185144 group . . . . .	57
Figure 4.27. Light curves of the HD190007 group . . . . .	58
Figure 4.28. Light curves of the HD201091/HD201092 group . . . . .	59
Figure 4.29. Light curves of the HD215704 group . . . . .	60
Figure 4.30. Light curves of the HD216385 group . . . . .	61
Figure 5. Observed and predicted cycle-to-cycle magnitude differences . . .	63
Figure 6. Distribution of differential airmasses . . . . .	64
Figure 7. Relation between seasonal rms magnitude dispersion and differential airmass . . . . .	64
Figure 8. Average intraseason dispersion as a function of difference in $(b - y)$ color . . . . .	66
Figure 9. Average intraseason dispersion as a function of difference in $V$ magnitude . . . . .	66
Figure 10. Average intraseason dispersion as a function of $V$ magnitude . .	66
Figure 11. Ratio of $s_b/s_y$ to $s_b$ . . . . .	67
Figure 12. Frequency histograms for intraseason variable, probably variable, and constant pairs of stars . . . . .	74
Figure 13. Average intraseason dispersion as a function of $B - V$ color . . .	75
Figure 14. Frequency histograms for interseason variable, probably variable, and constant pairs of stars . . . . .	79
Figure 15. Interseason range as a function of $B - V$ color . . . . .	80
Figure 16. $B - V$ colors as a function of color difference coded by variability range . . . . .	83
Figure 17. Intraseason dispersion as a function of chromospheric emission ratio . . . . .	85
Figure 18. Interseason range as a function of chromospheric emission ratio . . . . .	86



## List of Tables

	Page
Table 1. Observing list and variability summary . . . . .	4
Table 2. Error budget . . . . .	21
Table 3. Summary of annual mean differential magnitudes . . . . .	24
Table 4. Intraseason dispersion and interseason range. . . . .	68
Table 5. Intraseason variability and spectral type . . . . .	74
Table 6. Summary of rotation determinations . . . . .	77
Table 7. The least-variable stars . . . . .	81
Table 8. Strongly varying stars . . . . .	84

## 1. INTRODUCTION

### 1.1 Solar luminosity variation

The appearance and disappearance of sunspots during the 11-year solar cycle has long been suspected of causing slight fluctuations of the Sun's luminous output. Decades of pioneering efforts by Abbott and his coworkers (1963) from several sites, however, failed to demonstrate a convincing actual detection of solar variability. Groundbased observations, compromised by the necessity of accounting exactly for the variable amounts of sunlight absorbed and scattered by Earth's atmosphere, simply were not capable of revealing tiny intrinsic variations in the "solar constant."

In 1980, extremely precise measurements of total solar irradiance from space finally revealed small ( $<0.2\%$ ) dips of the total solar output accompanying the disk passage of large sunspot groups (Willson *et al.* 1981). Near solar maximum, a strong peak in the power spectrum of total irradiance at the solar rotation frequency is caused by the sunspot flux deficits in active regions (Willson 1982). A model of solar irradiance variation reconstructed from historic sunspot and faculae data predicted that owing to the flux blocking effects of sunspots, the solar output should vary inversely with solar activity, reaching a maximum at sunspot minimum and inversely (Hoyt and Eddy 1982).

Contrary to this simple scenario of irradiance variation, continuing measurements since 1980 showed that the solar constant decreased by almost 0.1% from sunspot maximum to sunspot minimum (Willson *et al.* 1986; Willson 1987). A new model of the radiation balance between sunspot flux deficits and faculae and bright magnetic network flux enhancements was proposed. In this model, excess radiation from faculae and network components compensates the flux blockage from sunspots to produce the observed decline of total irradiance between solar maximum and solar minimum (Foukal and Lean 1987, 1988; Lean and Foukal 1988).

With the existence of measurable solar variability now firmly established, the question of long-term irradiance changes and their effects on the solar-terrestrial environment becomes more than academic. Even though the sensitivity of terrestrial climate to solar variability is currently thought to be much smaller than anthropogenic trace gas and volcanic effects, the baseline of measured solar variations—less than one 11-year sunspot cycle—is still far too short to permit a comprehensive assessment of the causes of long-term climatic change (Dickinson 1987; Ramanathan 1988). Thus continuing irradiance monitoring is imperative.

The study of relationships between solar irradiance, solar activity, and terrestrial weather systems is also becoming important. Although past efforts were unconvincing (e.g., Abbott 1963), more sophisticated analysis reveals significant links between the solar cycle and some large-scale meteorological phenomena (Labitzke 1987; Tinsley 1988). Particularly intriguing is the situation prevailing during the so-called "Maunder minimum" from about 1645 until 1715, when sunspots were virtually absent (Eddy 1976). An accompanying period of unusual cold in northern Europe was so extraordinary that it has become known as the "Little Ice Age." Now that an apparent connection seems to exist between solar activity and irradiance, the

suggestion of a causal relation between these two very disparate phenomena—one solar and one climatological—seems hard to avoid.

It is in this context that the study of solar variability has undergone a renaissance. The Sun is now recognized as providing a varying input to the Earth radiation budget, and some component of this variability has observable terrestrial effects on solar-cycle time scales. But to characterize the nature and significance of solar variations by observing the Sun itself will require decades and many solar cycles. For a more timely understanding of past and present solar variability, we turn to the stars, especially those similar to the Sun in age, mass, and composition.

### 1.2 Activity cycles in Sun-like stars

Sun-like chromospheric-activity cycles were discovered by O. C. Wilson (1978) in the course of a decade-long study during which he monitored the strengths of the emission cores of the H and K lines of ionized calcium in a group of solar-type stars. It was Wilson's work that gave rise to the concept of "solar analogs," stars that truly mimic the Sun in all aspects of their spectral output and variability.

A basic indicator of the magnetic activity of these stars is provided by the variability of Wilson's index of composite H+K line strength,  $S$ , defined as the ratio of the emission in the line cores to the nearby continuum level. Stars with small, constant  $S$  indices were used as nightly calibration standards. Old main-sequence stars with the weak  $S$  indices signalling low chromospheric activity showed activity cycles remarkably similar to the Sun's, some comparable in length. Continuing Wilson's program, Vaughan *et al.* (1981) and Baliunas *et al.* (1983) found that young, chromospherically active stars displayed rotational modulation of the HK flux, attributable to the stellar analog of solar plage, thus accounting for some of the random fluctuations observed at lower time resolution by Wilson.

By subtracting the photospheric component of the  $S$  index, Noyes *et al.* (1984) derived a new parameter,  $R'_{HK}$ , the "chromospheric emission ratio," that quantitatively estimates the actual fraction of the star's total luminosity originating in the chromosphere. In the following discussion, we shall show that the magnitude of photometric variability is closely related to  $\log R'_{HK}$ .

### 1.3 Photometric variability of Sun-like stars

Measurements of the continuum brightness of young, chromospherically active stars in the Hyades open cluster showed that nearly all of these stars cooler than spectral type F7 are demonstrably variable, modulated like the Sun—though with much larger amplitudes—by the disk transit of spotted regions (Lockwood *et al.* 1984; Radick *et al.* 1987). Axial rotation periods that recur from year to year have now been determined for 18 stars. Repeated observations in successive seasons provided evidence of long-term changes as well: during seasons when the rotational modulation of brightness was most apparent, the mean brightness was reduced slightly and vice versa. A simple interpretation is that the presence of spots reduces the time-averaged stellar brightness—flux deficits associated with spots are not compensated by excess radiation elsewhere in the stellar atmosphere, as is evidently the case for the Sun.

However, in contrast to the clear picture that has emerged regarding the relation of chromospheric activity and photometric variability in young solar-type stars, essentially nothing was known about luminosity variations of common main-sequence stars. In fact, some of the Wilson stars exhibiting Sun-like chromospheric activity cycles are among those chosen decades ago and long accepted as photometric standard stars on the basis of their presumed stability. Nearly all these stars have appeared to be rock-steady in their light output. A photometric program carried out by Jerzykiewicz and Serkowski (1966) from 1955 to 1966 involving repeated measurements of thirteen mostly main-sequence F, G, and K stars uncovered no variability at the level of about 1%.

The present photometric study of stars similar to the Sun was undertaken in 1981 to look for analogs of solar variation in the mostly unexplored and technically difficult regime of stellar variability below 1%. Finding evidence of luminosity variations in a group of similar stars--especially ones with known Sun-like activity cycles--would help characterize the historic variability of the Sun and its possible modes of variability in solar cycles to come. With better instrumentation than Jerzykiewicz and Serkowski had available 25 years ago, we hoped to measure solar-like stellar variability at levels well below 0.5% on rotational as well as solar cycle time scales. In this report, we describe the results of the first four observing seasons of this program.

## 2. EXPERIMENTAL DESIGN

### 2.1 Selection of stars

#### 2.1.1 Program stars

Thirty six main-sequence and subgiant F, G, and K stars were selected for photometric monitoring, all but two from Wilson's (1978) survey of chromospheric activity in 91 main-sequence stars. These plus others suggested by D. K. Duncan (private communication) are currently also monitored spectroscopically in a continuation of the HK program at Mt. Wilson. Our list includes HK standards, young active stars, and solar-age stars with observed cyclic chromospheric activity. The program stars are listed in Table 1, organized together with the comparison stars required for differential photometry into 30 trio and quartet groups. Program stars are denoted by tabulated  $\log R'_{HK}$  or  $\langle S \rangle$  values. Four stars (HD82885, HD114710, HD120136, HD131156) were previously monitored by Jerzykiewicz and Serkowski (1966); several are *ucby* or *UBV* photometric standards, HK standards, or MK spectral standards and are so designated in the Stds column of Table 1.

In Table 1, the "intra" column indicates detected variability in each season, and the "inter" column indicates variability of the seasonal mean magnitudes, as discussed further in §§4 and 5.

TABLE 1. Observing List and Variability Summary

HD	HR	RA	Dec (2000)	V	B-V	Sp.	$\log R'_{HK}$	Intra	Inter	Stds	Notes
1	1835	88	0 <sup>h</sup> 22 <sup>m</sup> 9	-12°13'	6 <sup>m</sup> 4	G2V	-4.42	VVVV	V+		9 Cet=BE Cet. Hyades group. MK85 std
2	2488	...	0 28.6	-11.14	6.9	F5	...	CCCC	C		Rossiter 4146
3	1388	*	0 18.0	-13.27	6.5	G0V	...	CCCC	C		
1	10476	493	1 42.5	+20.16	5.2	K1V	-4.87	CCCC	V	4C	107 Psc. NSV 600
2	10137	508	1 44.9	+20.05	6.3	G5IV	...	CCCC	C		109 Psc. rv var?
3	11326	...	1 51.8	+18.17	6.7	G5	...	CCCV	C		
1	13421	635	2 11.4	+08.34	5.6	G0V	-5.21	VCC-	C	4C, HK	64 Cet
2	13611	649	2 13.0	+08.51	4.4	G6II-III CN-2	...	CCvC	V+		65= $\xi^1$ Cet. MK83 std, spec bin. <S>=0.15. NSV 749
3	13683	...	2 13.5	+05.01	6.6	F0	...	CCvC	C		spec bin
4	12414	...	2 01.9	+07.32	7.2	F2	...	---	C		
1	18256	869	2 56.4	+18.01	5.6	F6V	-4.79	CCC-	C		46= $\rho^3$ Ari
2	18404	878	2 58.1	+20.40	5.8	F5IV	...	CCC-	C		47 Ari. Hyades group
3	17659	...	2 50.7	+19.10	6.6	F8	...	CVC-	V?		
4	17918	856	2 53.2	+16.29	6.3	F5 III	...	---	V		
1	23140	...	3 44.8	+46.02	7.7	K2	...	VVv-	C		<S>=0.32 (D. K. Duncan 1984, private communication)
2	23256	...	3 45.6	+45.21	7.7	F2	...	CCC-	C		
3	22679	...	3 40.7	+46.01	7.6	G5	...	CCC-	C		ADS 2669
1	25998	1278	4 08.6	+38.02	5.5	F7V	-4.50	vVC	C		50 Persei. Hyades group; cpm w/HD 25893
2	24747	...	3 57.6	+36.30	6.9	F0	...	CCC	C		
3	23885	...	3 50.1	+37.52	6.6	F0	...	CCC	C		V491 Per=ADS 2995
4	25893	...	4 07.6	+38.04	7.1	K1V	...	-V	V		Hyades group. rv cst (Fekel <i>et al.</i> 1986)
1	35296	1780	5 24.4	+17.23	5.0	F8V	-4.38	CVVV	V+		111 Tau. Call em. HD 35171 (dK5) shares
2	33276	1676	5 09.7	+15.36	4.8	F2IV	...	CCCC	V?		cpm/rv. rv cst (Young <i>et al.</i> 1987)
3	39587	2047	5 54.4	+20.17	4.4	G0V	-4.44	CVVV	V+	4C	15 Ori
4	38558	1990	5 47.4	+17.44	5.5	F0III	...	CCCC	V?		54= $\chi^1$ Ori. in UMa cluster, Sirius group
1	76572	3563	8 58.0	+30.14	6.3	F6V	-4.94	CCCC	V	HK	rv cst (Young <i>et al.</i> 1987) MK85 std
2	73596	3423	8 40.3	+31.57	6.1	F5III	...	vvvC	C		130 Tau, MK85 std
3	78234	3620	9 08.1	+32.32	6.3	F2V	...	CCCC	C		61 Cnc=ADS 7107. UMa stream
4	75332	3499	8 50.5	+33.17	6.2	F7Vn	-4.44	-VV	V+		spec bin

TABLE 1. Observing List and Variability Summary (continued).

HD	HR	RA	Dec (2000)	V	B-V	Sp.	$\log R'_{HK}$	Intra	Inter	Stds	Notes
1	81809	3750	9 <sup>h</sup> 27 <sup>m</sup> 8	-06°04'	5 <sup>m</sup> 4	0 <sup>m</sup> 64	G2V	vvcv	V?	4C	Burnham 2530. spec bin 31= $\tau^1$ Hy=hl167
2	81997	3759	9 29.1	-02 46	4.6	0.46	F6V	CCVC	V?		
3	82074	3762	9 29.5	-04 15	6.3	0.84	G6IV	CCCC	V+		
1	82885	3815	9 35.7	+35 49	5.4	0.77	G8IV-V	CVVV	V+	4C	11 LMi=ADS 7441. CaII em. rv est (Young <i>et al.</i> 1987). Rot per: Skiff and Lockwood 1986 10 LMi. <S>=0.31. rv est (Young <i>et al.</i> 1987). Rot per: Skiff and Lockwood 1986) 13 LMi
2	82635	3800	9 34.2	+36 24	4.6	0.92	G8.5III	VVVV	V+	4C	
3	83951	3857	9 42.7	+35 06	6.1	0.36	F3V	CCCC	C		
4	83525	...	9 40.0	+35 20	7.0	0.5	F5	-CCC	C		
1	103095	4550	11 53.0	+37 43	6.4	0.75	G8VI	CCCC	C	4C	Groombridge 1830=CF UMa
2	103520	*	11 55.4	+38 45	7.0	0.99	K0III CN-1	vVVC	C		
3	101606	4501	11 41.6	+31 45	5.7	0.43	F4V	CCvv	V	4C	62 UMa
1	114710	4983	13 11.9	+27 53	4.3	0.57	F9.5V	CCCC	V?	4C	43= $\beta$ Com. spec bin? MK85 std
2	111812	4883	12 51.7	+27 32	4.9	0.67	G0IIIp	CCVC	V?	4C	31 Com. member of Coma cluster in Hertzprung gap. MK85 std: HK weak, very broad metallic lines 37 Com=ADS 8731. MK 85 std.
3	112989	4924	13 00.3	+30 47	4.9	1.17	G9III CN-2 FeI Ca-1	VVCV	V+		
1	115383	5011	13 16.8	+09 25	5.2	0.59	G0Vs	vVvC	V+	4C	e=59 Vir=Kui 62. rv est (Young <i>et al.</i> 1987)
2	117304	5081	13 29.2	+10 49	5.7	1.05	K0III	CCCC	V?		71 Vir. spec bin
3	117176	5072	13 28.4	+13 47	5.0	0.71	G4V	CCvC	V?	4C	70 Vir. MK85 std
1	115404	*	13 16.9	+17 01	6.5	0.94	K1V+M1V	VVVV	V+		ADS 8841. CaII em moderately strong in B comp
2	113848	4946	13 06.4	+21 09	6.0	0.39	F4V	CCCC	V?		39 Com. MK: weak lined A3p
3	114520	*	13 10.9	+21 14	6.7	0.4	F2II	CCCC	V?		
1	120136	5185	13 47.3	+17 27	4.5	0.48	F6IV	vCCC	V+		4= $\tau$ Boo=ADS 9025: 4.5,11.1;4.8;11(1970). NSV 6442
2	121107	5225	13 53.2	+17 56	5.7	0.84	G5III	VCCC	V?		7 Boo
3	121560	5243	13 55.8	+14 03	6.2	0.50	F6V	CCCC	V?		
1	124570	5323	14 14.1	+12 58	5.5	0.54	F6IV	CCCC	V?	HK	14 Boo. spec bin. NSV 6597
2	125451	5365	14 19.3	+13 00	5.4	0.38	F5IV	CCCC	V?		18 Boo. UMa stream
3	126246	...	14 24.1	+11 15	6.7	0.5	F8V+G1V	VVVv	V+		ADS 9251. AGK3 shows cpm, both incl in measures.

TABLE 1. Observing List and Variability Summary (continued).

HD	HR	RA (2000)	Dec	V	B-V	Sp.	$\log R'_{HK}$	Intra	Inter	Stds	Notes
1 129333	...	14 <sup>h</sup> 39 <sup>m</sup> 0	+64°18'	7 <sup>m</sup> 5	0 <sup>m</sup> 6	G0	-4.23	VVVV	V+		Call em
2 129390	...	14 39.4	+64 09	7.5	0.4	F2	...	CCCC	C		
3 131330	...	14 49.9	+64 35	8.2	...	F8	...	CCCC	C		
1 131156	5544	14 51.4	+19 06	4.6	0.76	G8V+K4V	-4.36	CVVV	C		37= $\xi$ Boo=ADS 9413, both incl., both show Call em, both rv cst (Young <i>et al.</i> 1987)
2 129972	5502	14 45.2	+16 58	4.6	0.98	G8.5III	...	CCCC	V+		35= $\sigma$ Boo. barium star. MK85 std
3 131511	5553	14 53.4	+19 09	6.0	0.83	K2V	...	VVVV	V+		Hyades group. NSV 6847.
4 132146	5575	14 57.2	+16 23	5.7	0.94	gG5	...	-CCC	C		
1 143761	5968	16 01.0	+33 18	5.4	0.60	G0+Va Fe-1	-5.02	VCCC	C	HK, 4C	15= $\rho$ CrB. MK85 std
2 142091	5901	15 51.2	+35 39	4.8	1.00	K1IVa	...	CCCC	V		11= $\kappa$ CrB. MK85 std
3 140716	5855	15 44.0	+32 31	5.6	1.06	gG9	...	VvC	C		9= $\pi$ CrB
1 149661	6171	16 36.4	-02 19	5.8	0.82	K2V	-4.54	VVCC	V+		12 Oph=V2133 Oph. Call em. poss rv var (Young <i>et al.</i> 1987)
2 150050	...	16 38.7	-01 14	6.7	1.1	K0	...	CCCC	C		
3 152391	*	16 53.0	-00 02	6.6	0.76	G7V	-4.45	CCVV	V+		
4 152569	6277	16 54.2	-01 37	6.3	0.28	F0V	...	VVVV	C		
1 157856	6489	17 26.0	-01 39	6.4	0.46	F3V	-4.70	CCCC	V		
2 156635	...	17 18.8	-02 49	6.7	0.5	F8	...	CCCC	C		
3 158614	6516	17 30.4	-01 04	5.3	0.72	G9IV-V H61	-4.99	CCvC	V+		ADS10598. Also classed G5V (Abt 1981)
4 157347	6465	17 22.9	-02 23	6.3	0.68	G5IV	...	CCCC	C		
1 160346	*	17 39.3	+03 33	6.5	0.96	K3V	-4.71	CCCC	C		
2 160385	...	17 39.5	+03 24	6.8	1.1	K3IIIb	...	VVVv	C		ADS10688. closer, brtr comp incl in measures
3 160823	...	17 41.9	+04 22	6.9	0.6	G0	...	CCVC	V+		
1 161239	6608	17 43.4	+24 20	5.7	0.65	G2IIIb	-5.14	CCCC	V+	HK	84 Her. shows long-term cycle despite low HK flux. MK85 std.
2 162211	6644	17 48.8	+25 37	5.1	1.16	K2III	...	CVVV	V?		87 Her.
3 162076	6638	17 48.4	+20 34	5.7	0.94	G5IV	...	VVVv	V?		
4 160935	...	17 41.8	+21 30	6.9	0.5	F5	...	-CCC	V+		

TABLE 1. Observing List and Variability Summary (continued).

HD	HR	RA (2000)	Dec	V	B-V	Sp.	$\log R'_{HK}$	Intra	Inter	Stds	Notes
1	176095	7163	18 <sup>h</sup> 58 <sup>m</sup> .4	+06 <sup>s</sup> 14'	6 <sup>m</sup> .2	0 <sup>m</sup> .46	F5IV	-4.68	CCCC	C	
2	175515	7135	18 55.5	+06 37	5.6	1.04	K0III	...	CCCC	C	62 Ser. spec bin. NSV 11536(in IR)
3	175637	...	18 56.0	+07 08	7.3	0.4	F0	...	VVVV	C	
1	182572	7373	19 25.0	+11 57	5.2	0.77	G8IV Hδ1	-5.03	vCCC	C	31 Aql. MK85 std; NSV 11994. 61 Cygni group
2	180868	7315	19 17.8	+11 36	5.3	0.20	F0IV	...	CCCV	C	25=ω <sup>1</sup> Aql
3	185018	7456	19 36.9	+11 16	6.0	0.88	G0Ib-II	...	CVCC	V	ADS12670; mag 12.5 comp excluded from measures.
1	185144	7462	19 32.4	+69 40	4.7	0.79	K0V	-4.75	CCCC	V+	4C
2	176524	7180	18 54.4	+71 18	4.8	1.15	K0III Ba0.2	...	vCCv	V+	61=σ Dra. NSV 12176. MK85 std
3	190940	7685	20 02.8	+67 52	4.5	1.32	K3III	...	vvvV	V+	52=ν Dra, spec bin
1	190007	...	20 02.8	+03 20	7.5	1.14	K4	-4.59	VVVV	V+	67=ρ Dra=LD52447
2	189533	...	20 00.4	+03 20	6.8	0.8	G5	...	CCCV	V?	
3	190521	...	20 05.2	+03 26	7.8	1.1	K0	...	CCCC	V?	
1	201091	8085	21 06.9	+38 45	5.2	1.18	K5V	-4.80	VVVV	V?	4C
2	200031	*	20 59.7	+38 49	6.8	0.80	G5III	...	CCCV	V?	61 Cyg A=V1803 Cyg=ADS14636A: 29.7,148(1990). NSV 13543. CalI em. MK85 std; rv cst (Young <i>et al.</i> 1987)
3	201092	8086	21 06.9	+38 45	6.0	1.37	K7V	-4.91	CVVC	V?	4C
4	200577	8063	21 03.1	+38 39	6.1	1.01	G8III	...	CCvC	V?	61 Cyg B=ADS14636B. NSV 13546 CalI em. MK85 std; rv cst (Young <i>et al.</i> 1987)
1	215704	...	22 46.3	+50 13	7.9	0.80	K0	...	CCCC	V?	<S>=0.25 (Duncan 1984 private communication)
2	215427	...	22 44.3	+49 25	7.2	1.4	K5	...	VVVV	V+	
3	216175	...	22 49.9	+50 01	8.0	0.9	G5	...	CCCC	V?	
1	216385	8697	22 52.4	+09 50	5.2	0.48	F7IV	-5.03	CCCC	V	HK
2	216048	8681	22 49.6	+10 29	6.5	0.29	F0IV-V	...	CvVV	C	49=σ Peg. spec bin
3	217232	8739	22 59.2	+11 44	5.8	0.32	A8V+F6V	...	VvVC	C	52 Peg=ADS16428:6.0,7.3,0.67,3.15(1990).

\*Star is listed in YBS Supplement.



## SUPPLEMENTARY NOTES – TABLE 1

The information in these notes is derived in large part from a bibliographic search kindly conducted for us by Dr. W. H. Warren, Jr., National Space Science Data Center, using the SIMBAD astronomical literature database. We acknowledge with gratitude this extremely useful service.

In general, all the program stars and many of the comparison stars are F2–K7 dwarfs of apparent magnitude  $4.5 < V < 7$  and consequently lie close to Earth, many within 10 pc. Many of the stars are thus included in high proper-motion and parallax catalogues of Gliese, Luyten, Woolley, Lowell, Yale, etc. Information about the dynamical aspects of any particular star should be sought in these sources. Membership of several stars in dynamical groups such as the Hyades are noted in the table. The Mount Wilson HK data for nearly all the Wilson stars have been analyzed by Vaughan *et al.* (1981) and Baliunas *et al.* (1983, 1985).

HD1835 = HR 88 = 9 Ceti = BE Ceti. This Wilson star, 1985 MK G2V standard, and Hyades group member has been frequently studied as a solar analog. However, because it is younger and much more chromospherically active than the Sun, it has not proven to be a perfect match (cf. Hardorp 1978; Cayrel de Strobel *et al.* 1981; Hardorp 1982). Chugainov (1980) found rotational variability ( $\Delta V = 0.032$ ,  $\Delta B = 0.037$ ) with a period of 7.655 days, using HD2488 as the comparison star (included in our trio with HD1835). Campbell and Cayrel (1984) found molecular lines characteristic of sunspot umbrae in high-resolution spectra that suggested spot coverage of  $\sim 3\%$  of the surface.

HD10476 = HR493 = 107 Piscium = NSV 600. This Wilson star is a photometric standard on the *UBV* (fundamental), *uvby*, and DAO systems. The suspected variability is due to Gutierrez-Moreno *et al.* (1966), who claim a range of 0.12 in *V*, which is clearly discredited by our observations (the star is nevertheless a long-term microvariable). The star is a suspected spectroscopic binary, but unresolved via speckle interferometry (Hartkopf and McAlister 1984).

HD13421 = HR635 = 64 Ceti. A Wilson star that has received relatively little attention apart from analysis of the Mount Wilson HK data. It is included as a standard in Perry *et al.* (1987). MK classification suggests this is a subgiant.

HD13611 = HR649 =  $\xi^1$  Ceti = 65 Ceti = NSV 749. This luminous marginal barium star is a 1983 MK and DDO standard. It was suspected of variability by Argue (1966), who suggested it was an eclipsing binary of amplitude  $V = 0.03$  from two nights' data (!). Our data also show variability, but of a different kind; short-term variation at the 3% level is ruled out. It was observed by Wilson (1982) during a quick-look survey of HK emission in late-type giants and found to be inactive. The star has a diameter determined via lunar occultation (cf. White and Feerman 1987). It is a spectroscopic binary with several published orbits (most recently Griffin 1982), which is resolved via speckle interferometry (McAlister *et al.* 1984); the companion was detected using *IUE* and interpreted as a white dwarf (common among Ba stars) by Bohm-Vitense and Johnson (1985). The last three observations have not been correlated directly.

### Supplementary Notes continued.

HD18256 = HR869 =  $\rho$  Arietis = 46 Arietis. A relatively low HK flux Wilson star. The reality of its spectroscopic binarity has been disputed (cf. Morbey and Griffin 1987).

HD23140 = SAO 39072. Included in D. K. Duncan's 1984 list of stars then actively observed in HK at Mount Wilson.

HD25893 = ADS 2995 = V491 Persei. A Hyades group star having common proper-motion with the brighter Wilson star HD25998 (see below). It was added to program because of probable variability. HK emission was noticed by Bidelman (1983) on objective-prism plates. This led Boyd *et al.* (1984) to check it for variability using an automated telescope; they found a  $V$  amplitude of 0.03 mag and a period of 7.37 days. Our data, though not as extensive, suggest a period of about 11 days (more concordant with expectations from other Hyades stars of this spectral type), and 1986/7 season amplitude  $\Delta y = 0.05$ .

HD25998 = HR1278 = 50 Persei. A Wilson star and Hyades group member having common proper-motion with the binary HD25893 (above). Aside from analysis of Mount Wilson HK data, no other relevant study.

HD35296 = HR1780 = 111 Tauri. A bright Wilson star whose chromospheric activity is well-studied in many lines from the UV to IR. Boyd *et al.* (1984) used this as a comparison star for the long-period variable 119=CE Tauri, but did not notice the variability found in the present observations.

HD39587 = HR2047 =  $\chi^1$  Orionis = 54 Orionis. Among the most thoroughly studied Wilson stars, and among the brightest on our observing list. Also a Strömgren photometric, zero-polarization, and 1985 MK standard. Its angular diameter has been measured via lunar occultation (cf. White and Feigman 1987).

HD75332 = HR3499. An active Wilson star without much astrophysical study apart from Mount Wilson HK analysis. It is included as a "highly accurate" photoelectric standard in Khaliullin *et al.*'s (1985) WBVR system, but with only two nights' observation, they missed the 2% interannual variation we see. UBV measures have been made by a Canadian amateur (Kaitting 1985), who also found no variations (his rms dispersion was 0.02).

HD76572 = HR3563 = 61 Cancri = ADS 7107. A low-flux Wilson HK standard. Classed as F6V by Cowley and Bidelman (1979), but moderate-dispersion classification by Abt (1986) shows it to have slightly weak metallic lines (F4V/F2met/F4 G-band). Observed by Radick *et al.* (1983) in 1978/9, who found no variability at the 4 mmag level in  $y$ .

**Supplementary Notes** continued.

HD81809 = HR3750 = Burnham 2530. This Wilson star is often considered a solar analog (see, however, Neckel 1986). Observed by Radick *et al.* (1983) in 1978/9, who found no variability at the 4 mmag level in *y*. Duquennoy and Mayor (1988) present the results of nine years of CORAVEL radial velocity measures, which are consistent with the 35-year visual binary orbit of Baize (1985); the implied mass ratio suggests a G0V+G9V pair.

HD82635 = HR3800 = 10 Leonis Minoris. This chromospherically active giant was chosen as a comparison star for HD82885 = 11 LMi (see next). A rotation period was found by Skiff and Lockwood (1986). The star is a standard on the *uvby* system. It was observed by Wilson (1982) in a quick-look survey of H&K emission in cool giants, where the activity was about double that of the Sun. About the same time, Middelkoop (1982) found a similar *S* value.

HD82885 = HK3815 = 11 Leonis Minoris = ADS 7441. An active and well-studied Wilson star. The star is a fundamental *UBV* standard, *uvby*, DAO, zero-polarization, and "Lowell 10-Year" (Jerzykiewicz and Serkowski 1966) standard. Radick *et al.* (1983) found no variations in 1978/9 at the 4 mmag level. Nevertheless, Skiff and Lockwood (1986) found a rotation period with an amplitude over 3% in 1984/5. The spectral type has been disputed. In the original *UBV* paper (Johnson and Morgan 1953), Morgan classed it as G8IV-V; later the YBS listed it as G8III. However, the large parallax and proper-motion indicate that the star cannot be other than a dwarf. More recently, Abt (1981) has classed it as G8V. The star has a mag. 13 M-dwarf companion which has an orbital period near 200 years (Heintz 1988).

HD103095 = HR4550 = NSV 5374 = CF Ursae Majoris = Groombridge 1830. This thoroughly studied Wilson star is a famous high-velocity halo subdwarf 8 parsecs from the Sun. It has the third-highest known proper-motion, amounting to 7.1 arcsec-yr<sup>-1</sup>. The star is used as a *UBV*, Strömgren, Washington, Lowell "10-Year," and radial-velocity standard. Flares have been reported twice by parallax observers (see Heintz 1984 for summary), but these almost certainly arose from instrumental effects; the variable star designations were thus assigned prematurely, and we find only long-term changes in our measures. There is an extensive literature of detailed spectroscopy and spectrophotometry examining various aspects of the star's low metal abundance (roughly ten times less than solar). The star will pass near another field star ( $V = 13.90$ ,  $b - y = 0.27$ , based on two nights differential photometry relative to HD103095) around the turn of the century.

HD111812 = HR4883 = 31 Comae. This star is a rapidly rotating G-giant that appears to be a member of the Coma cluster, but lies in the Hertzsprung gap. It is a fundamental *UBV* standard, Strömgren, and 1985 MK standard. Well-studied spectroscopically because of its unusual properties. The rapid rotation and similarity to FK Comae-type variables led Boyd *et al.* (1984, 1985) to search for variability using an automatic telescope; none was found at the 1% level (Strassmeier and Hall 1988); our measures show significant seasonal and interannual variations. Simon (1986) sought rotational modulation in *IUE* spectra without success.

**Supplementary Notes** continued.

HD112989 = HR4924 = 37 Comae = ADS 8731. This chemically peculiar K-giant is a 1985 MK standard (G9III CH-2Fe1Ca1) and has been much studied as a member of the class of metal-weak stars. The visual binary companion is very faint ( $V = 13$ ) and not important to the present photometry. Eggen (1973) included the star in a list of young, disk population giants. It has twice been classified as cooler than the standard: K1IIIp (weak G band) by Schild (1973) and K1II-III by Abt (1981). The star was observed photoelectrically by Boyd *et al.* (1984, 1985); no variability was found (Strassmeier and Hall 1988).

HD114710 = HR4983 =  $\beta$  Comae = 43 Comae Berenices. This thoroughly studied Wilson star is a relatively inactive nearby dwarf and 1985 MK standard.

HD115383 = HR5011 = 59 Virginis =  $\epsilon$  Virginis. A fairly active Wilson star and Strömgren standard. No directly relevant study apart from HK analysis. Not previously known to be variable.

HD115404 = ADS 8841 = SAO 100491. A chromospherically active pair involving K1 and M1 dwarfs. Variability was first reported by Radick *et al.* (1983), who found a range of  $\sim 3\%$  and a period of 18 days, consistent with Mount Wilson HK measurements.

HD120136 = HR5185 = 4 Bootis =  $\tau$  Bootis = NSV 6444 = ADS 9025. This Wilson star is a *UBV* and Lowell "10-year" standard, but has been suspected of variability for many years. The chromospheric activity is relatively weak as measured in the HK lines and in He I lines (see Wolff *et al.* 1986). We find a small, gradual change in mean brightness after four seasons unrelated to the originally suspected  $\delta$  Scuti-like variations, which do not exist in our data. The faint ( $V = 10.7$ ) companion is an M3 dwarf (Joy and Abt 1974).

HD124570 = HR 5323 = 14 Bootis = NSV 6597. This Wilson HK standard was observed for short-period variability by Breger (1969), who found no variations at the 3 mmag level during 2.4 hours of monitoring. The spectroscopic binary companion is undetectable either via secondary lines (Gomez and Abt 1982) or via speckle interferometry (most recently: Blaziti *et al.* 1987).

HD129333 = SAO 16453. A relatively faint star on the HK program at Mount Wilson in later years. The most active star in our photometric program. Well observed in the Geneva system, but not suspected of variability (see Rufener 1981). HK emission analysis only by Soderblom (1985) and Soderblom and Clements (1987). Photometric activity quite variable, ranging from 0.03–0.09 mag in  $y$  over one season, and changes of 0.05 mag or so over several years.

HD131156 = HR5544 = 37 Bootis =  $\xi$  Bootis = ADS 9413. Another active double star long suspected of variability; we find clear evidence of rotation despite its being a Lowell "10-year standard" (Jerzykiewicz and Serkowski 1966). The secondary star is 2.23 magnitudes fainter in  $V$  on average, though both stars are likely to be variable.

**Supplementary Notes** continued.

HD131511 = HR5553 = NSV 6847. This star was chosen as a comparison for HD131156, but as it is a member of the Hyades moving group, it was not surprising to find it variable; our data provide a rotation period of about 10 days, near what is expected for Hyades K2V stars. The spectroscopic binary ( $P \sim 125$  days) is unresolved via speckle interferometry.

HD143761 = HR5968 = 15 Coronae Borealis =  $\rho$  Coronae Borealis. This low HK-flux high-velocity halo star is a Strömgren, radial-velocity, and 1985 MK standard.

HD149661 = HR6171 = 12 Ophiuchi = V2133 Ophiuchi. An active Wilson star first discovered to be variable by Dorren and Guinan (1982) after null results published by Blanco *et al.* (1979), who observed the star for four seasons, and Rybka (1979), who analyzed relatively noisy observations. Radick *et al.* (1983) also found no variability at the 5 mmag level.

HD152391 = SAO121921. An active Wilson star, but photometric variability varies from nil to obvious between seasons. A light curve was first published by Chugainov (1976). Variability was also observed by Dorren and Guinan (1982), who derived a rotation period, and by Radick *et al.* (1983).

HD157856 = HR6489. A low HK-flux Wilson star.

HD158614 = HR6516 = ADS10598. Another inactive Wilson star. Keenan and Pitts (1980) included it their 1980 list of MK standards as G9IV-V H $\delta$ 1, however Abt (1981) classed it as G5V.

HD160346. Relatively inactive Wilson star and 1983 MK standard. Blanco *et al.* (1979) found it to be constant at the 1% level.

HD161239 = HR6608 = 84 Herculis. The sole true giant on the Wilson list (relatively inactive), and a 1985 MK standard (G2IIb).

HD162211 = HR6644 = 87 Herculis. This slightly variable comparison star has traditionally been used as a comparison star for the extensively observed UU-Herculis variable 89 Her; the variability we find has not been previously suspected (e.g., Fernie, 1986, where Strömgren photometry is given).

HD176095 = HR7163. A relatively hot Wilson star.

HD182572 = HR7373 = b Aquilae = 31 Aquilae = NSV 11994. This Wilson star has attracted attention largely because of its high velocity and its strong-lined spectrum. It is a radial-velocity (extensive high-precision observations indicate it is single) and 1985 MK standard.

HD185018 = HR7456 = ADS12670. This supergiant was selected as a comparison star before we were aware of its luminous nature. It lies just outside the Cepheid instability strip, and variability has not been demonstrated before the present observations (Eggen, 1985, found it nonvariable at the 3 mmag level on four nights).

**Supplementary Notes continued.**

HD185144 = HR7462 = 61 Draconis =  $\sigma$  Draconis = NSV 12176. This bright, nearby K dwarf is a *UBV*, Strömgren, and 1985 MK standard. The suspected variability ( $\Delta V = 0.07$ ) was found visually and can be discounted from our data.

HD190007 = SAO 125379. A cool, active Wilson star. A marginal detection of variability was found by Dorren and Guinan (1982), but there were insufficient data to make a firm statement. Radick *et al.* (1983) also came to an uncertain conclusion based on Strömgren data whose *y*-filter rms dispersion was 0.009 mag.

HD201091 = HR8085 = 61 Cygni A = V1803 Cygni = ADS14636A. This famous, exhaustively studied star (and *UBV*, Strömgren, and 1985 MK standard) was first clearly observed to be variable by Dorren and Guinan (1982). They found an amplitude of 0.03 mag in the blue that correlated well with the HK-derived rotation period. They observed near the cyclic HK-flux maximum about 1981. In contrast, Perry *et al.* (1987) find no variability on 18 nights; likewise our observations do not show this short-period variability.

HD201092 = HR8086 = 61 Cygni B = NSV 13546 = ADS14636B. A standard on many systems: *UBV*, Strömgren, DAO, 1985 MK, and others. This star has also been suspected of variability ( $\Delta V = 0.07$ ), which is ruled out by the present observations. Neff (1968) claimed "rapid irregular light variations on several occasions." Blanco *et al.* (1979) saw no variations over five seasons; Dorren and Guinan (1982) had insufficient data to come to a conclusion about variability; finally, Perry *et al.* (1987) found no variability over 18 nights.

HD215427 = SAO 52320. A new semiregular variable among our comparison stars for HD215704. No citations in the SIMBAD database.

HD215704 = SAO 52353. A relatively faint, low HK-flux star from the 1984 Duncan observing list.

HD216385 = HR8697 = 49 Pegasi =  $\sigma$  Pegasi. *UBV* and Wilson HK standard.

Figure 1 shows the relationship between the chromospheric emission ratio ( $\log R'_{HK}$ ) and  $B - V$  color for the program stars. The designation "Y" or "O" refers to the classification of the stars as "young" or "old," according to their position in an  $[< S >, B - V]$  diagram (Vaughan 1980). On this diagram the Sun's position is bracketed in color and activity level by program stars that cover the full range of both quantities. In these parameters, the closest solar analog is HD81809, a G2V spectroscopic binary. The location of the Sun on Figure 1 suggests that it may be among the hottest of the old stars having a measurable activity cycle. At the lower left, the six stars denoted by filled symbols are HK standards with low and constant  $< S >$  values; two of them (HD13421, G0V; HD143761, G0+Va) happen to be *uvby* photometric standards as well, and all have subsolar activity levels according to their low values of  $\log R'_{HK}$ .

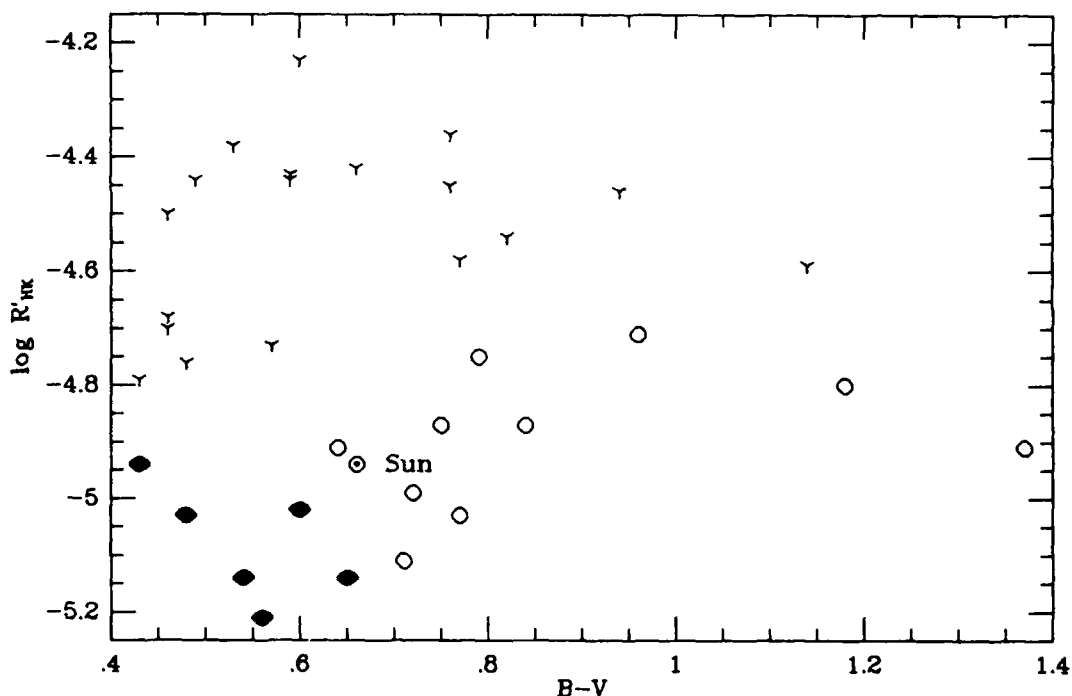


**Figure 1.** Chromospheric emission ratio  $\log R'_{HK}$  as a function of  $B - V$  color for the program stars. (Y) - young, active stars, (O) - old stars, (filled circles) - inactive HK standards. The designations "old" and "young" are from Vaughan (1980).

### 2.1.2 Comparison stars

Optimal differential photometry requires the measurement of two or more field comparison stars of comparable apparent magnitude and color. A minimal configuration is thus a trio containing one program star and two comparison stars located within a few degrees of one another on the sky. In six cases initially, quartet groups were formed containing two program stars and two comparison stars. In Table 1, the entries are organized into the resulting 30 such groups. When more than one star

in a trio exhibited variability, an additional comparison star was added, eventually making several new quartet groups.

Figure 2 shows the location of the groups on the sky. The star symbols are program stars. In most cases, the group members are so close together that their airmasses are very nearly the same, thus minimizing differential extinction effects.

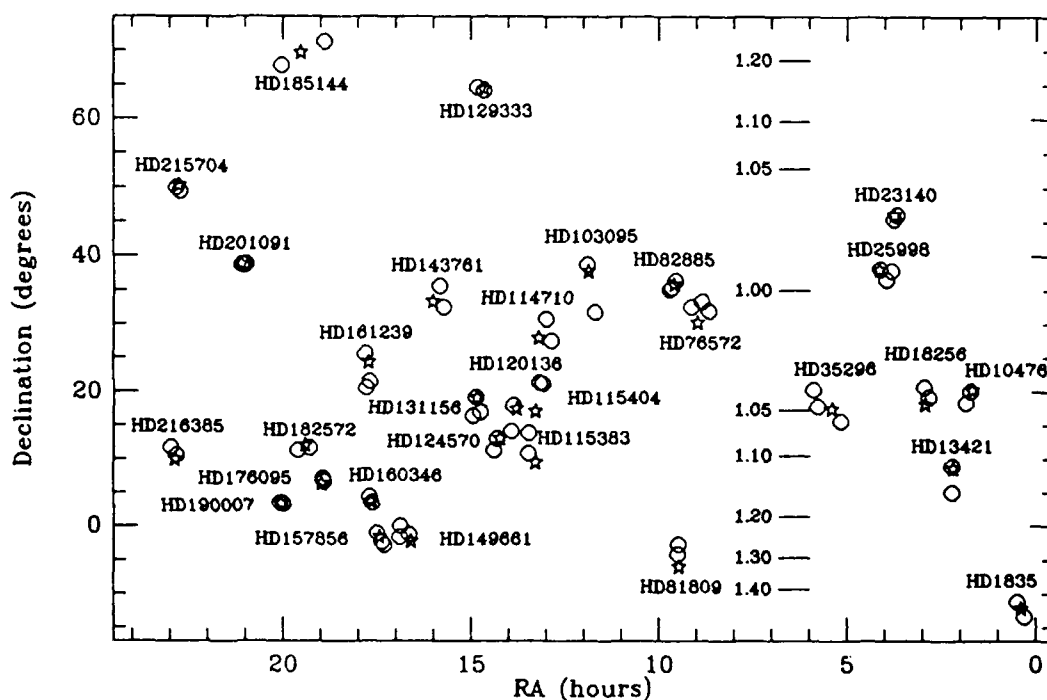


**Figure 2.** Location of the trio and quartet groups on the sky. (stars) – program stars. Differential airmasses may be estimated by the separate scale showing the airmass at meridian transit.

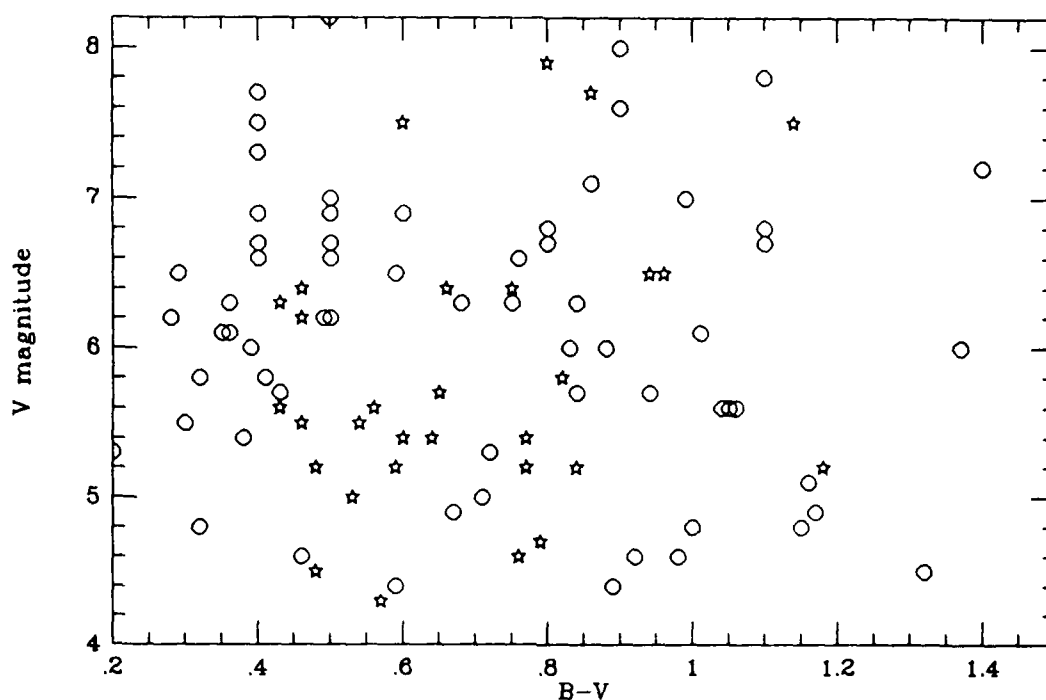
### 2.1.3 Distribution of color and apparent magnitude

Figure 3 shows that the distributions of apparent  $V$  magnitudes and  $B - V$  colors for the program stars and comparison stars are similar, though the comparison stars are on average about 0.5 mag fainter and 0.04 mag redder in  $B - V$ .

### 2.2 The observational facility

All observations were made using the 0.5-m reflecting telescope of Lowell Observatory, located on a wooded mesa at an elevation of 2200 m about 1 km west and 100 m above downtown Flagstaff. The telescope is a manually slewed f/16 Cassegrainian housed in a building with a roll-off roof; it was originally used in the 1950s by H. L. Johnson in the early days of  $UBV$  photometry. Recent photographs of the telescope may be found in Lockwood (1983) and Lockwood and Skiff (1987).





**Figure 3.** Apparent visual magnitudes and measured or estimated  $B - V$  colors for the program stars (*stars*) and comparison stars (*open circles*).

Despite the proximity of city lights, the sky brightness is only a couple of stellar magnitudes brighter at the zenith than the natural celestial background and is therefore essentially negligible for bright-star photometry. Local aerosols are usually trapped below the level of the Observatory by a nighttime temperature inversion, a significant factor in winter when woodstoves are in use.

Since 1974, the telescope has been equipped with a photoelectric photometer of conventional design, pulse-counting electronics, and a data-acquisition microcomputer, currently a Digital Equipment Corporation LSI-11/03 and associated standard interface and control circuit cards. Data are displayed on a video terminal and recorded on DEC RX02 flexible disks for subsequent analysis on the Observatory's VAX-750 computer. Recently, funds provided by this contract were used to equip the telescope with a computerized coordinate display system.

The photometer utilizes a thermoelectrically cooled EMI 6256S photomultiplier and standard intermediate-band Strömberg *uvby* interference filters. An  $\text{Sr}^{90}$  Cerenkov source provides a stable light output used to monitor the nominal performance of the detector and electronics. The same photomultiplier and filters have been in constant use since 1971, a factor contributing significantly to the long-term stability and precision of results obtained with this facility.

### 2.3 The basic observation sequence

Following the methodology recommended to us by Jerzykiewicz 15 years ago, the basic data unit in precision differential photometry is a "cycle" comprising sequential observations of the three stars of a trio or the four stars of a quartet through a single filter. In this program we utilize only the *b* (472 nm) and *y* (551 nm) filters of the Strömgren four-color system. Typically, a standard nightly observation consists of four cycles in the filter order *y, b, b, y*. Within each cycle, each star is measured for a total of six 10-second intervals as follows:

					dark	Sr <sup>90</sup>	Sr <sup>90</sup>
			*sky 2	sky 2	†star 2	star 2	star 2
star 1	star 1	star 1	sky 1	sky 1	star 1	star 1	star 1
[star 4	star 4	star 4	sky 4	sky 4	star 4	star 4	star 4]**
star 3	star 3	star 3	sky 3	sky 3	star 3	star 3	star 3
star 2	star 2	star 2	sky 2	sky 2			
			....	....	Sr <sup>90</sup>	Sr <sup>90</sup>	dark

\*\* - quartet only.

Subsequent cycles in the same filter begin at †; subsequent cycles in a different filter begin at \*

A sample complete observation is given in the Appendix. Each set of *n* cycles is preceded and followed by a dark count and standard light source sequence that serves as an archived indicator of system performance.

An important element of the experimental design is the equal statistical weight (in terms of total integration) of each stellar measurement, regardless of whether it is a program or a comparison star. The various pairwise differential combinations (i.e., star 1–star 2, star 1–star 3, ..., star 3–star 4) are thus statistically equivalent except for time order and the splitting of the observations of star 2 (normally a comparison star) into two half-weight sequences beginning and ending each cycle. Every nightly differential magnitude set for a group contains an internal noise measure provided by two presumably quiescent comparison stars. The most stable pairwise differential magnitude defines the night-to-night noise baseline, which in the absence of variability is typically in the 0.002–0.003 mag range.

### 2.4 Expected precision levels

Attaining the highest possible long-term precision is a major goal of this program. If they mimic the Sun exactly, our solar analog program stars will have rotational amplitudes under 0.5% and cycle amplitudes under 0.1%. This is a formidable challenge to conventional stellar photometry, one which has few precedents in the astronomical literature and little in the way of technical guidance (cf. Young 1974, for a litany of photometry pitfalls relevant to this program).

We have previously found (e.g., Lockwood 1984) that intermediate-band photoelectric photometry yields nightly mean differential magnitudes with a standard deviation of about 0.003 mag (0.3%). If there are no systematic errors, 8-16 nights should theoretically yield seasonal mean values with a precision on the order of 0.001 mag (0.1%). Obviously, at this demanding level of precision, the long-term stability of the photometer and the interference filters is of paramount importance. Earlier long-term monitoring of solar system objects using the same equipment yielded results that appear to be stable to about 0.003 mag and perhaps better, but this prior experience offers no certain proof of performance at the even higher precision required here (Lockwood *et al.* 1980; Lockwood and Thompson 1986a).

Ultimately, the uncertainty of differential magnitudes propagates from the measurement errors of the simplest data element, the photon-counting statistics of individual 10-second integrations, plus random or systematic measurement errors due to a variety of causes. As a fundamental, observationally testable statistic of the error budget, we estimate how precisely the differential magnitudes should repeat from cycle to cycle within the nightly sequence  $y, b, b, y$ . Known or suspected components of error include (1) photon counting statistics and the correction for dead time, (2) sky background measurements, (3) differential extinction, (4) sky transparency changes during the cycle, (5) photometer sensitivity changes during the cycle, (6) scintillation, and (7) effects of seeing and image motion within the star diaphragm. In the following sections, we estimate as best we can the relative importance of these various components.

#### 2.4.1 Photon-counting errors

The throughput of the telescope + photometer system changes only slowly with time, as evidenced by the constancy of stellar and  $\text{Sr}^{90}$  count rates. Photon-counting errors are thus a simple function of stellar magnitude, since the observations are deliberately made in an identical way each night. The stars in Table 1 have a median  $V$  magnitude of 6.1 mag; the faintest is 8.2 mag. Three-quarters of the stars are brighter than  $V = 6.7$  mag, corresponding to an observed count rate in the  $y$  filter  $> 25,000 \text{ sec}^{-1}$ , and greater still in  $b$  for stars hotter than  $B - V \sim 1.4$  (K7V, K3III). Six 10-second integrations therefore yield an internal photon-counting error  $< 0.001$  mag for  $V < 6.7$  (i.e., for 75% of the stars in Table 1). In §3.7.1 we illustrate the predicted photon-counting error distribution for the actual set of differential star pairs in the observing program.

#### 2.4.2 Sky background

Under dark sky conditions, the observed count rate through the 49 arcsec diameter star diaphragm normally used was  $\sim 250 \text{ sec}^{-1}$ , yielding a negligible ( $< 1\%$ ) sky contribution to the stellar signal and a completely negligible ( $< 0.1\%$ ) uncertainty in the resulting sky-subtracted count.

An unseen 12th magnitude background star will contaminate the measurement of a 7th magnitude star at the 1% level, whether it is included in the diaphragm with the star or is accidentally encountered during the separate measurement of sky

brightness. Fortunately, the density of 12th magnitude stars averaged over the whole sky is fairly low (Roach and Gordon 1973): the probability of accidentally including a background star in a 49 arcsec diaphragm is  $\sim 0.03$  in the magnitude range  $12.5 < V < 13.5$  and  $< 0.05$  for all stars brighter than  $V = 14.0$ , a negligible risk. Nonetheless, great care has been taken to avoid including faint background stars (see §3.2).

#### 2.4.3 Extinction and airmass

Scintillation noise and atmospheric extinction effects are minimized in this program because all but one of the star groups transit the meridian at an airmass  $< 1.3$ . Differential airmasses within groups are usually negligibly small (Figure 2). If, for example, the differential airmass range is as large as 0.03—a condition occurring only rarely—and the assumed mean extinction coefficient is incorrect by 0.03 mag airmass<sup>-1</sup>, a typical uncertainty (Lockwood and Thompson 1986b), the resulting differential magnitude error is  $< 0.001$  mag. Note, however, that this error systematically affects all observations of a particular group in the same way on a given night; it contributes therefore to the night-to-night dispersion and can in principle masquerade as stellar variability. In §3.7.2 we test some data with especially “large” values of the differential airmass for possible extinction-related systematic effects.

#### 2.4.4 Temporal atmospheric transparency changes

The observation of a single cycle requires at most 10 minutes for a quartet and 7 minutes for a trio. If the sky transparency changes during this interval (due to vanishingly thin cirrus clouds, for example), random errors are introduced into the differential magnitudes. Termination of observations is at the discretion of the observer (see §3.2); but generally, problems with sky transparency become noticeable only when they reach the 1–2% level.

Certainly, on truly “photometric” nights, repeated observations of bright stars should approach the scintillation + photon limit. In some earlier measurements (cf. Lockwood 1984), we looked for evidence of sky transparency fluctuations over intervals of a few minutes by examining the relative precision of the differential magnitudes of the various pairs of stars within cycles. Over the 2–7 minute time interval in which the various pairs of stars within quartets were measured, we found no evidence for systematic effects—the precision attained for each of the pairs was the same.

#### 2.4.5 Temporal changes in photometer sensitivity

The recorded output of the  $\text{Sr}^{90}$  standard source light that precedes and concludes each four-cycle data set provides confirmation of the temporal stability of the photometer electronics. Apart from a slow ( $< 1\% \text{ hr}^{-1}$ ) drift in the count rate, evidently related to ambient temperature changes as the night progresses, the source output repeats in accord with photon-counting statistics, i.e., about 0.16% rms (10-second integrations).

#### 2.4.6 Scintillation error

The relevant formulas are given by Young (1974). For a 0.5-m telescope, the expected standard deviation for a single 10-second integration is 0.0008-0.0018 mag in the airmass range of interest, depending on the angle between the line of sight and the upper-air wind direction. Combining six 10-second integrations thus is expected to provide an essentially negligible 0.0005 mag contribution to the error budget.

#### 2.4.7 Errors caused by seeing and image motion

The observed brightness of decentered stars can vary because of inhomogeneities in the sensitivity across the focal plane aperture of the photometer. In addition, decentered or moving images result in a position-dependent occultation of different parts of the extended faint wings of stellar images by the circular diaphragm. Variable seeing, image motion, and telescope tracking errors combine to degrade measurement precision unpredictably.

Drift scans in perpendicular directions across the 29- and 49-arcsec apertures indicate that the photometer response is uniform within 0.3% or so over the central third of each aperture where most observations are made (cf. §3.2). Random decentering of star images may contribute significantly to the error budget, but we can only guess an approximate amount.

#### 2.4.8 A hypothetical error budget

A hypothetical error budget for a single stellar magnitude determined from six 10-second integrations includes the terms in Table 2. In this example, more than half the variance is conceivably contributed by the poorly estimated component related to image motion. When two individual stellar measurements are combined to create a differential magnitude, the variance is doubled, leading to an expected cycle-to-cycle rms dispersion of 0.002-0.005 mag. In §3.7.1, we compare the error budget with real data, and in §3.7.2 we will show that the value 0.002 corresponding to the low estimate above is achieved for the most stable stars.

### 3. THE DATA

#### 3.1 Observations obtained

The stars listed in Table 1 are organized into 30 groups of trios and quartets. Trios were promoted to quartets if, during the course of the program, more than one star was found to vary. Nearly 2000 nightly observations, about 60 nights per group, were obtained on 350+ nights between March 1984 and December 1987 — three full seasons for all groups and four, or part of a fourth, for nearly all groups. All observations were made and reduced to differential magnitudes by B. A. Skiff. A typical original data record is given in the Appendix.

#### 3.2 Observational procedures

Observations were about evenly split between diaphragm 3 (29 arcsec) and diaphragm 4 (49 arcsec). One or the other was selected based on the apparent

TABLE 2. Error Budget

	Low Estimation (mag)	High Estimation (mag)
Photon counting ( $V = 6.7$ )	0.001	0.001
Sky subtraction	0.0005	0.001
Differential extinction	<0.0005	0.001
Scintillation	0.0003	0.0007
Sensitivity drift	...	0.0005
Centering/tracking	0.001	0.003
Root mean square	0.0016	0.0036

image size of bright ( $V < 2$ ) stars: if the seeing disk was less than 6 to 8 arcsec (corresponding roughly to FWHM and estimated using the known sizes of the diaphragms), then the smaller aperture was used; worse seeing dictated the use of the larger aperture. Observations were not made (or halted at some convenient point) if the images were larger than about 25 arcsec, a condition that occurred a few nights each year associated with passage of winter storms. The estimated seeing is recorded in the comments line of each file header.

Observations were begun during late twilight when the sky counts declined to about double the expected full-dark level for the appropriate diaphragm size. Measurements were not made closer than 20 to 30 degrees from the Moon or when the sky counts exceeded  $1000 \text{ sec}^{-1}$  in the  $b$  filter due to moonlight. At high galactic latitudes, the sky readings were made by simply flipping the declination slow-motion crank either north or south about a full turn; tests showed this corresponds to a typical offset "throw" of 4 or 5 arcminutes. Except during the first few months of the project, the first two cycles have sky readings to the south and the last two to the north. At low galactic latitudes, sky readings were taken at locations selected during dark time and used consistently; for several groups this meant taking all the sky readings in one direction. All the low-latitude groups could be measured using diaphragm 4.

Stars were carefully centered in the diaphragm, usually within the central one-third of the diameter. The telescope drive often exhibited a slow drift caused by a small periodic error in the worm, and stars were usually offset to one side or the other of the central one-third of the field to let the star drift across dead center. For the numerous double stars where both components were visible, pairs were set on the weighted photocenter (determined roughly by eye), which generally was very close to the primary star. The fields were usually observed within one hour of meridian passage, and rarely up to 2.5 hours hour angle.

Contamination of both star and sky counts by faint field stars was anticipated both in planning and in observing. Bright stars were thoroughly examined by various double star observers about 100 years ago with large telescopes. Thus, any significant close companions are recorded in double star catalogs (and noted in Table 1). Many more of our program stars are also in double star catalogs by virtue of their large proper motions—micrometric measurements of faint background stars being used to ascertain this independent of meridian circle measurements. These ended up being listed as double stars because not a few of the faint companions turned out to have common motion. At any rate, the point is that we know about reasonably bright ( $V < 14$ ) stars near the program/comparison stars that would be included in the diaphragm.

The declination offset throws were not done completely blindly: the "WPHOT" computer program that records data warns the observer of overbright readings on the sky ( $> 2\times$  normal). The readings that were noted as even slightly above normal (indicated by the one-second integrations on a frequency counter) were repeated at a slightly different location to try to get the offending star out of the diaphragm as the integrations continued. Regarding the discussion in §2.4.2, stars  $V < 14$  were hardly ever included in sky readings, not so much because the odds of inclusion are so small, but because the observing technique specifically attended to this point. Certain stars have a faint "companion" consistently falling in the normal "sky" position, and these have all their sky readings taken in the opposite direction.

Finally, it is also worth noting that the sky background at low galactic latitudes is noticeably brighter due to the presence of stars below the limit of visibility of the telescope ( $V > 15$  on dark nights).

### 3.3 Data rejection criteria

Integrations were monitored regularly for anomalous counts both as they were taken and using a summary facility in the photometry program. Generally, the batches of repeated 10-second "star" integrations would show a total range of 1% or a bit more; larger ranges were indicative of clouds, miscentered stars, or poor seeing (i.e., too-small a diaphragm). A set of integrations would be repeated only due to observer or mechanical error, viz. the wrong star, miscentering due to drive motor drift or wind. The rms noise on a set of six integrations was typically 0.3–0.5%; on the most stable nights (generally associated with the best seeing), the rms would consistently reach 0.1–0.3%; and on poor nights, increase to 0.5–0.8%—these last often preceding the arrival of cirrus, easily discernable photometrically at the 1–2% level. The repeated cyclic measurements provided further checks on photometric stability. If a star did not repeat to within about half a percent between cycles (after compensating mentally for airmass changes), suspicions were raised; usually, continued observations would show persistent deviations (either cycle-to-cycle or intra cycle), thus ending the night.

### 3.4 Reductions

Utilizing data reduction procedures that have been highly standardized for many years, the raw observations were corrected for pulse pair "dead time," the sky background was subtracted, and differential magnitudes were computed using seasonally adjusted mean values of the extinction coefficients (Lockwood and Thompson 1986b). The principal raw data archive is maintained on the original 8-inch flexible disks.

Each reduced observation yields a printed output and one data "record" per cycle that is appended to the master file for each group. Every cycle produces a set of three differential magnitudes for a trio (star 1-star 2, 1-3, 2-3), six for a quartet (star 1-star 2, 1-3, 1-4, 2-3, 2-4, 3-4). Examples of the printed nightly output file are shown in the Appendix.

### 3.5 Seasonal mean differential magnitudes

Table 3 contains the seasonal mean Julian Date, the mean differential  $b$  and  $y$  magnitudes, and their standard deviations for each group. Nomenclature of the pairwise magnitude combinations corresponds to the star numbers assigned within each group in Table 1. The number of observations,  $n$ , is the number of cycles obtained in each filter; hence the number of nights is  $n/2$ .

### 3.6 Light Curves

Figures 4.1-4.30 show the light curves for each group. Because the light curves in  $b$  and  $y$  are essentially identical, the data have been condensed for presentation by averaging the  $y$  magnitudes of cycle 1 with the  $b$  magnitudes of cycle 2, and the  $b$  magnitudes of cycle 3 with the  $y$  magnitudes of cycle 4. Individual data points for the averaged  $(b + y)/2$  cycles are shown on the left-hand panels, using the same vertical scale (0.05, 0.1, or 0.2 mag full range as required) for all the panels of a given group.

Seasonal mean magnitudes are summarized on the right-hand panels, where the mean values are connected by solid lines. The error bars are 95% confidence intervals about the means. Median differential magnitudes are shown as open circles: by comparing the relative locations of means and medians, some feeling for the asymmetry of the data can be obtained, particularly useful in assessing the importance of outliers that may be observed on the left-hand panels. Note that the 95% confidence intervals are sensitive to not only the rms dispersion of the data, but also to the number of data points: large confidence intervals often indicate sparseness of data rather than variability.

### 3.7 Observed precision levels

Before attempting to determine which stars may be varying, it is important to establish a clear picture of the magnitude of various error sources; i.e., a statistical profile of the data as a whole. In this section we partition the data in different ways to examine (1) cycle-to-cycle magnitude variations, (2) errors related to differential extinction, and (3) errors associated with bad nights or a particular star group.



TABLE 3. Summary of Annual Mean Differential Magnitudes

Group	Mean JD 2,440,000+	n	1-2		1-3		1-4		2-3		2-4		3-4	
			$\Delta m$ (mag)	s.d. (mag)	$\Delta m$ (mag)	s.d. (mag)	$\Delta m$ (mag)	s.d. (mag)	$\Delta m$ (mag)	s.d. (mag)	$\Delta m$ (mag)	s.d. (mag)	$\Delta m$ (mag)	s.d. (mag)
HD1835 b	6030.6	28	-0.4097	0.0038	-0.0837	0.0034			0.3260	0.0018				
	6347.4	53	-0.4245	0.0031	-0.0974	0.0032			0.3271	0.0013				
	6713.4	38	-0.4135	0.0030	-0.0867	0.0031			0.3268	0.0013				
	7085.6	28	-0.4219	0.0034	-0.0960	0.0034			0.3259	0.0014				
y	6030.6	28	-0.4763	0.0035	-0.1155	0.0037			0.3608	0.0015				
	6347.4	53	-0.4885	0.0027	-0.1264	0.0029			0.3621	0.0010				
	6713.4	38	-0.4797	0.0031	-0.1185	0.0030			0.3613	0.0010				
	7085.6	28	-0.4863	0.0029	-0.1255	0.0028			0.3608	0.0010				
HD10476 b	6016.3	30	-0.9926	0.0006	-1.5099	0.0011			-0.5173	0.0010				
	6364.4	30	-0.9927	0.0008	-1.5100	0.0010			-0.5172	0.0011				
	6712.8	28	-0.9881	0.0010	-1.5046	0.0011			-0.5166	0.0007				
	7089.1	28	-0.9890	0.0007	-1.5056	0.0011			-0.5167	0.0012				
y	6016.3	30	-1.0470	0.0011	-1.3495	0.0008			-0.3024	0.0008				
	6364.4	30	-1.0466	0.0010	-1.3490	0.0010			-0.3024	0.0010				
	6712.8	28	-1.0442	0.0008	-1.3455	0.0008			-0.3013	0.0011				
	7089.1	28	-1.0444	0.0005	-1.3460	0.0009			-0.3016	0.0010				
HD13421 b	6009.0	24	1.1226	0.0012	-0.7520	0.0017			-1.8746	0.0016				
	6381.0	18	1.1235	0.0013	-0.7529	0.0015			-1.8765	0.0015				
	6731.9	29	1.1149	0.0008	-0.7514	0.0011			-1.8663	0.0011				
	7098.8	14	1.1057	0.0015	-0.7510	0.0018	-1.3907	0.0021	-1.8566	0.0013	-2.4964	0.0014	-0.6397	0.0013
y	6009.0	24	1.2938	0.0019	-0.8868	0.0016			-2.1805	0.0012				
	6381.0	18	1.2925	0.0012	-0.8859	0.0012			-2.1784	0.0012				
	6731.9	29	1.2861	0.0012	-0.8854	0.0010			-2.1715	0.0012				
	7098.8	14	1.2790	0.0017	-0.8838	0.0021	-1.4306	0.0013	-2.1628	0.0015	-2.7096	0.0016	-0.5408	0.0015
HD18256 b	6015.3	18	-0.1826	0.0016	-1.1083	0.0018			-0.9257	0.0016				
	6389.6	19	-0.1823	0.0006	-1.1079	0.0015			-0.9256	0.0015				
	6739.8	15	-0.1815	0.0011	-1.1047	0.0010			-0.9231	0.0012				
	7099.8	11	-0.1820	0.0013	-1.1047	0.0018	-1.4118	0.0054	-0.9227	0.0015	-1.2298	0.0060	-0.3071	0.0057
y	6015.3	18	-0.2069	0.0010	-1.0429	0.0008			-0.8360	0.0010				
	6389.6	19	-0.2071	0.0011	-1.0429	0.0015			-0.8358	0.0010				
	6739.8	15	-0.2058	0.0012	-1.0408	0.0014			-0.8351	0.0012				
	7099.8	11	-0.2051	0.0013	-1.0391	0.0019	-1.3134	0.0051	-0.8340	0.0020	-1.1084	0.0053	-0.2743	0.0047

TABLE 3. Summary of Annual Mean Differential Magnitudes (continued)

Group	Mean JD	n	1-2		1-3		1-4		2-3		2-4		3-4	
			$\Delta m$ (mag)	s.d. (mag)	$\Delta m$ (mag)	s.d. (mag)	$\Delta m$ (mag)	s.d. (mag)	$\Delta m$ (mag)	s.d. (mag)	$\Delta m$ (mag)	s.d. (mag)	$\Delta m$ (mag)	s.d. (mag)
HD23140 <i>b</i>	6046.1	22	0.2950	0.0024	0.2602	0.0025			-0.0348	0.0015				
	6397.3	22	0.2941	0.0019	0.2619	0.0018			-0.0322	0.0010				
	6744.3	15	0.2919	0.0022	0.2589	0.0028			-0.0330	0.0015				
<i>y</i>	6046.1	22	0.0483	0.0017	0.3066	0.0017			0.2582	0.0012				
	6397.3	22	0.0472	0.0019	0.3066	0.0018			0.2594	0.0010				
	6744.3	15	0.0461	0.0023	0.3043	0.0025			0.2582	0.0017				
HD25998 <i>b</i>	6042.6	16	-1.4157	0.0035	-0.9478	0.0044			0.4679	0.0030				
	6390.3	24	-1.4150	0.0033	-0.9458	0.0025			0.4691	0.0019				
	6708.0*	12	-1.4114	0.0020	-0.9455	0.0034			0.4658	0.0025				
<i>y</i>	*6766.2	11	-1.4097	0.0034	-0.9433	0.0047	-1.7895	0.0144	0.4664	0.0033	-0.3797	0.0146	-0.8462	0.0146
	6042.6	16	-1.4729	0.0031	-1.0987	0.0034			0.3741	0.0028				
	6390.3	24	-1.4734	0.0021	-1.0969	0.0018			0.3764	0.0015				
HD35296/ HD39587 <i>b</i>	6708.0*	12	-1.4689	0.0023	-1.0938	0.0027			0.3752	0.0027				
	*6766.2	11	-1.4689	0.0031	-1.0934	0.0044	-1.6055	0.0044	0.3755	0.0030	-0.1366	0.0118	-0.5121	0.0130
	5769.2	10	0.3158	0.0044	0.5888	0.0052	-0.3440	0.0041	0.2730	0.0033	-0.6598	0.0035	-0.9328	0.0024
<i>y</i>	6088.7	30	0.3108	0.0035	0.5770	0.0039	-0.3481	0.0027	0.2662	0.0035	-0.6589	0.0019	-0.9250	0.0025
	6420.1	63	0.3176	0.0018	0.5758	0.0020	-0.3442	0.0019	0.2582	0.0016	-0.6618	0.0006	-0.9200	0.0017
	6776.1	32	0.3207	0.0023	0.5798	0.0032	-0.3367	0.0024	0.2591	0.0026	-0.6575	0.0010	-0.9166	0.0025
<i>y</i>	5769.2	10	0.1817	0.0050	0.6165	0.0056	-0.4775	0.0040	0.4348	0.0034	-0.6592	0.0035	-1.0940	0.0030
	6088.7	30	0.1792	0.0031	0.6074	0.0034	-0.4788	0.0024	0.4281	0.0029	-0.6580	0.0021	-1.0861	0.0023
	6420.1	63	0.1855	0.0016	0.6063	0.0018	-0.4763	0.0017	0.4208	0.0014	-0.6619	0.0005	-1.0827	0.0014
HD76572/ HD75332† <i>b</i>	6776.1	32	0.1900	0.0019	0.6118	0.0030	-0.4693	0.0020	0.4218	0.0022	-0.6593	0.0007	-1.0811	0.0020
	5782.7	23	0.0766	0.0015	-0.1714	0.0015			-0.2481	0.0016				
	6119.5	27	0.0775	0.0011	-0.1698	0.0011			-0.2473	0.0010				
<i>y</i>	6432.6	34	0.0773	0.0007	-0.1703	0.0008	0.0040	0.0018	-0.2476	0.0006	-0.0733	0.0018	0.1743	0.0018
	6847.8	29	0.0787	0.0007	-0.1687	0.0007	-0.0142	0.0045	-0.2474	0.0008	-0.0929	0.0047	0.1545	0.0044
	5782.7	23	0.0384	0.0021	-0.2187	0.0012			-0.2571	0.0021				
<i>y</i>	6119.5	27	0.0395	0.0008	-0.2170	0.0007			-0.2565	0.0011				
	6432.6	34	0.0400	0.0007	-0.2172	0.0006	0.0374	0.0017	-0.2571	0.0007	-0.0025	0.0018	0.2546	0.0017
	6847.8	29	0.0411	0.0006	-0.2159	0.0010	0.0224	0.0038	-0.2570	0.0008	-0.0137	0.0038	0.2382	0.0035

TABLE 3. Summary of Annual Mean Differential Magnitudes (continued)

Group	Mean JD 2,440,000+	n	1-2		1-3		1-4		2-3		2-4		3-4	
			$\Delta m$ (mag)	s.d. (mag)	$\Delta m$ (mag)	s.d. (mag)	$\Delta m$ (mag)	s.d. (mag)	$\Delta m$ (mag)	s.d. (mag)	$\Delta m$ (mag)	s.d. (mag)	$\Delta m$ (mag)	s.d. (mag)
HD81809 <i>b</i>	5786.3	19	0.8809	0.0016	-0.9673	0.0016			-1.8482	0.0016				
	6122.7	26	0.8804	0.0012	-0.9687	0.0015			-1.8491	0.0011				
	6464.7	14	0.8761	0.0033	-0.9679	0.0015			-1.8440	0.0037				
	6864.6	28	0.8765	0.0016	-0.9620	0.0013			-1.8384	0.0013				
<i>y</i>	5786.3	19	0.7755	0.0015	-0.8758	0.0013			-1.6513	0.0010				
	6122.7	26	0.7754	0.0011	-0.8764	0.0010			-1.6517	0.0010				
	6464.7	14	0.7729	0.0021	-0.8755	0.0011			-1.6484	0.0023				
	6864.6	28	0.7731	0.0018	-0.8721	0.0017			-1.6452	0.0011				
HD82885/ HD82635† <i>b</i>	5790.0	19	0.7683	0.0065	-0.5265	0.0034			-1.2947	0.0052				
	6137.6	54	0.7842	0.0042	-0.5162	0.0038	-1.3643	0.0037	-1.3004	0.0017	-2.1485	0.0014	-0.8481	0.0006
	6486.7	55	0.7773	0.0026	-0.5233	0.0017	-1.3709	0.0014	-1.3006	0.0017	-2.1483	0.0019	-0.8476	0.0008
	6864.8	41	0.7716	0.0024	-0.5255	0.0014	-1.3716	0.0014	-1.2971	0.0018	-2.1432	0.0018	-0.8461	0.0007
<i>y</i>	5790.0	19	0.8436	0.0063	-0.7358	0.0031			-1.5795	0.0054				
	6137.6	54	0.8588	0.0035	-0.7263	0.0032	-1.5016	0.0035	-1.5851	0.0013	-2.3603	0.0013	-0.7753	0.0011
	6486.7	55	0.8533	0.0020	-0.7319	0.0016	-1.5062	0.0014	-1.5851	0.0016	-2.3595	0.0016	-0.7744	0.0006
	6864.8	41	0.8491	0.0022	-0.7339	0.0011	-1.5076	0.0011	-1.5831	0.0016	-2.3567	0.0016	-0.7736	0.0007
HD103095 <i>b</i>	5795.5	20	-0.7047	0.0013	0.8384	0.0010			1.5432	0.0011				
	6119.7	28	-0.7046	0.0011	0.8393	0.0008			1.5439	0.0011				
	6496.3	21	-0.7038	0.0008	0.8367	0.0010			1.5406	0.0012				
	6872.5	20	-0.7030	0.0013	0.8366	0.0017			1.5397	0.0015				
<i>y</i>	5795.5	20	-0.5924	0.0011	0.6754	0.0008			1.2678	0.0011				
	6119.7	28	-0.5928	0.0010	0.6773	0.0006			1.2702	0.0008				
	6496.3	21	-0.5921	0.0010	0.6753	0.0007			1.2675	0.0010				
	6872.5	20	-0.5914	0.0013	0.6744	0.0013			1.2658	0.0012				
HD114710 <i>b</i>	5795.5	18	-0.7411	0.0013	-0.9497	0.0022			-0.2087	0.0021				
	6163.8	18	-0.7410	0.0015	-0.9413	0.0034			-0.2003	0.0034				
	6519.8	27	-0.7352	0.0029	-0.9302	0.0023			-0.1950	0.0030				
	6908.4	12	-0.7361	0.0020	-0.9361	0.0077			-0.2000	0.0064				
<i>y</i>	5795.5	18	-0.6813	0.0011	-0.6193	0.0018			0.0620	0.0016				
	6163.8	18	-0.6822	0.0017	-0.6138	0.0025			0.0683	0.0028				
	6519.8	27	-0.6784	0.0018	-0.6080	0.0018			0.0704	0.0027				
	6908.4	12	-0.6774	0.0022	-0.6107	0.0049			0.0667	0.0047				

TABLE 3. Summary of Annual Mean Differential Magnitudes (continued)

Group	Mean JD 2,440,000+	n	1-2		1-3		1-4		2-3		2-4		3-4	
			$\Delta m$ (mag)	s.d. (mag)	$\Delta m$ (mag)	s.d. (mag)	$\Delta m$ (mag)	s.d. (mag)	$\Delta m$ (mag)	s.d. (mag)	$\Delta m$ (mag)	s.d. (mag)	$\Delta m$ (mag)	s.d. (mag)
HD115383/ HD117176 b	5802.6	12	-0.6916	0.0016	0.1682	0.0015			0.8598	0.0010				
	6156.3	12	-0.7044	0.0038	0.1556	0.0039			0.8600	0.0014				
	6520.6	21	-0.7055	0.0010	0.1496	0.0017			0.8551	0.0015				
	6907.7	9	-0.6938	0.0020	0.1560	0.0030			0.8558	0.0016				
y	5802.6	12	-0.4425	0.0017	0.2362	0.0012			0.6787	0.0014				
	6156.3	12	-0.4524	0.0026	0.2268	0.0025			0.6791	0.0009				
	6520.6	21	-0.4554	0.0017	0.2207	0.0018			0.6761	0.0013				
	6907.7	9	-0.4504	0.0022	0.2247	0.0020			0.6751	0.0016				
HD115404 b	5823.9	18	0.7594	0.0029	-0.0831	0.0028			-0.8426	0.0013				
	6189.8	39	0.7499	0.0023	-0.0906	0.0023			-0.8406	0.0007				
	6517.2	25	0.7424	0.0040	-0.0963	0.0042			-0.8388	0.0010				
	6912.6	11	0.7480	0.0061	-0.0887	0.0059			-0.8368	0.0018				
y	5823.9	18	0.4943	0.0031	-0.3489	0.0025			-0.8432	0.0021				
	6189.8	39	0.4858	0.0019	-0.3544	0.0022			-0.8402	0.0008				
	6517.2	25	0.4805	0.0036	-0.3575	0.0031			-0.8380	0.0012				
	6912.6	11	0.4845	0.0057	-0.3524	0.0059			-0.8369	0.0021				
HD120136 b	5830.8	24	-1.4080	0.0016	-1.7036	0.0012			-0.2956	0.0011				
	6180.9	16	-1.4056	0.0010	-1.7028	0.0010			-0.2971	0.0010				
	6546.1	15	-1.4003	0.0030	-1.6943	0.0031			-0.2939	0.0023				
	6932.7	16	-1.3946	0.0015	-1.6927	0.0016			-0.2980	0.0013				
y	5830.8	24	-1.2155	0.0016	-1.6841	0.0012			-0.4686	0.0013				
	6180.9	16	-1.2135	0.0012	-1.6830	0.0017			-0.4694	0.0015				
	6546.1	15	-1.2108	0.0020	-1.6766	0.0020			-0.4658	0.0021				
	6932.7	16	-1.2057	0.0012	-1.6751	0.0017			-0.4694	0.0011				
HD124570 b	5814.4	16	0.2088	0.0013	-1.2876	0.0041			-1.4964	0.0034				
	6187.8	20	0.2078	0.0007	-1.2711	0.0025			-1.4788	0.0025				
	6549.6	29	0.2066	0.0008	-1.2686	0.0012			-1.4752	0.0012				
	6930.7	14	0.2058	0.0018	-1.2756	0.0026			-1.4814	0.0027				
y	5814.4	16	0.1342	0.0010	-1.2674	0.0028			-1.4016	0.0027				
	6187.8	20	0.1337	0.0011	-1.2523	0.0019			-1.3860	0.0019				
	6549.6	29	0.1321	0.0007	-1.2517	0.0011			-1.3838	0.0013				
	6930.7	14	0.1322	0.0015	-1.2580	0.0020			-1.3902	0.0017				

TABLE 3. Summary of Annual Mean Differential Magnitudes (continued)

Group	Mean JD 2,440,000+	n	1-2		1-3		1-4		2-3		2-4		3-4	
			$\Delta m$ (mag)	s.d. (mag)	$\Delta m$ (mag)	s.d. (mag)	$\Delta m$ (mag)	s.d. (mag)	$\Delta m$ (mag)	s.d. (mag)	$\Delta m$ (mag)	s.d. (mag)	$\Delta m$ (mag)	s.d. (mag)
HD129333 <i>b</i>	5842.9	14	0.1064	0.0093	-0.8722	0.0095			-0.9786	0.0021				
	6209.3	53	0.1056	0.0064	-0.8732	0.0071			-0.9787	0.0018				
	6554.8	52	0.1269	0.0042	-0.8512	0.0043			-0.9781	0.0008				
	6880.4	9	0.1537	0.0085	-0.8222	0.0085			-0.9758	0.0030				
<i>y</i>	5842.9	14	-0.0167	0.0081	-0.9660	0.0089			-0.9493	0.0020				
	6209.3	53	-0.0163	0.0054	-0.9650	0.0055			-0.9487	0.0010				
	6554.8	52	0.0029	0.0036	-0.9455	0.0036			-0.9484	0.0011				
	6880.4	9	0.0297	0.0072	-0.9197	0.0068			-0.9493	0.0022				
HD131156 <i>b</i>	5839.4	28	-0.1495	0.0029	-1.4776	0.0031			-1.3280	0.0033				
	6204.6	43	-0.1481	0.0019	-1.4775	0.0030	-1.2536	0.0022	-1.3295	0.0020	-1.1085	0.0007	0.2209	0.0020
	6553.1	33	-0.1540	0.0031	-1.4715	0.0052	-1.2563	0.0026	-1.3175	0.0048	-1.1024	0.0011	0.2151	0.0047
	6942.6	35	-0.1572	0.0028	-1.4723	0.0024	-1.2593	0.0029	-1.3151	0.0017	-1.1021	0.0007	0.2130	0.0017
<i>y</i>	5839.4	28	-0.0535	0.0024	-1.4534	0.0029			-1.3999	0.0030				
	6204.6	43	-0.0523	0.0017	-1.4528	0.0026	-1.1679	0.0017	-1.4006	0.0018	-1.1157	0.0005	0.2849	0.0018
	6553.1	33	-0.0571	0.0028	-1.4489	0.0044	-1.1688	0.0024	-1.3918	0.0042	-1.1118	0.0010	0.2800	0.0041
	6942.6	35	-0.0606	0.0025	-1.4477	0.0022	-1.1707	0.0024	-1.3871	0.0018	-1.1101	0.0007	0.2771	0.0016
HD143761 <i>b</i>	5838.8	22	0.4170	0.0011	-0.4057	0.0010			-0.8228	0.0010				
	6193.7	18	0.4158	0.0010	-0.4072	0.0012			-0.8230	0.0013				
	6552.5	18	0.4160	0.0011	-0.4055	0.0011			-0.8215	0.0016				
	6942.8	20	0.4151	0.0011	-0.4051	0.0008			-0.8202	0.0006				
<i>y</i>	5838.8	22	0.6161	0.0013	-0.1589	0.0024			-0.7749	0.0019				
	6193.7	18	0.6157	0.0007	-0.1598	0.0008			-0.7755	0.0010				
	6552.5	18	0.6135	0.0013	-0.1590	0.0010			-0.7724	0.0015				
	6942.8	20	0.6136	0.0007	-0.1591	0.0012			-0.7727	0.0010				
HD149661/ HD152391 <i>b</i>	5841.3	18	-1.2144	0.0025	-0.8143	0.0041	-0.2050	0.0041	0.4000	0.0025	1.0093	0.0030	0.6093	0.0021
	6223.4	26	-1.2166	0.0029	-0.8103	0.0039	-0.2098	0.0031	0.4062	0.0023	1.0068	0.0027	0.6005	0.0033
	6611.5	20	-1.2231	0.0021	-0.8360	0.0034	-0.2132	0.0044	0.3871	0.0035	1.0099	0.0039	0.6228	0.0044
	6965.4	20	-1.2115	0.0022	-0.8299	0.0041	-0.2061	0.0038	0.3816	0.0046	1.0053	0.0042	0.6237	0.0064
<i>y</i>	5841.3	18	-0.9408	0.0023	-0.8519	0.0029	-0.5031	0.0047	0.0889	0.0018	0.4377	0.0040	0.3488	0.0036
	6223.4	26	-0.9428	0.0027	-0.8493	0.0033	-0.5067	0.0030	0.0935	0.0024	0.4361	0.0021	0.3427	0.0028
	6611.5	20	-0.9501	0.0023	-0.8729	0.0036	-0.5123	0.0034	0.0772	0.0031	0.4378	0.0027	0.3606	0.0038
	6965.4	20	-0.9400	0.0017	-0.8675	0.0031	-0.5013	0.0025	0.0725	0.0035	0.4357	0.0024	0.3631	0.0045

TABLE 3. Summary of Annual Mean Differential Magnitudes (continued)

Group	Mean JD	n	1 2		1 3		1 4		2 3		2 1		3 4	
			$\Delta m$ (mag)	s.d. (mag)	$\Delta m$ (mag)	s.d. (mag)	$\Delta m$ (mag)	s.d. (mag)	$\Delta m$ (mag)	s.d. (mag)	$\Delta m$ (mag)	s.d. (mag)	$\Delta m$ (mag)	s.d. (mag)
HD157856/ HD158624 b	5850.7	14	-0.2534	0.0027	1.0130	0.0030	0.0542	0.0030	1.2663	0.0027	0.3076	0.0026	-0.9588	0.0015
	6228.1	14	-0.2569	0.0018	1.0101	0.0027	0.0501	0.0023	1.2670	0.0022	0.3069	0.0021	-0.9600	0.0020
	6592.1	12	-0.2504	0.0017	1.0093	0.0023	0.0550	0.0021	1.2597	0.0023	0.3054	0.0014	-0.9543	0.0030
	6965.0	18	-0.2555	0.0015	1.0070	0.0011	0.0513	0.0010	1.2626	0.0016	0.3068	0.0015	-0.9557	0.0011
y	5850.7	14	-0.2227	0.0015	1.1400	0.0014	0.1625	0.0023	1.3627	0.0016	0.3852	0.0016	-0.9775	0.0022
	6228.1	14	-0.2239	0.0017	1.1385	0.0014	0.1614	0.0012	1.3624	0.0014	0.3853	0.0015	-0.9771	0.0012
	6592.1	12	-0.2235	0.0014	1.1337	0.0026	0.1608	0.0023	1.3572	0.0017	0.3843	0.0020	-0.9729	0.0022
	6965.0	18	-0.2234	0.0018	1.1337	0.0016	0.1607	0.0013	1.3571	0.0016	0.3841	0.0013	-0.9730	0.0013
HD160346 b	5838.5	14	-0.4847	0.0033	-0.5390	0.0014			-0.0542	0.0030				
	6232.1	23	-0.4877	0.0029	-0.5379	0.0022			-0.0502	0.0029				
	6602.5	21	-0.4857	0.0019	-0.5415	0.0015			-0.0558	0.0025				
	6966.5	14	-0.4833	0.0022	-0.5403	0.0018			-0.0569	0.0026				
y	5838.5	14	-0.1022	0.0023	-0.4831	0.0009			-0.3809	0.0026				
	6232.1	23	-0.1055	0.0021	-0.4829	0.0017			-0.3773	0.0017				
	6602.5	21	-0.1043	0.0015	-0.4873	0.0015			-0.3831	0.0023				
	6966.5	14	-0.1031	0.0018	-0.4856	0.0015			-0.3826	0.0026				
HD161239 b	5880.5	21	0.4254	0.0034	-0.0998	0.0023			-0.5253	0.0049				
	6228.5	30	0.4258	0.0025	-0.0984	0.0013	-0.9286	0.0011	-0.5242	0.0024	-1.3544	0.0028	-0.8302	0.0015
	6612.3	21	0.4283	0.0023	-0.0944	0.0019	-0.9257	0.0010	-0.5226	0.0024	-1.3540	0.0025	-0.8313	0.0022
	6958.5	12	0.4201	0.0026	-0.0983	0.0018	-0.9244	0.0007	-0.5183	0.0025	-1.3444	0.0028	-0.8261	0.0020
y	5880.5	21	0.6863	0.0021	0.0472	0.0022			-0.6371	0.0034				
	6228.5	30	0.6864	0.0025	0.0487	0.0012	-1.0008	0.0008	-0.6377	0.0022	-1.6872	0.0027	-1.0495	0.0013
	6612.3	21	0.6882	0.0019	0.0520	0.0017	-0.9993	0.0008	-0.6361	0.0021	-1.6875	0.0019	-1.0514	0.0016
	6958.5	12	0.6818	0.0023	0.0487	0.0021	-0.9983	0.0018	-0.6331	0.0021	-1.6801	0.0022	-1.0469	0.0023
HD176095 b	5909.8	22	0.3733	0.0021	-1.0250	0.0042			-1.3583	0.0040				
	6253.1	31	0.3720	0.0011	-1.0284	0.0038			-1.4004	0.0037				
	6637.0	22	0.3714	0.0012	-1.0296	0.0045			-1.4011	0.0045				
	7005.7	23	0.3712	0.0008	-1.0276	0.0035			-1.3987	0.0038				
y	5909.8	22	0.6729	0.0016	-1.1346	0.0040			-1.8075	0.0033				
	6253.1	31	0.6708	0.0010	-1.1379	0.0031			-1.8088	0.0034				
	6637.0	22	0.6698	0.0012	-1.1385	0.0042			-1.8083	0.0039				
	7005.7	23	0.6704	0.0007	-1.1355	0.0038			-1.8059	0.0039				

TABLE 3. Summary of Annual Mean Differential Magnitudes (continued)

Group	Mean JD 2,440,000+	n	1-2		1-3		1-4		2-3		2-4		3-4	
			$\Delta m$ (mag)	s.d. (mag)	$\Delta m$ (mag)	s.d. (mag)	$\Delta m$ (mag)	s.d. (mag)	$\Delta m$ (mag)	s.d. (mag)	$\Delta m$ (mag)	s.d. (mag)	$\Delta m$ (mag)	s.d. (mag)
HD182572 b	5937.4	28	0.1731	0.0011	-0.8895	0.0010			-1.0626	0.0010				
	6249.9	21	0.1735	0.0011	-0.8866	0.0013			-1.0601	0.0012				
	6634.6	22	0.1713	0.0010	-0.8833	0.0010			-1.0546	0.0012				
	7004.9	25	0.1697	0.0009	-0.8843	0.0009			-1.0540	0.0009				
y	5937.4	28	-0.1477	0.0008	-0.8064	0.0008			-0.6587	0.0010				
	6249.9	21	-0.1471	0.0010	-0.8064	0.0012			-0.6593	0.0011				
	6634.6	22	-0.1464	0.0010	-0.8035	0.0010			-0.6572	0.0010				
	7004.9	25	-0.1467	0.0009	-0.8032	0.0009			-0.6565	0.0009				
HD185141 b	5939.7	30	-0.3465	0.0010	-0.1362	0.0012			0.2103	0.0012				
	6267.0	18	-0.3456	0.0011	-0.1371	0.0016			0.2085	0.0011				
	6641.9	14	-0.3399	0.0012	-0.1303	0.0016			0.2096	0.0018				
	7015.1	22	-0.3412	0.0016	-0.1267	0.0015			0.2146	0.0018				
y	5939.7	30	-0.1435	0.0019	0.1800	0.0013			0.3236	0.0018				
	6267.0	18	-0.1439	0.0013	0.1764	0.0017			0.3203	0.0017				
	6641.9	14	-0.1393	0.0010	0.1815	0.0011			0.3209	0.0012				
	7015.1	22	-0.1403	0.0011	0.1844	0.0014			0.3247	0.0021				
HD190007 b	5957.3	36	0.5971	0.0031	-0.1961	0.0029			-0.7932	0.0012				
	6269.2	37	0.5971	0.0014	-0.1925	0.0017			-0.7896	0.0012				
	6640.8	48	0.6049	0.0020	-0.1847	0.0020			-0.7897	0.0008				
	7020.6	58	0.5940	0.0027	-0.1955	0.0023			-0.7895	0.0010				
y	5957.3	36	0.7333	0.0030	-0.1598	0.0029			-0.8931	0.0014				
	6269.2	37	0.7334	0.0013	-0.1571	0.0013			-0.8905	0.0010				
	6640.8	48	0.7394	0.0018	-0.1510	0.0017			-0.8905	0.0011				
	7020.6	58	0.7298	0.0024	-0.1607	0.0022			-0.8904	0.0008				
HD201091/ HD201092 b	5957.3	39	-1.3740	0.0013	-0.9719	0.0012	-0.8130	0.0013	0.4021	0.0010	0.5609	0.0008	0.1588	0.0008
	6301.8	34	-1.3759	0.0008	-0.9733	0.0016	-0.8137	0.0011	0.4026	0.0014	0.5621	0.0012	0.1596	0.0010
	6657.6	28	-1.3708	0.0008	-0.9667	0.0011	-0.8095	0.0010	0.4041	0.0008	0.5613	0.0008	0.1572	0.0011
	7038.3	39	-1.3723	0.0012	-0.9697	0.0010	-0.8127	0.0010	0.4025	0.0007	0.5596	0.0008	0.1571	0.0007
y	5957.3	39	-1.5815	0.0012	-0.8220	0.0012	-0.9110	0.0011	0.7595	0.0010	0.6705	0.0011	-0.0890	0.0011
	6301.8	34	-1.5846	0.0012	-0.8225	0.0010	-0.9127	0.0011	0.7620	0.0007	0.6718	0.0010	-0.0902	0.0008
	6657.6	28	-1.5806	0.0008	-0.8201	0.0008	-0.9104	0.0008	0.7605	0.0010	0.6702	0.0008	-0.0903	0.0008
	7038.3	39	-1.5817	0.0008	-0.8212	0.0008	-0.9127	0.0008	0.7605	0.0006	0.6690	0.0006	-0.0915	0.0006

TABLE 3. Summary of Annual Mean Differential Magnitudes (continued)

Group	Mean JD 2 440,000+	n	1 2		1 3		1 4		2 3		2 4		3 4	
			$\Delta m$ (mag)	s.d. (mag)	$\Delta m$ (mag)	s.d. (mag)	$\Delta m$ (mag)	s.d. (mag)	$\Delta m$ (mag)	s.d. (mag)	$\Delta m$ (mag)	s.d. (mag)	$\Delta m$ (mag)	s.d. (mag)
HD215704 <i>b</i>	5978.8	34	0.2628	0.0043	0.0376	0.0010			-0.2252	0.0044				
	6342.2	72	0.2275	0.0025	0.0399	0.0007			-0.1876	0.0024				
	6643.3	73	0.2487	0.0029	0.0401	0.0007			-0.2086	0.0029				
	7062.0	44	0.2623	0.0034	0.0401	0.0009			-0.2222	0.0033				
<i>y</i>	5978.8	34	0.8614	0.0036	-0.0683	0.0012			-0.9297	0.0038				
	6342.2	72	0.8355	0.0023	-0.0666	0.0010			-0.9021	0.0023				
	6643.3	73	0.8532	0.0024	-0.0657	0.0007			-0.9189	0.0024				
	7062.0	44	0.8629	0.0029	-0.0659	0.0011			-0.9288	0.0031				
HD216385 <i>b</i>	5989.9	26	-1.2662	0.0010	-0.4791	0.0015			0.7871	0.0012				
	6337.4	33	-1.2674	0.0010	-0.4796	0.0008			0.7878	0.0007				
	6658.2	22	-1.2628	0.0010	-0.4763	0.0010			0.7865	0.0010				
	7074.6	36	-1.2626	0.0009	-0.4764	0.0006			0.7862	0.0009				
<i>y</i>	5989.9	26	-1.3903	0.0011	-0.6101	0.0010			0.7802	0.0012				
	6337.4	33	-1.3906	0.0010	-0.6110	0.0010			0.7796	0.0010				
	6658.2	22	-1.3877	0.0012	-0.6079	0.0015			0.7798	0.0024				
	7074.6	36	-1.3871	0.0007	-0.6088	0.0007			0.7783	0.0008				



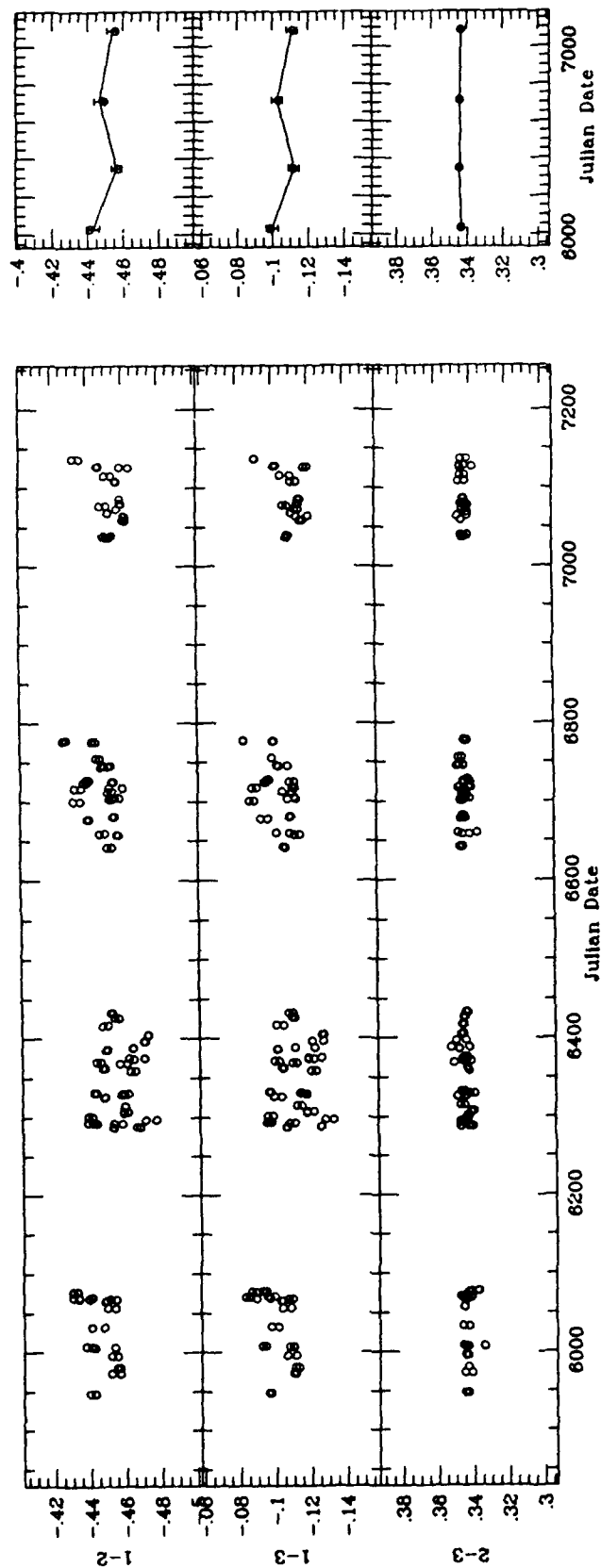


Figure 4.1. Light curves of the HD1835 group, compressed scale,  $b$  and  $y$  averaged. (left) - individual data points,  $b$  and  $y$  averaged. (right) - seasonal mean magnitudes (connected by solid lines), and medians (solid dots). Error bars denote 95% confidence intervals. Star 1 = HD1835 (G2V) is strongly variable and has an observed photometric rotation period of 7.7 days (Table 6).

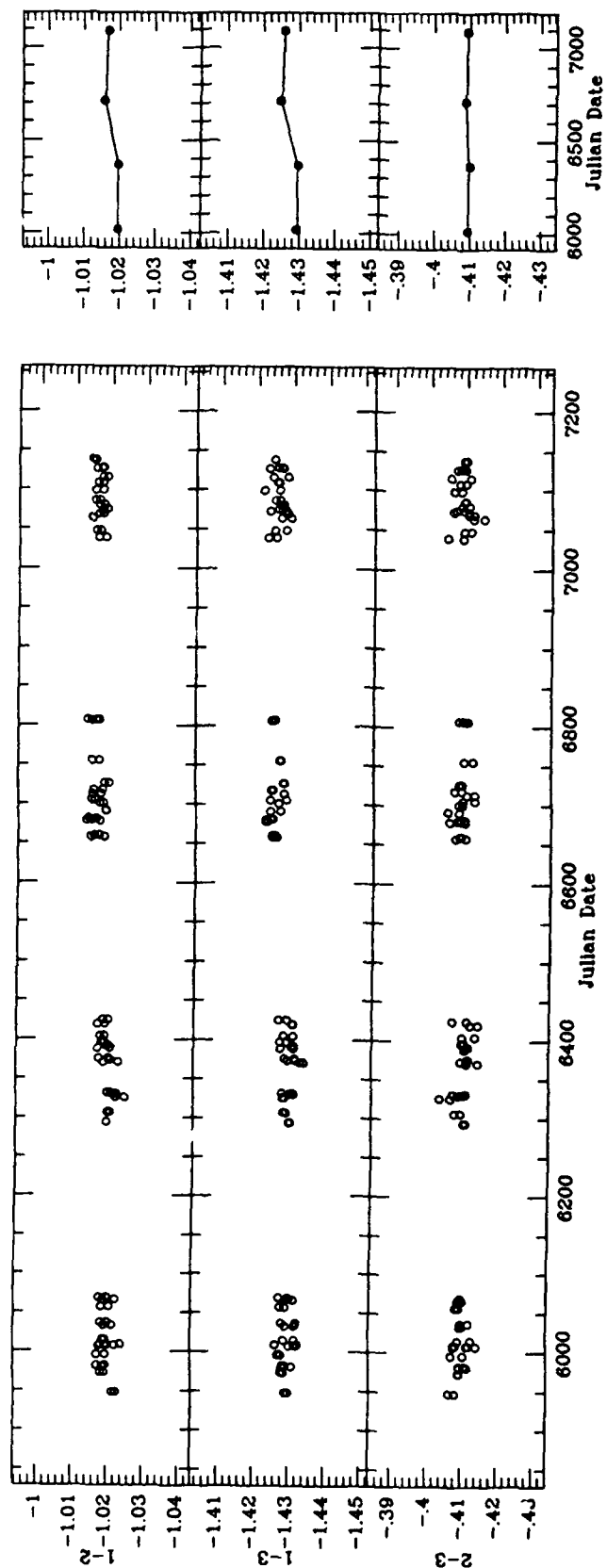


Figure 4.2. Light curves of the HD10476 group. Star 1 = HD10476 (K1V) is variable from year to year, but all three stars are unusually stable each season. The range of star 1—star 3 is only 0.0009 mag in four seasons.

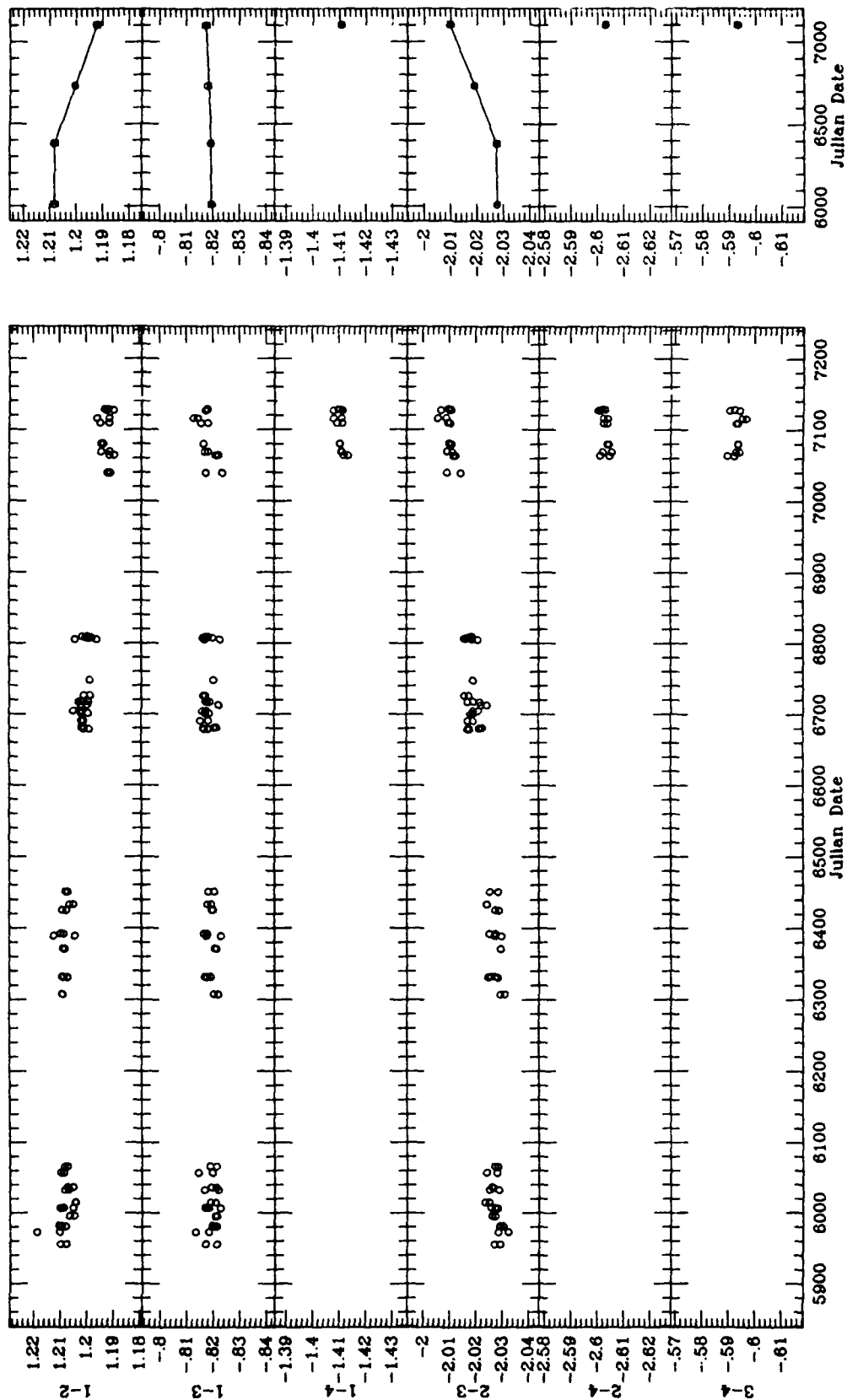


Figure 4.3. Light curves of the HD13421 group. Star 2 = HD13611 (G6II-III), an MK standard star, is strongly variable from year to year.

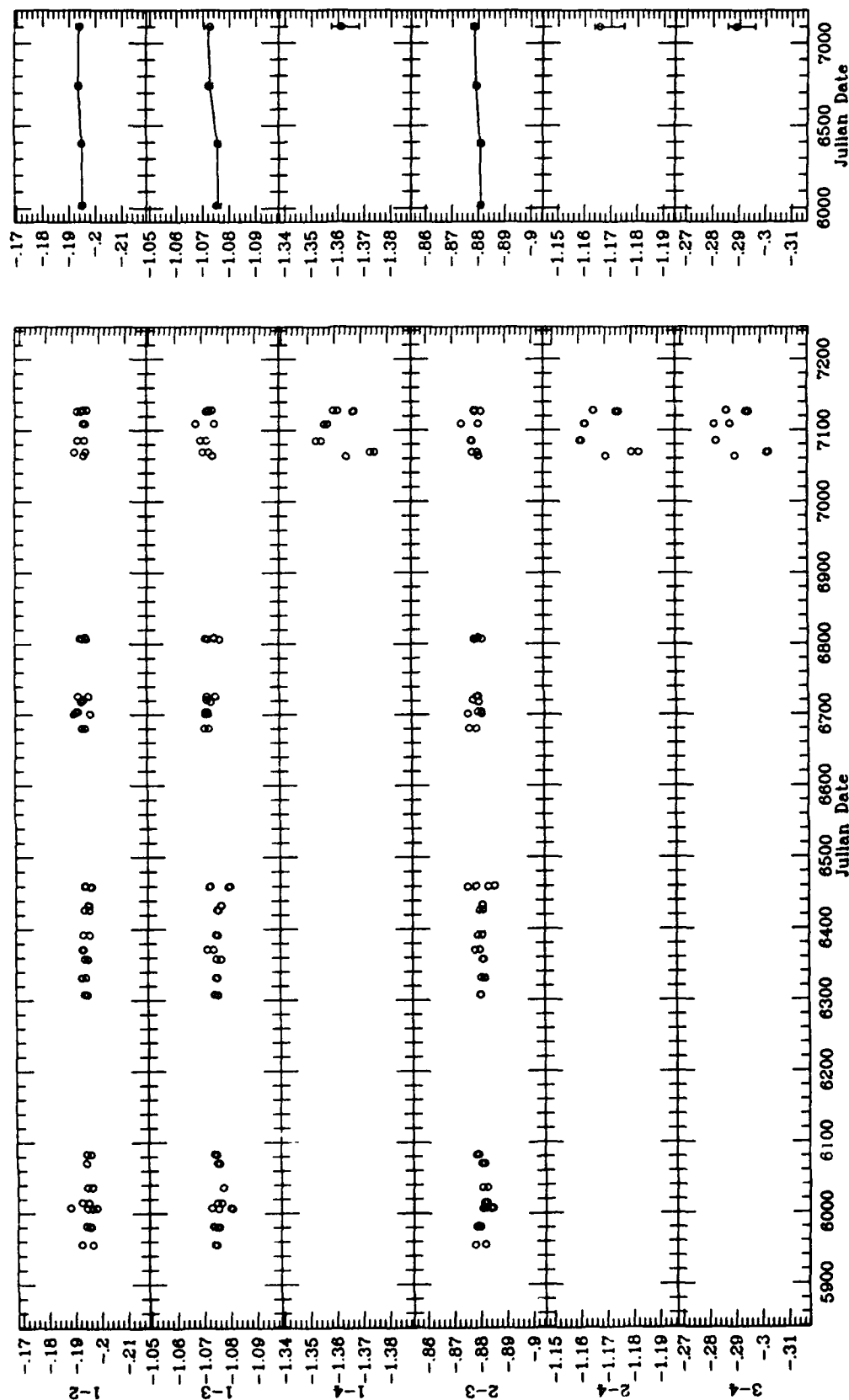


Figure 4.4. Light curves of the HD18256 group. This group is exceptionally quiescent, but star 3 = HD17659 (F8) may vary slightly from year to year.

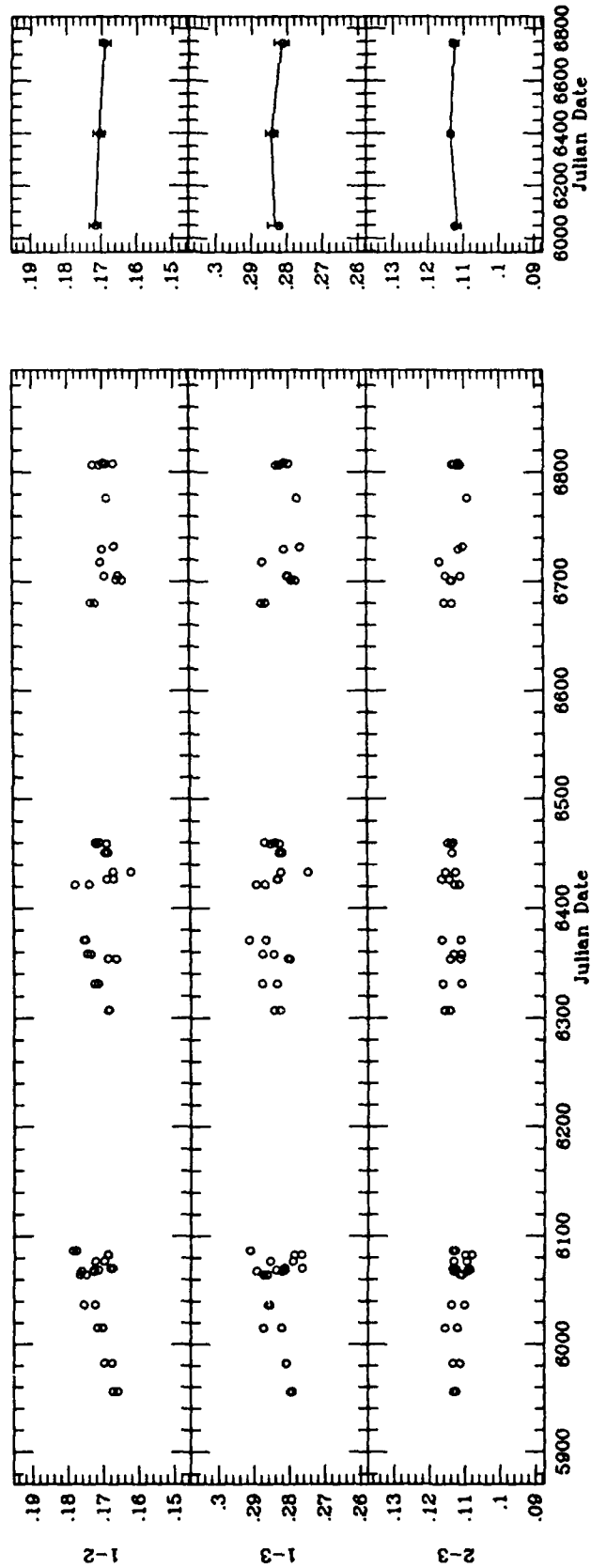


Figure 4.5. Light curves of the HD23140 group. Star 1 = HD23140 (K2) varied in two seasons, but none of the stars showed long-term variability.

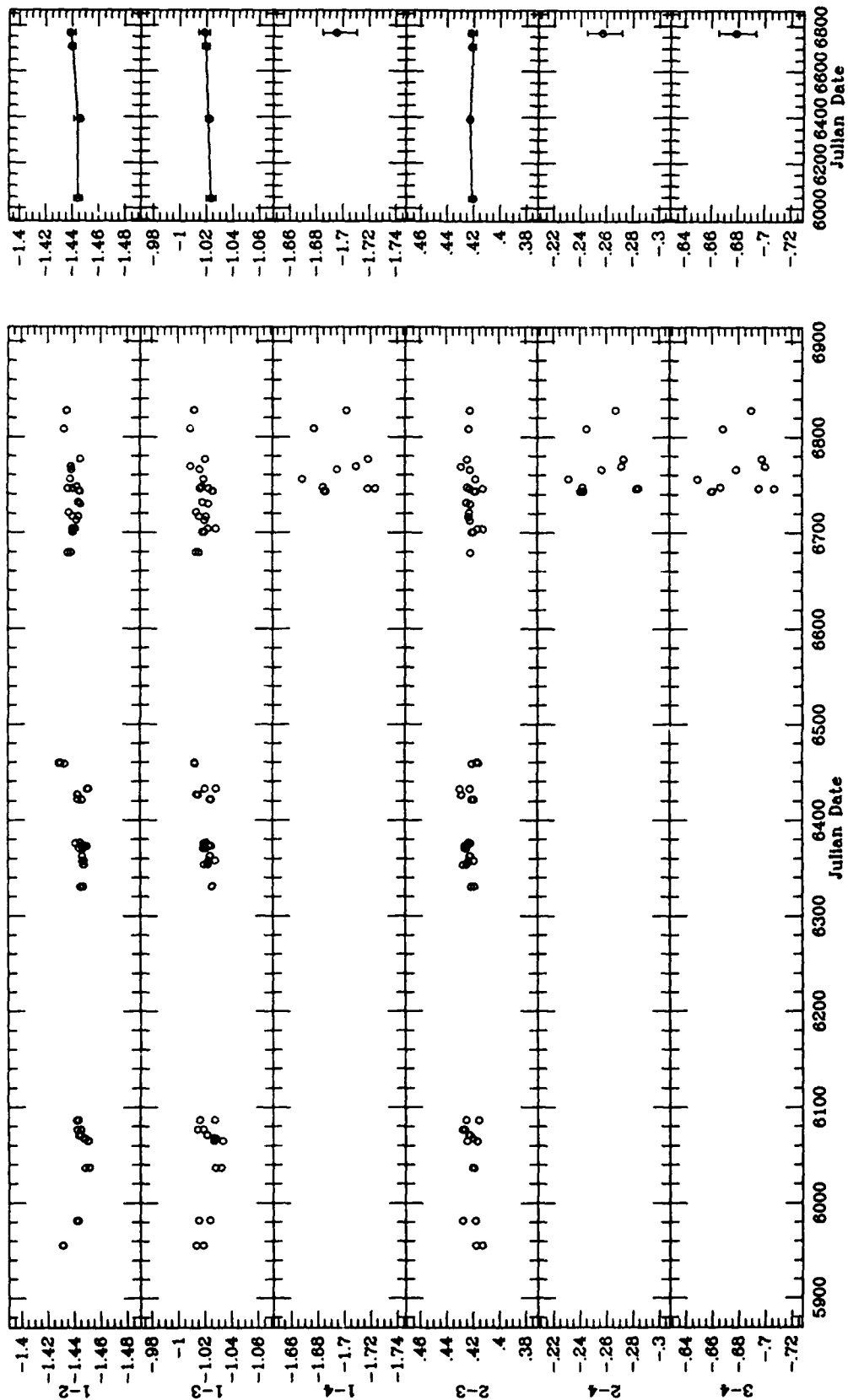


Figure 4.6. Light curves of the HD25998 group, compressed scale. Star 1 = HD25998 (F7V), a member of the Hyades group, varied slightly in the first two seasons. Comparison stars 2 and 3 are slightly noisy. Star 4 = HD25893 = V491 Persei (K1V) shares a common proper motion with HD25998 and is photometrically active.

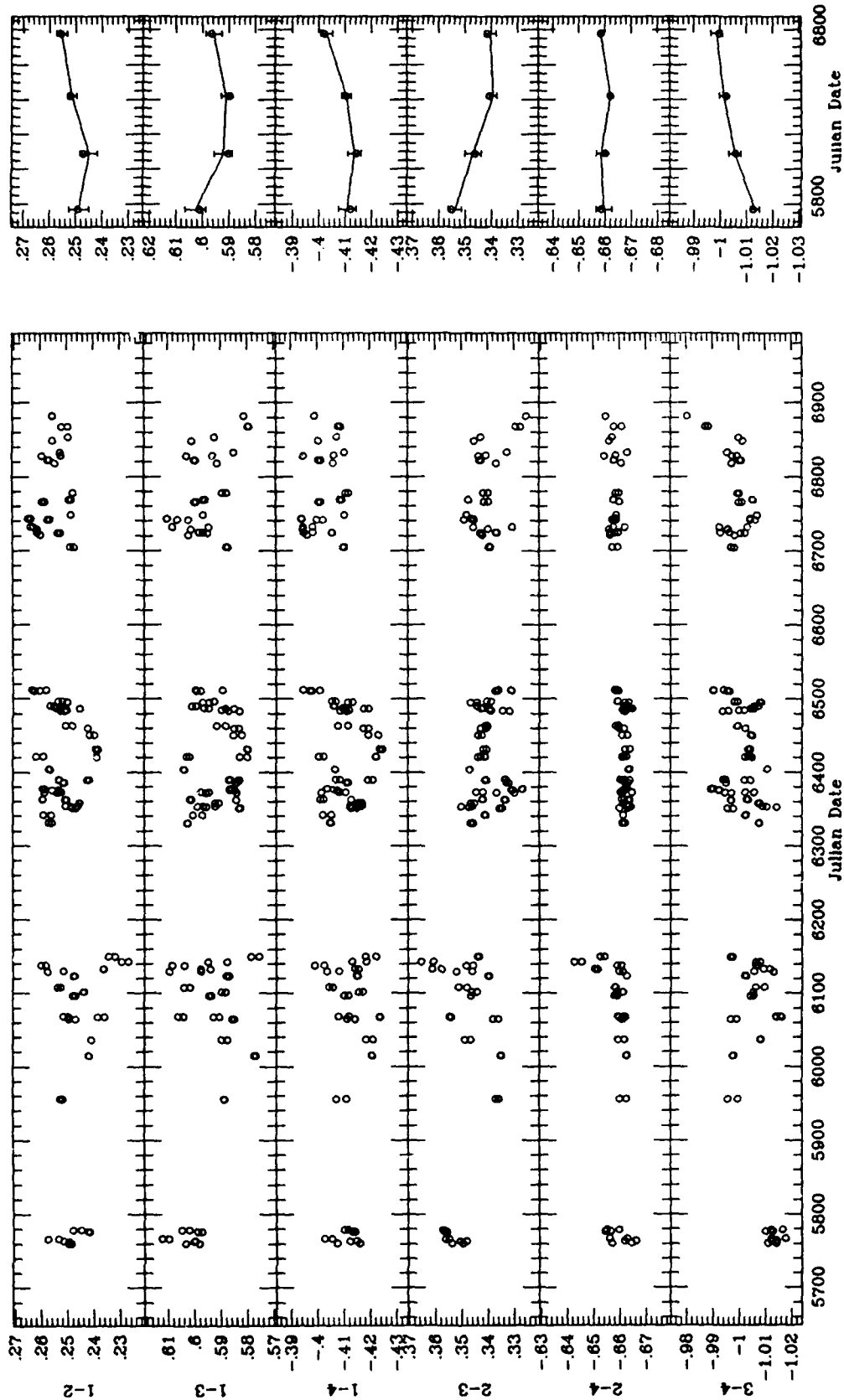


Figure 4.7. Light curves of the HD35296/HD39587 group. Star 1 = HD35296 (F8V) and star 3 = HD39587 (G0V) were variable each year and varied strongly from year to year as well. We find photometric rotation periods of 2.3 and 4.9 days, respectively, the latter in good agreement with the HK period. One or both of the comparison stars appeared to vary slightly during two seasons and from year to year. Note the variation of star 2 just at the end of the second season.

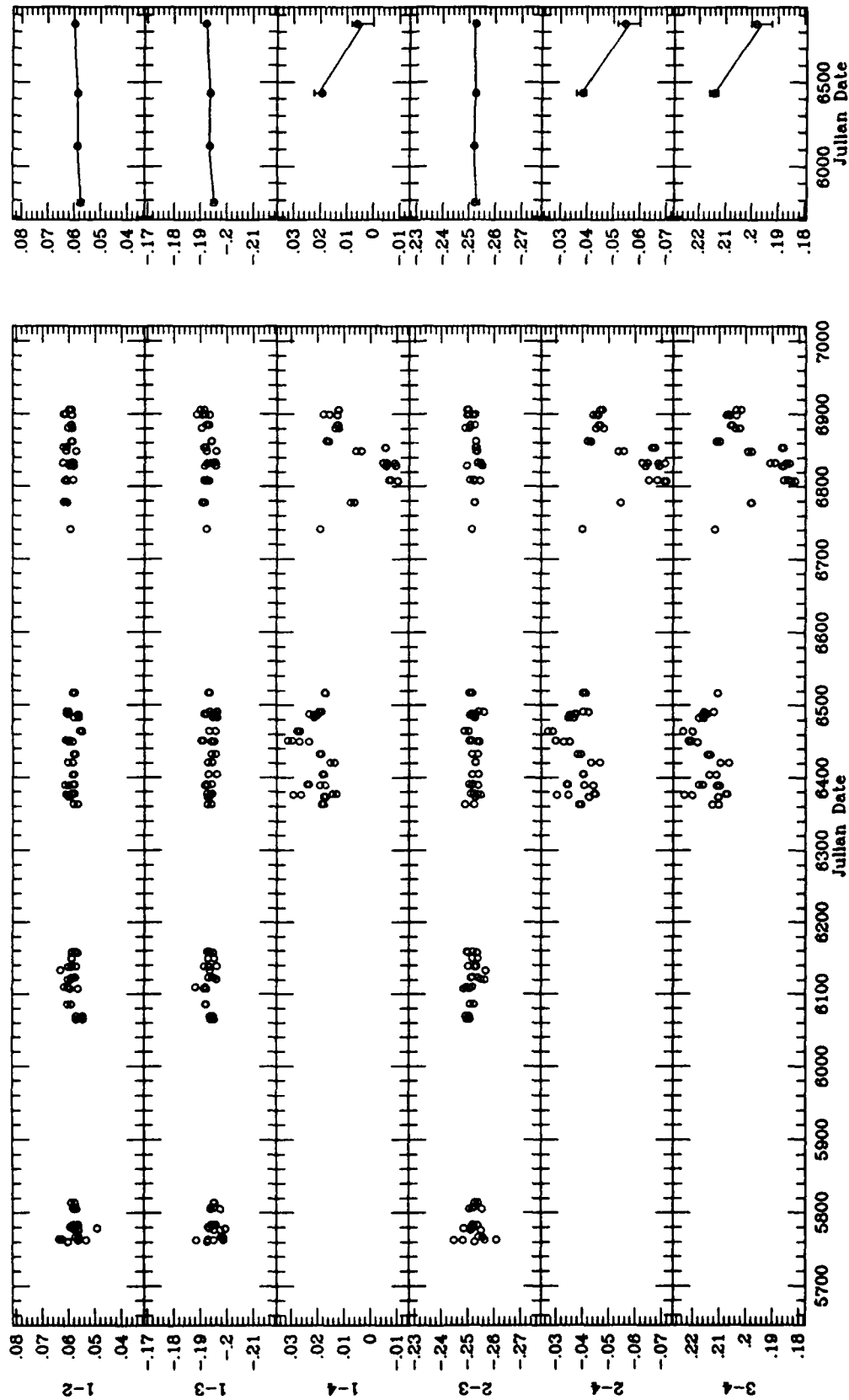


Figure 4.8. Light curves of the HD76572/HD75332 group. All three of the original trio pairs are very stable, with the four-season range of star 2—star 3, 0.0007 mag, the smallest observed. Star 2 = HD73596 (F5III) may vary slightly on short time scales. Star 4 = HD75332 (F7Vn) is very active.



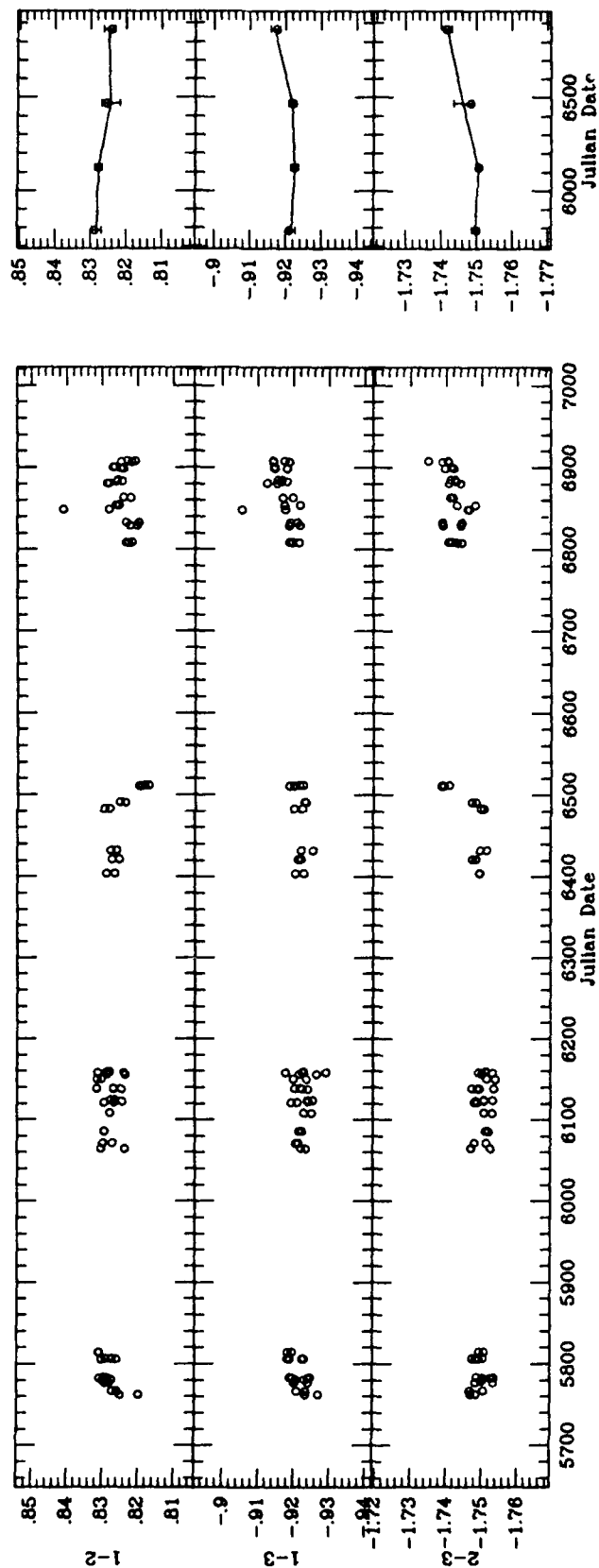


Figure 4.9. Light curves of the HD81809 group. Comparison star 3 = HD82074 (G6IV) varied strongly from year to year. Star 1 = HD81809 (G2V) may fluctuate slightly.

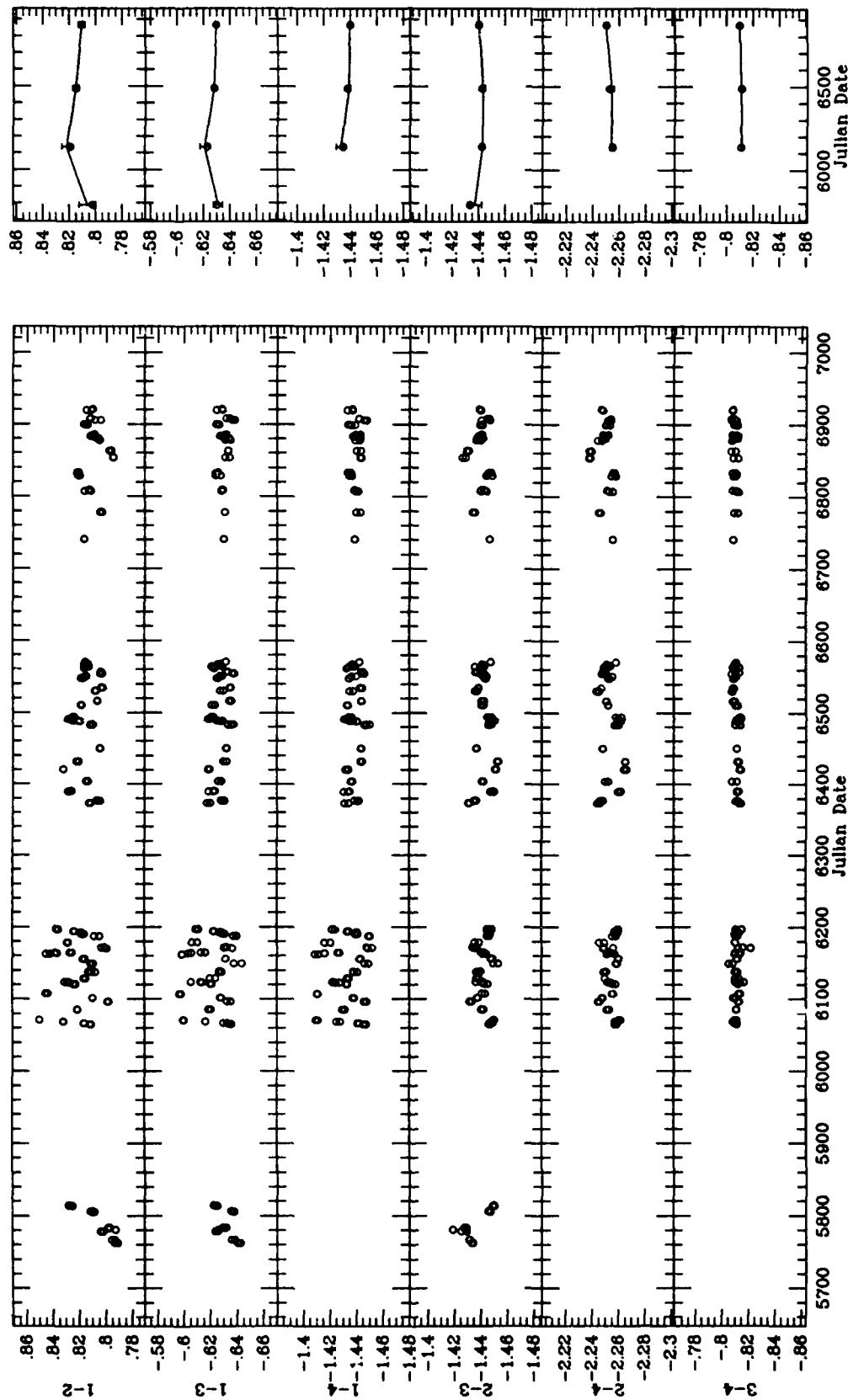
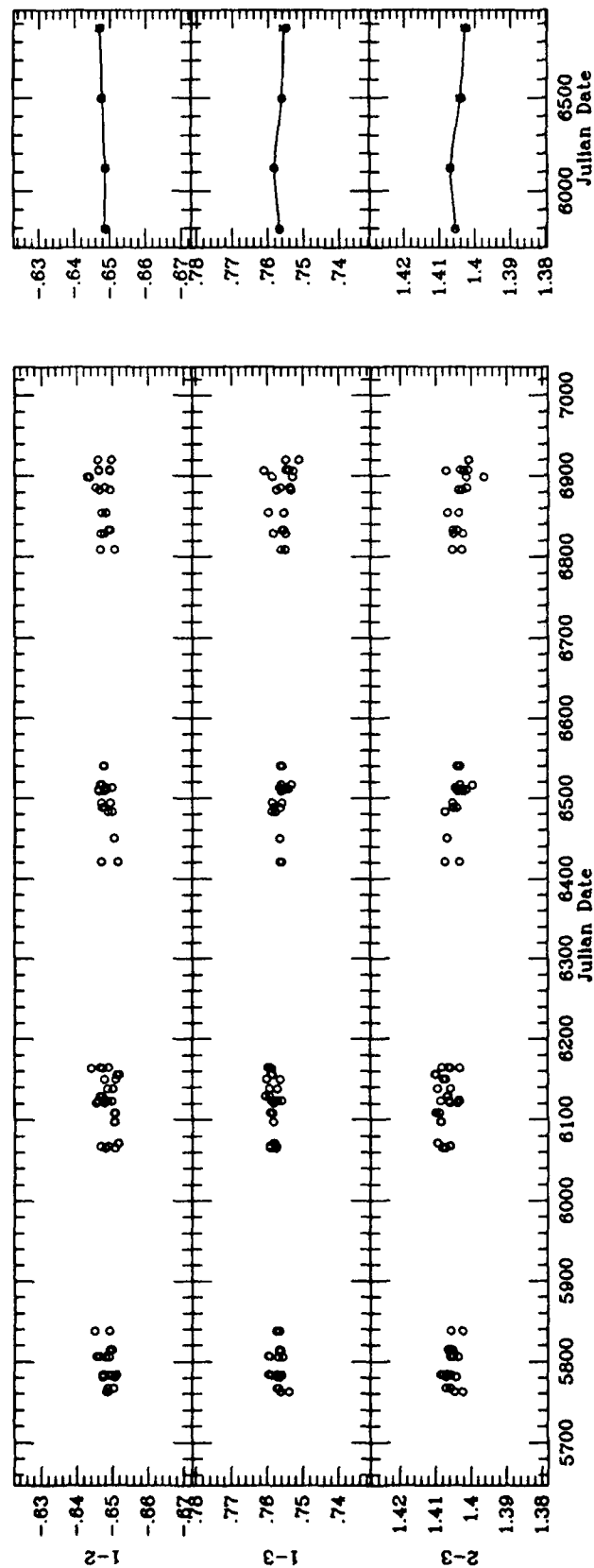


Figure 4.10. Light curves of the HD82885/HD82635 group, compressed scale. This group was expanded into a quartet because of the large dispersions in all of the original trio differential magnitudes. In the second season, star 1 = HD82885 (G8IV-V), a *wavy* standard star, exhibited a rotational light curve with a period of 18.0 days and an amplitude of 0.03 mag. The same year, star 2 = HD82635 (G8.5III), also a *wavy* standard, displayed a rotational light curve with a period of 40.4 days and an amplitude of 0.01 mag. Both stars vary strongly from year to year, but the large-amplitude light curve of star 1 disappeared in the following two seasons. Comparison stars 3 and 4 are quiescent.



**Figure 4.11.** Light curves of the HD103095 group. Star 3 = HD101606 (F4V), a *uvby* standard, may be slightly variable, long term, but this group is essentially quiescent.

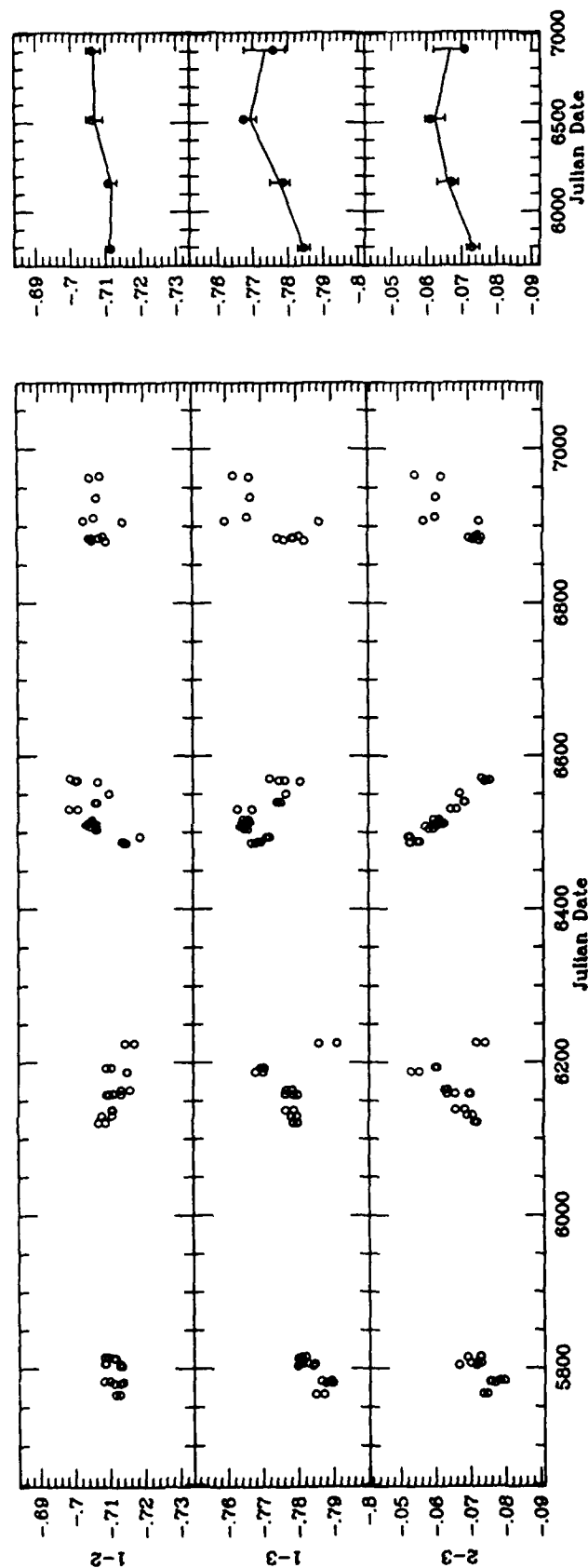
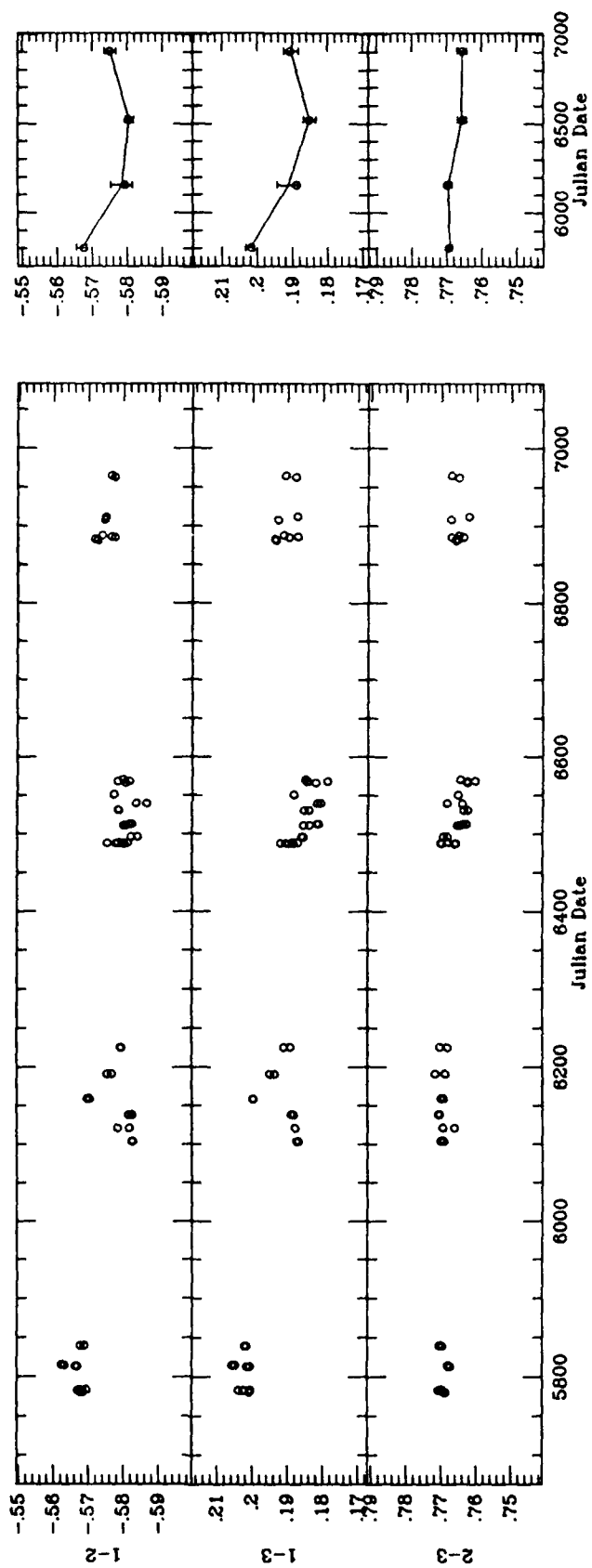
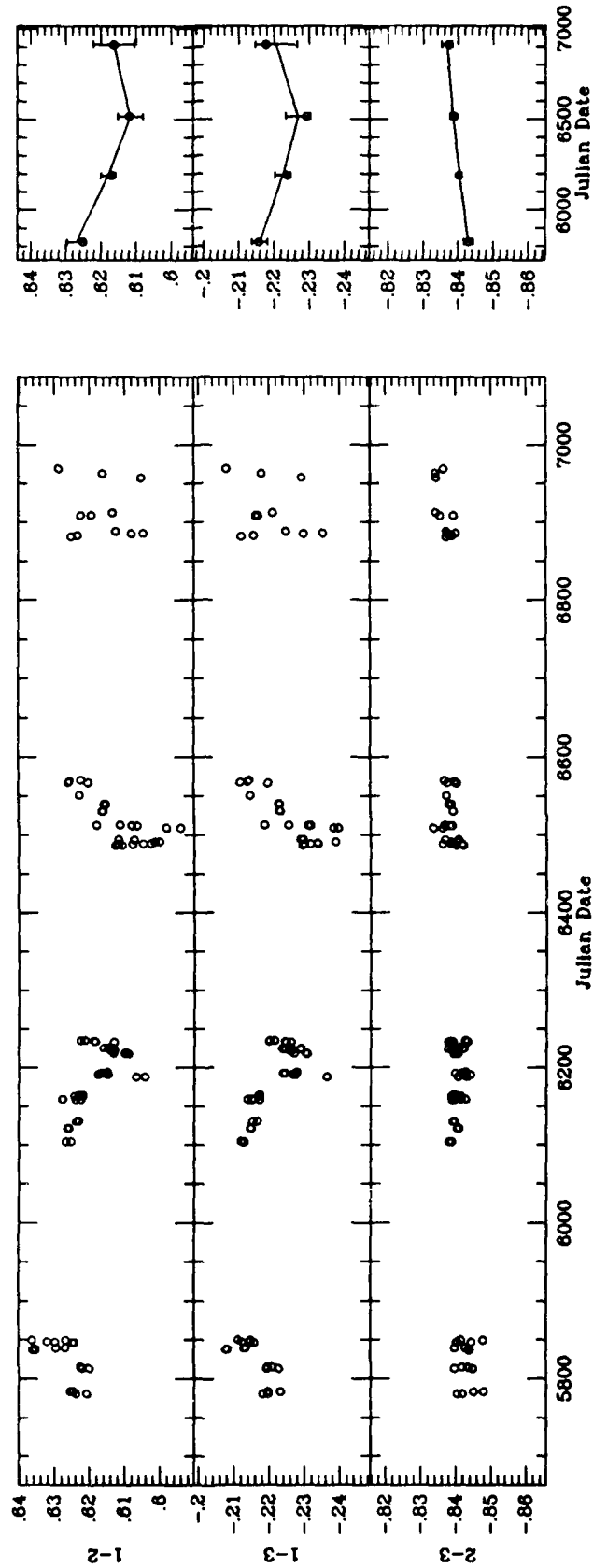


Figure 4.12. Light curves of the HD114710 group. Star 3 = HD112980 (G9III) is consistently and strongly variable.



**Figure 4.13.** Light curves of the HD115383/HD117176 group. Star 1 = HD115383 (G0Vs), a *unby* and MK standard star, varies strongly from year to year.



**Figure 4.14.** Light curves of the HD115404 group. Star 1 = HD115404 (K1V + M1V) varies strongly. The derived photometric rotation period of 11.0 days is probably spurious: it is not in accord with the well-determined HK period of 18.8 days. Star 2—star 3, though quiescent, vary from year to year.

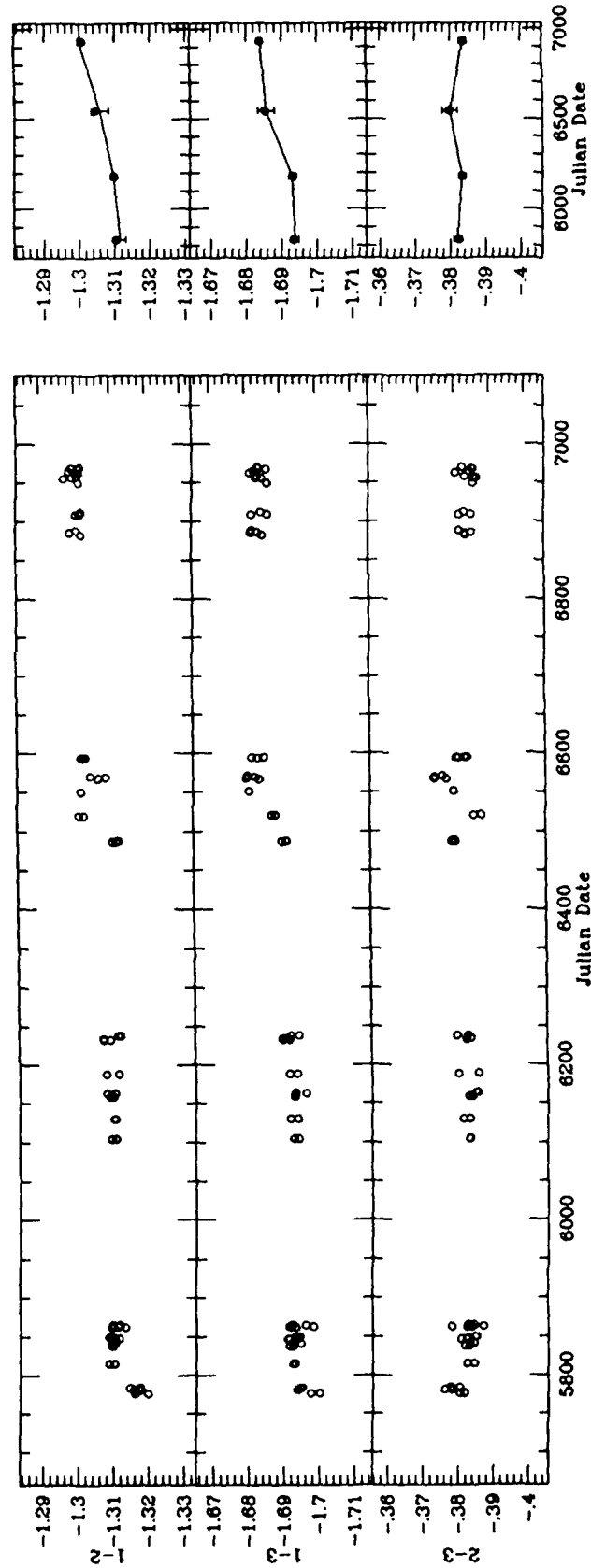


**Figure 4.15.** Light curves of the HD120136 group. Star 1 = HD120136 (F6IV) seems to vary strongly from year to year but neither of the comparison stars is particularly stable.

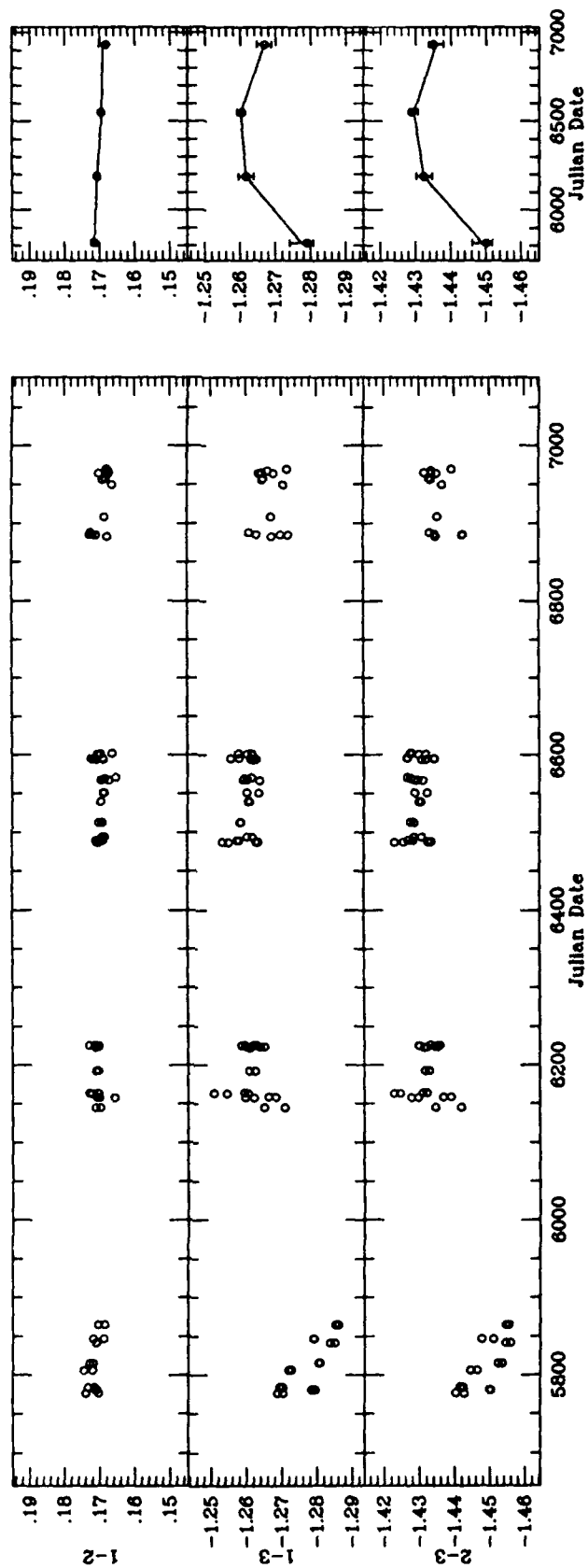


Figure 4.16. Light curves of the HD126246 (F8V + G1V) varies strongly with a range of nearly 0.02 mag.



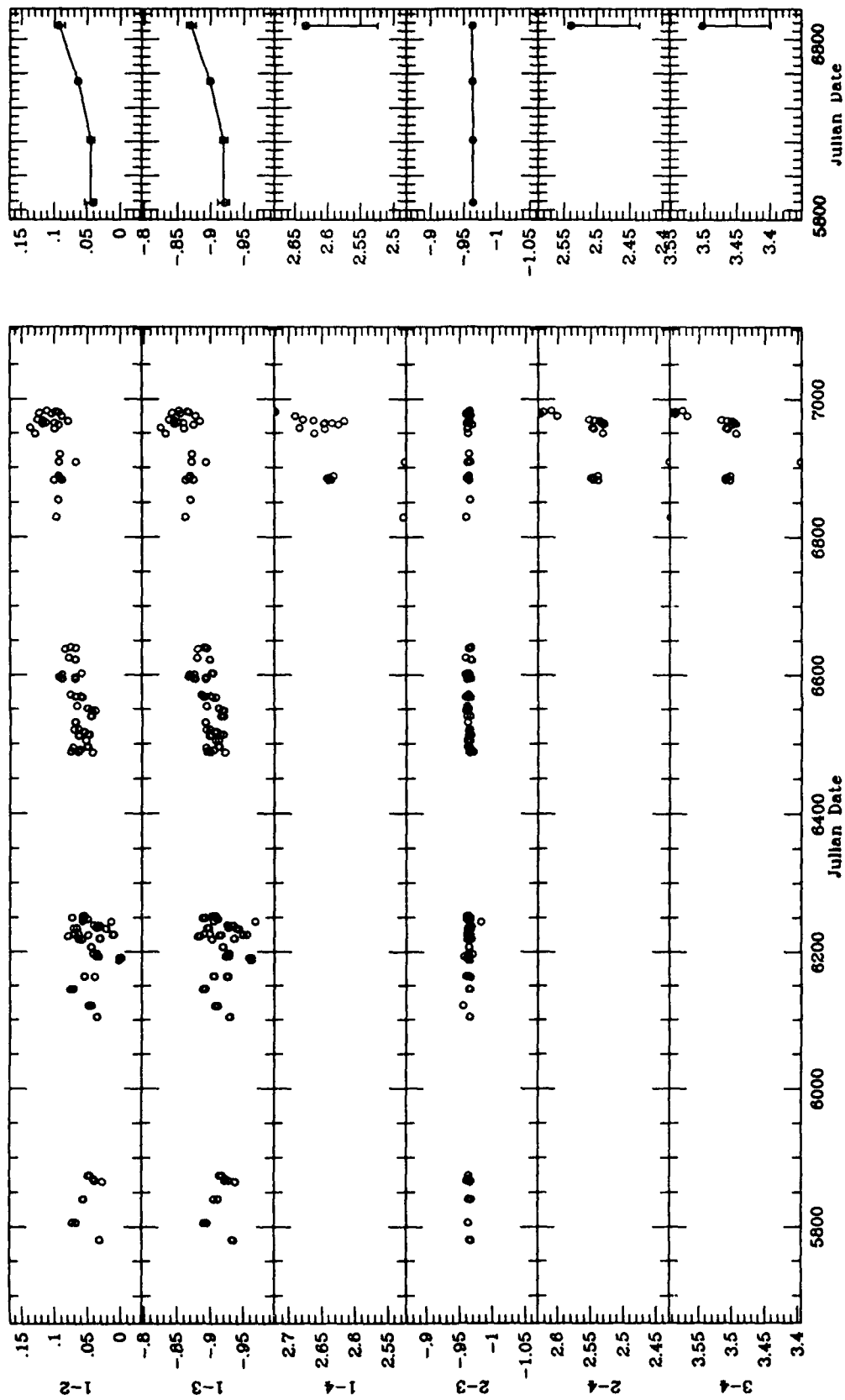


Figure 4.17. Light curves of the HD129333 group, compressed scale. Star 1 = HD129333 (G0) has the largest  $\log R'_{HK}$  value on our program and the greatest range of variability (0.05 mag). Its photometric rotation period in two seasons was 2.7 and 2.0 days.

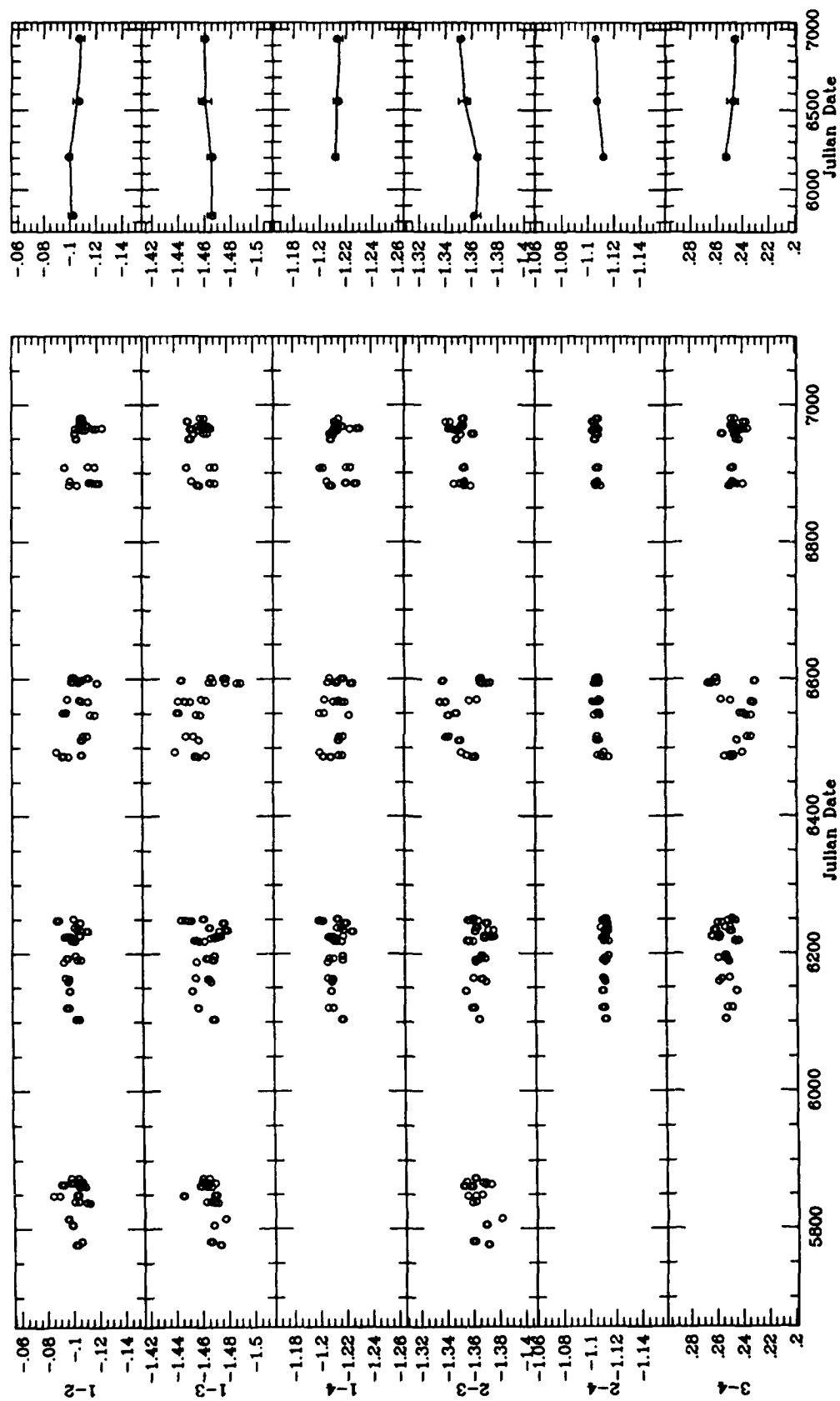


Figure 4.18. Light curves of the HD131156 group, compressed scale. Star 1 = HD131156 (G8V + K4V) and star 3 = HD131511 (K2V) are consistently variable each year, but the long-term light curves are confused, with only star 2 = HD129972 (G8.5III) showing a clear signal thus far.

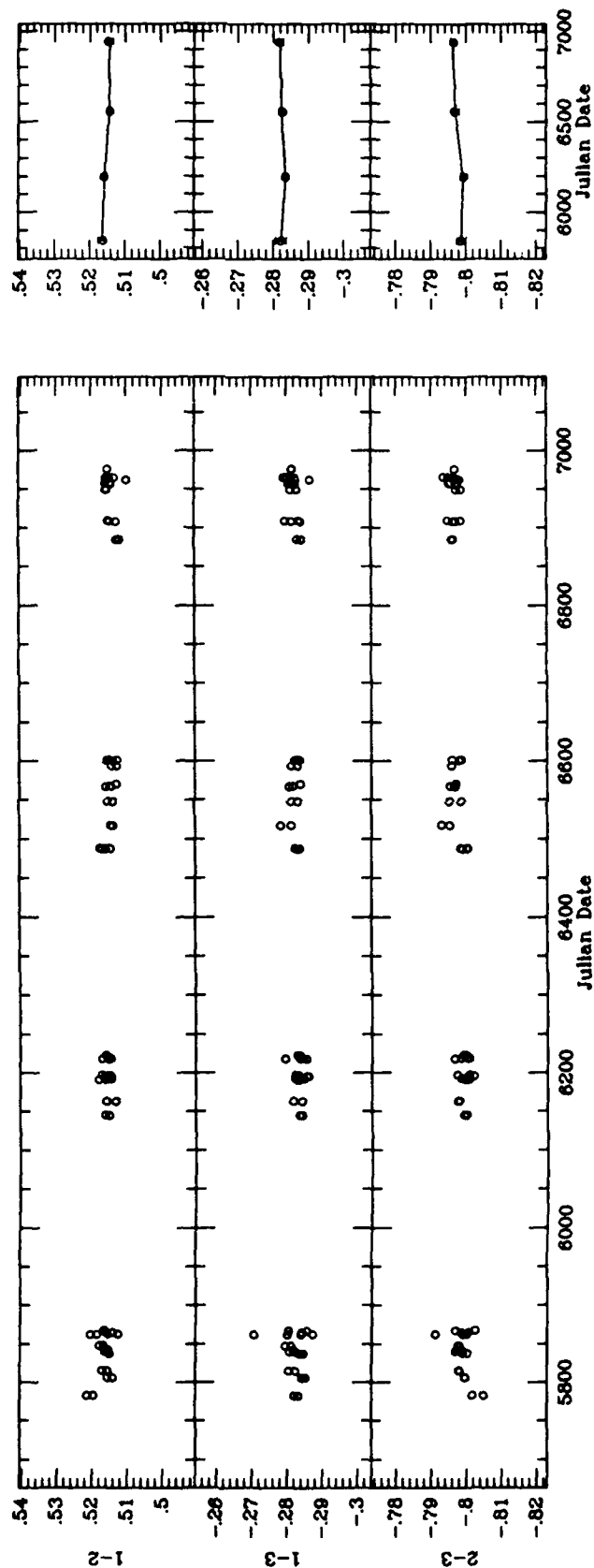


Figure 4.19. Light curves of the HD143761 group. Star 1 = HD143761 (G0+Va), a *wby*, MK, and HK standard is exceptionally stable. Star 3 = HD140716 (gG:9) may fluctuate slightly.

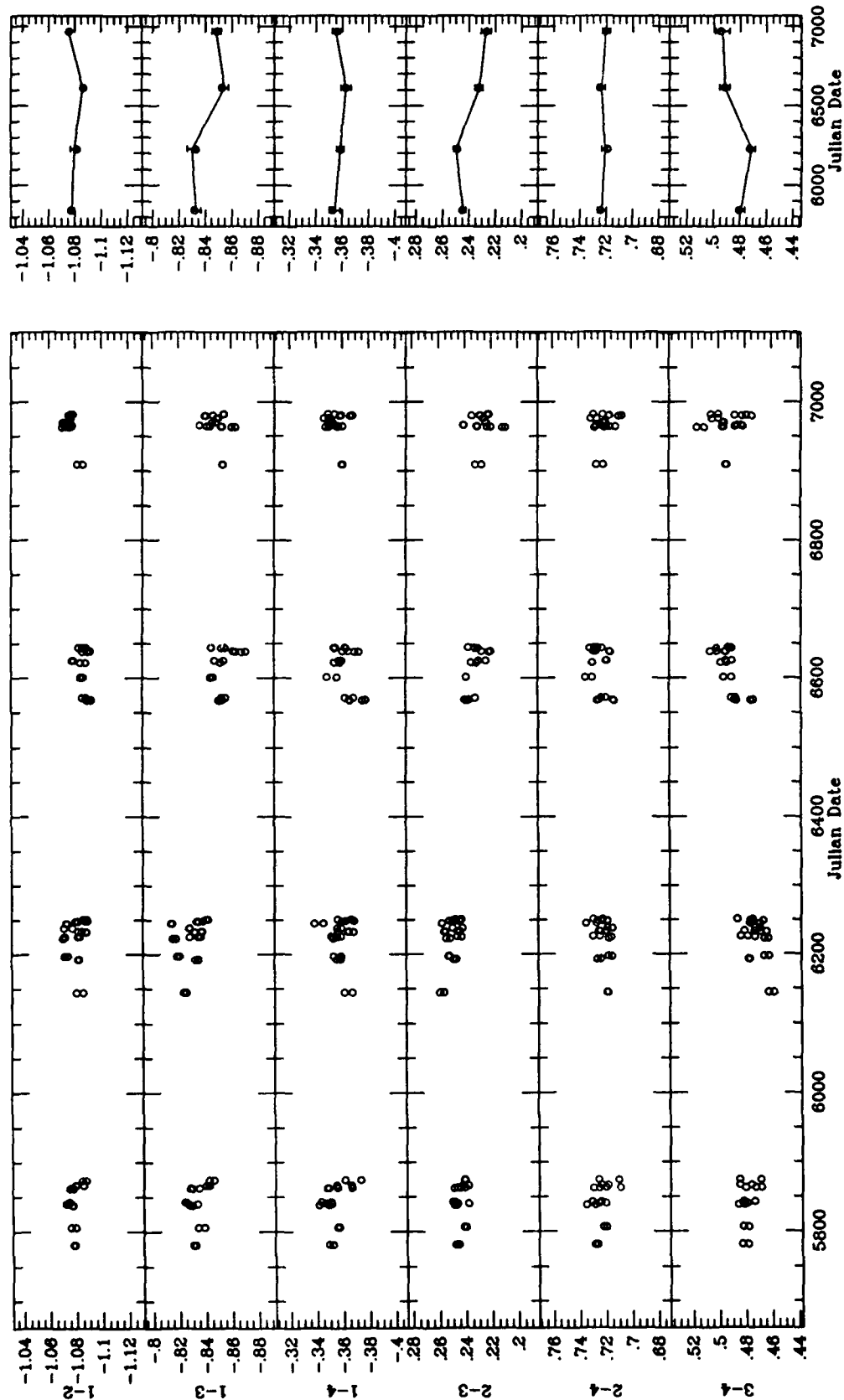


Figure 4.20. Light curves of the HD149661/HD152391 group, compressed scale. Star 1 = HD149661 (K2V) and star 3 = HD152391 (G7V) both vary strongly with ranges of 0.01 and 0.02 mag, respectively. One or both comparison stars is slightly active also, but the long-term range is small, about 0.003.

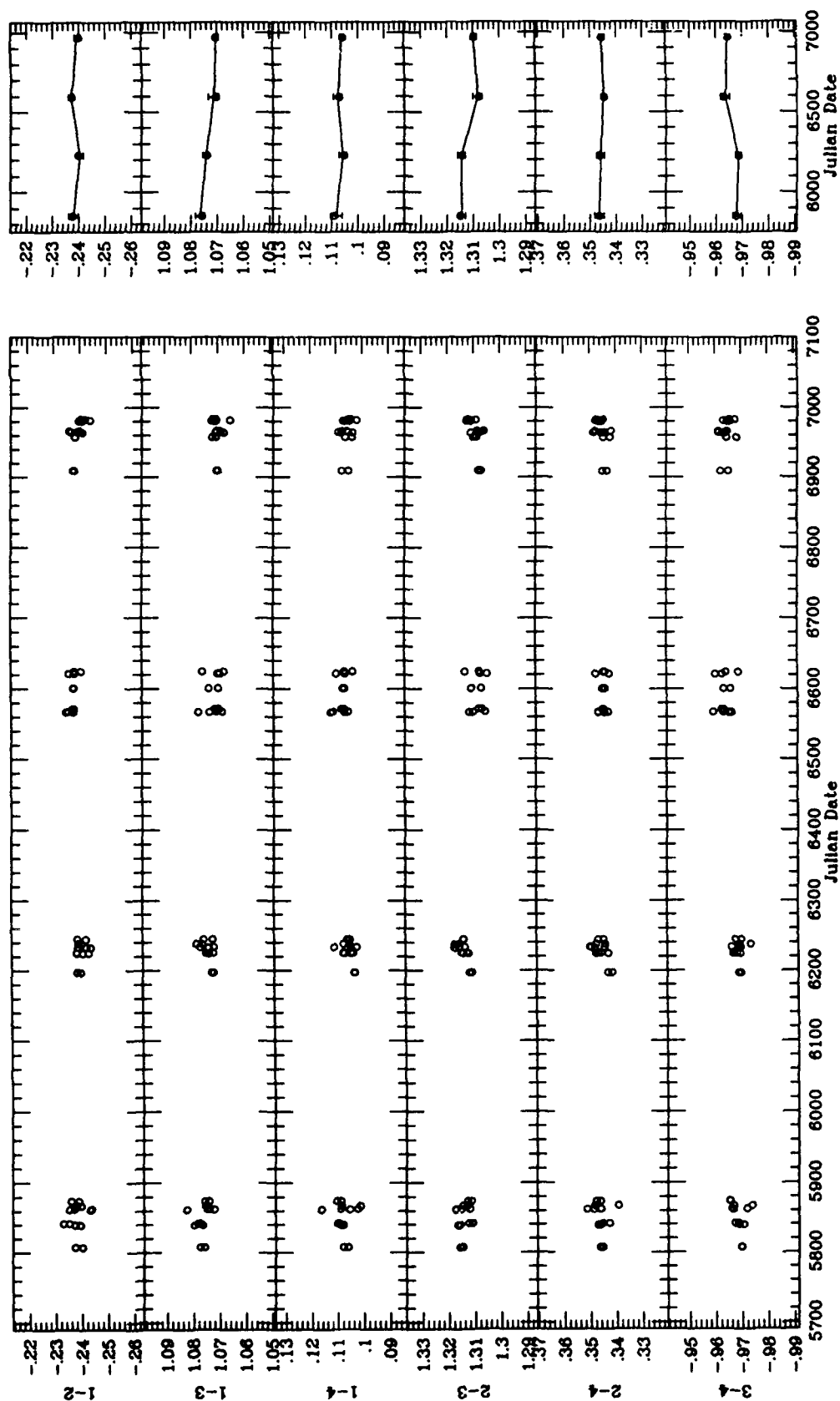


Figure 4.21. Light curves of the HD157856/HD158614 group. Though consistently quiescent, star 1 = HD157856 (F3V) may show long-term variation. Star 3 = HD158614 (G8IV) varies strongly from year to year. Both comparison stars are stable.

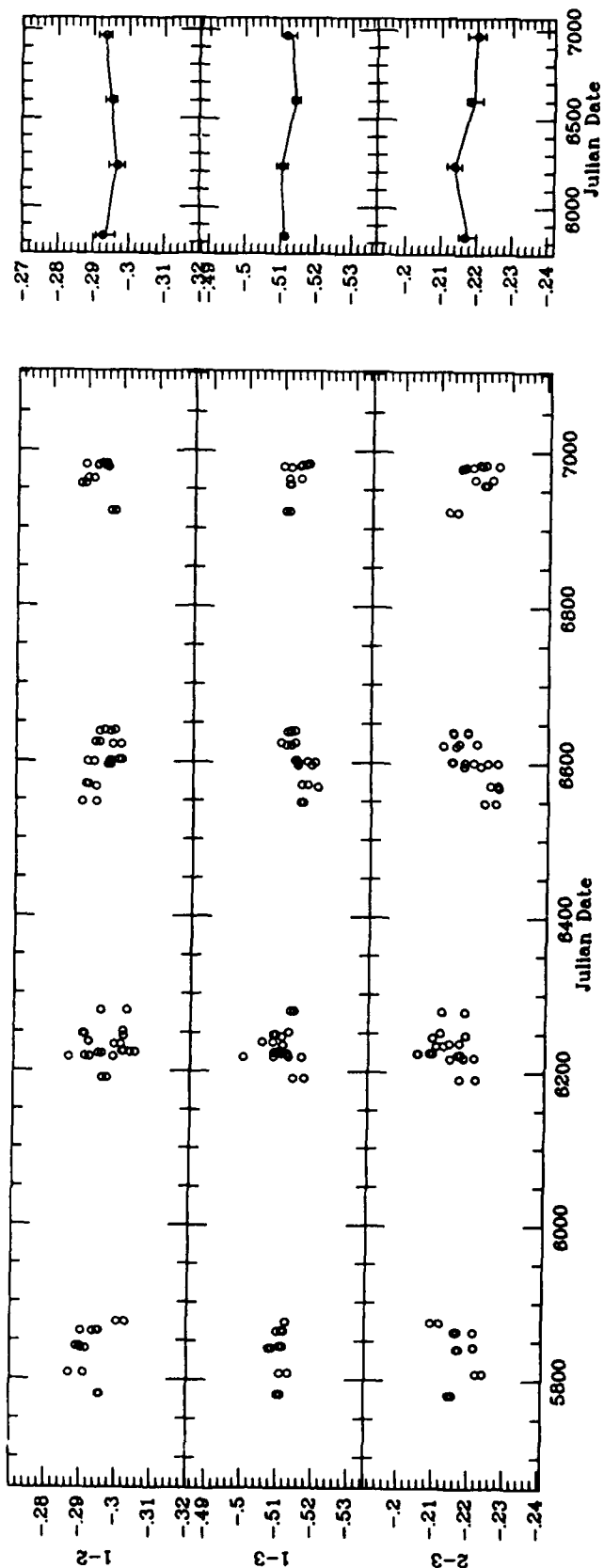


Figure 4.22. Light curves of the HD160346 group. This group lacks a quiescent stars. Star 2 = HD160385 (K3IIb) was variable every year but is stable long term. Star 3 = HD160823 (G0) varies strongly from year to year.

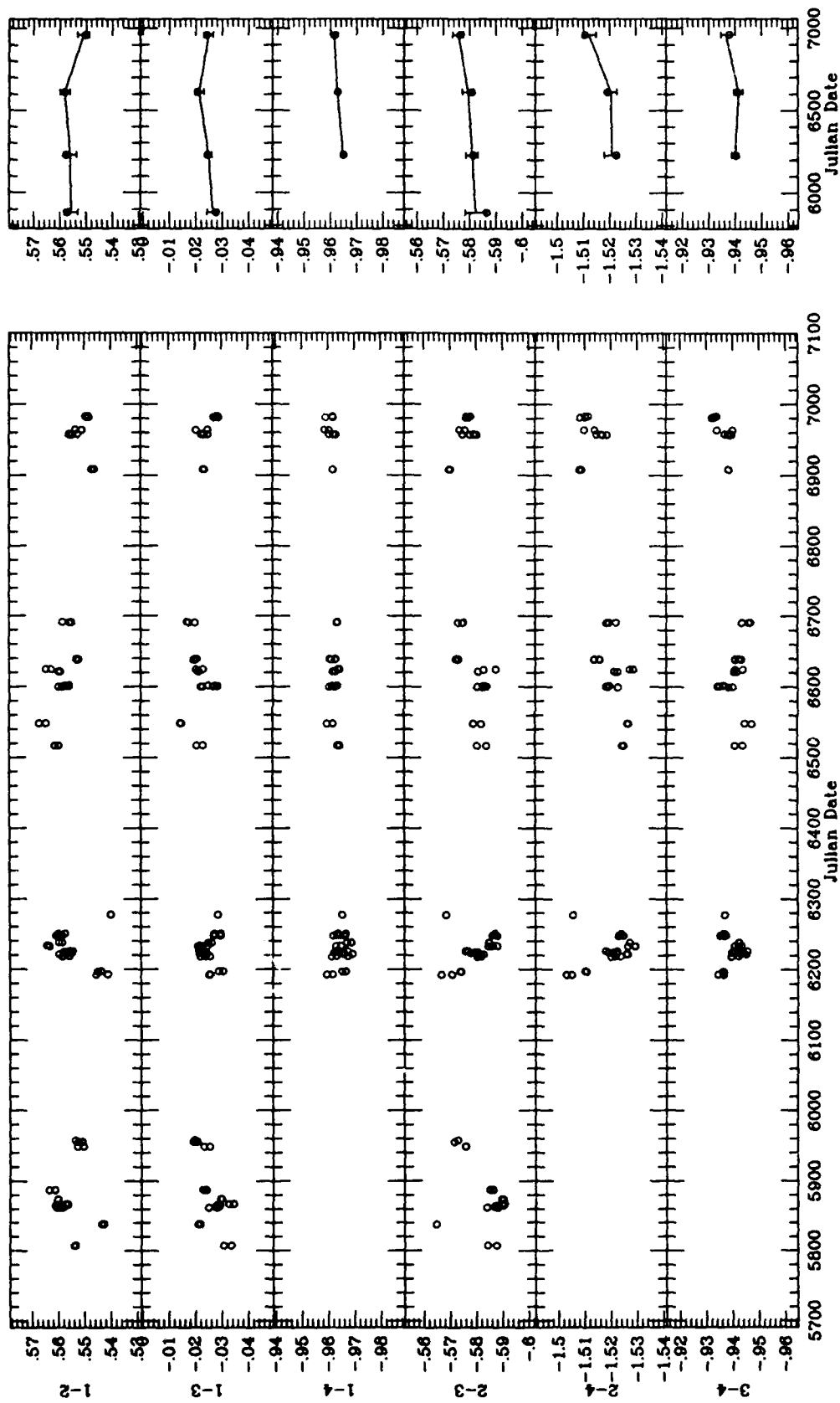


Figure 4.23. Light curves of the HD161239 group. Both star 2 = HD162211 (K2III) and star 3 = HD162076 (G5IV) fluctuate slightly, and star 4 = HD160935 (F5) seems to vary strongly from year to year. The long-term light curves are confused.

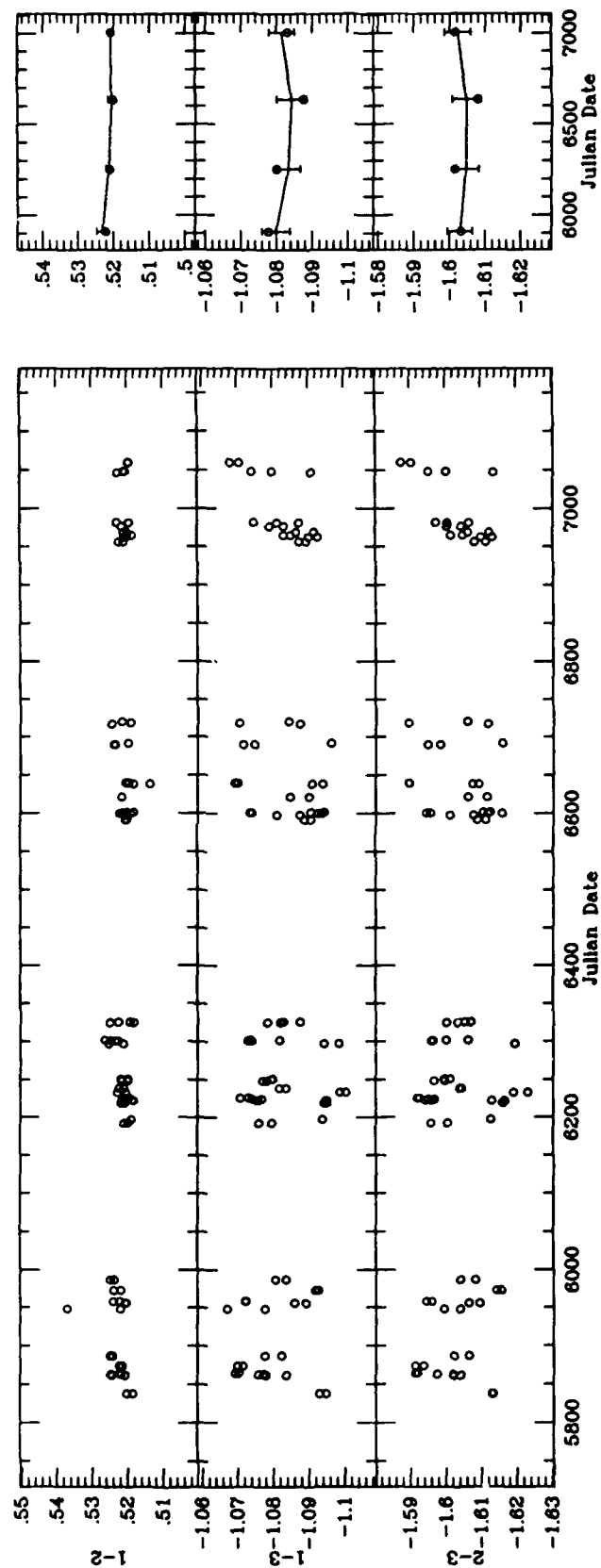


Figure 4.24. Light curves of the HD176095 group. Star 3 = HD175637 (F0) was variable each year and is suspected of being a  $\delta$  Scuti star.



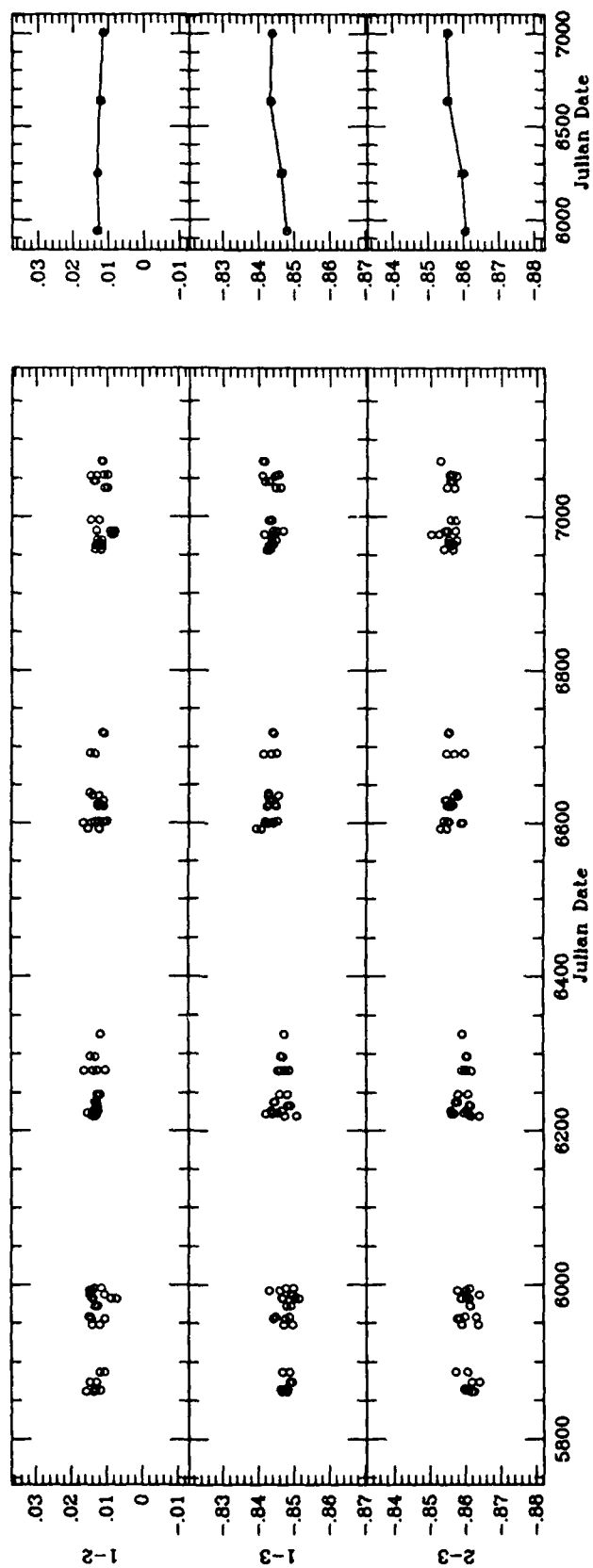


Figure 4.25. Light curves of the HD182572 group. Star 3 = HD185018 (G0Ib-II) may vary slightly from year to year.

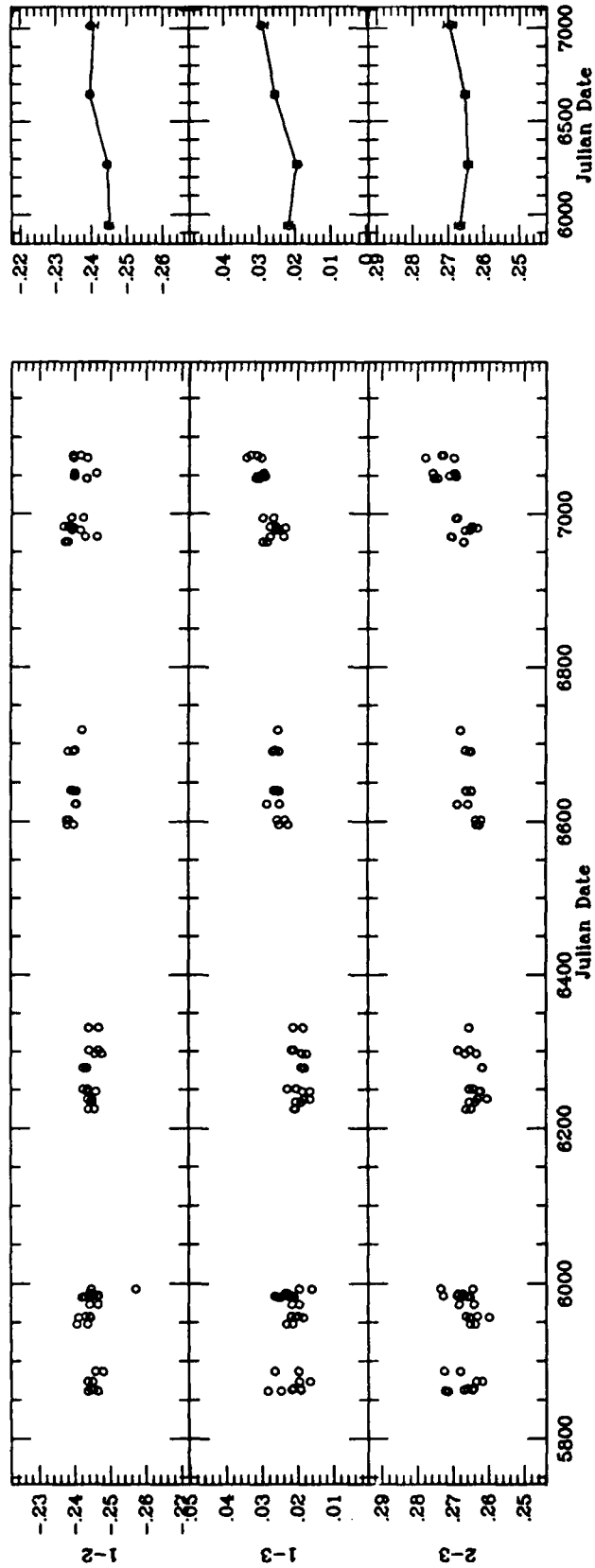


Figure 4.26. Light curves of the HD185144 group. All three stars were essentially quiescent each year, although both of the K-giant comparison stars may fluctuate slightly. The strong variation in each of the interseason light curves makes it impossible to tell which star is variable.

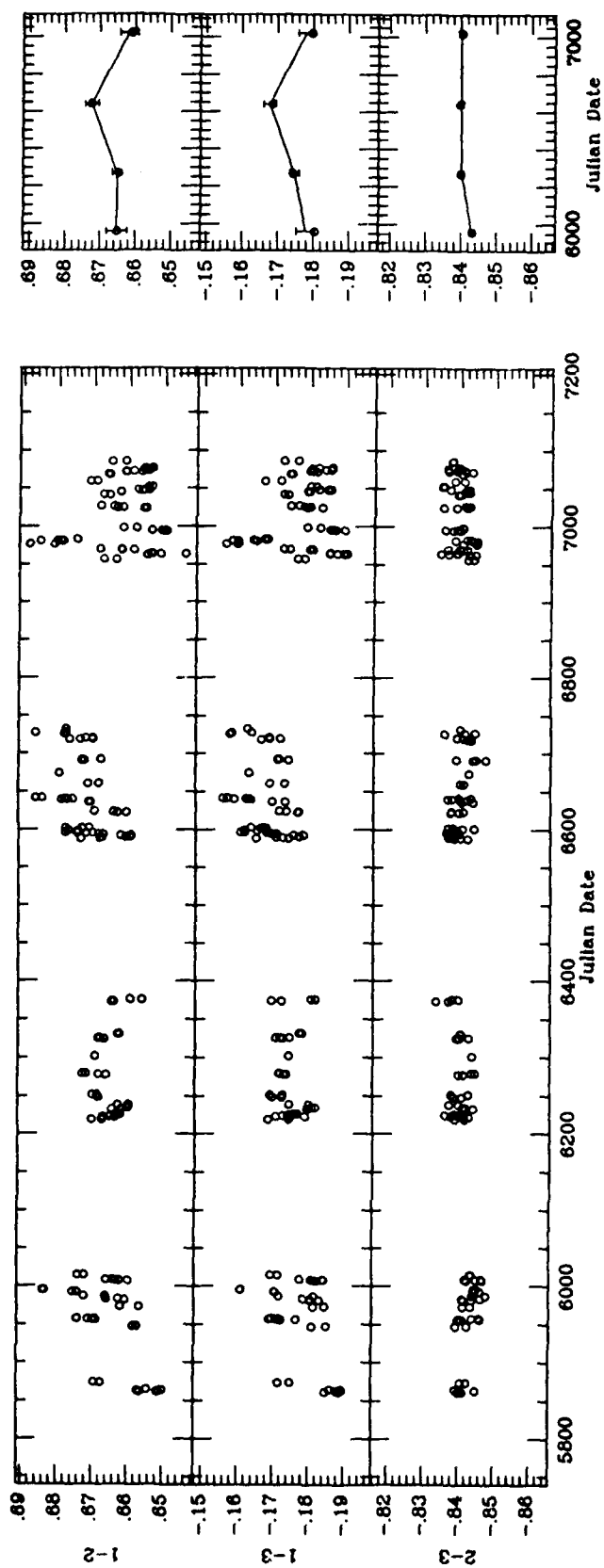


Figure 4.27. Light curves of the HD190007 group. Star 1 = HD190007 (K4) varies strongly on all time scales.

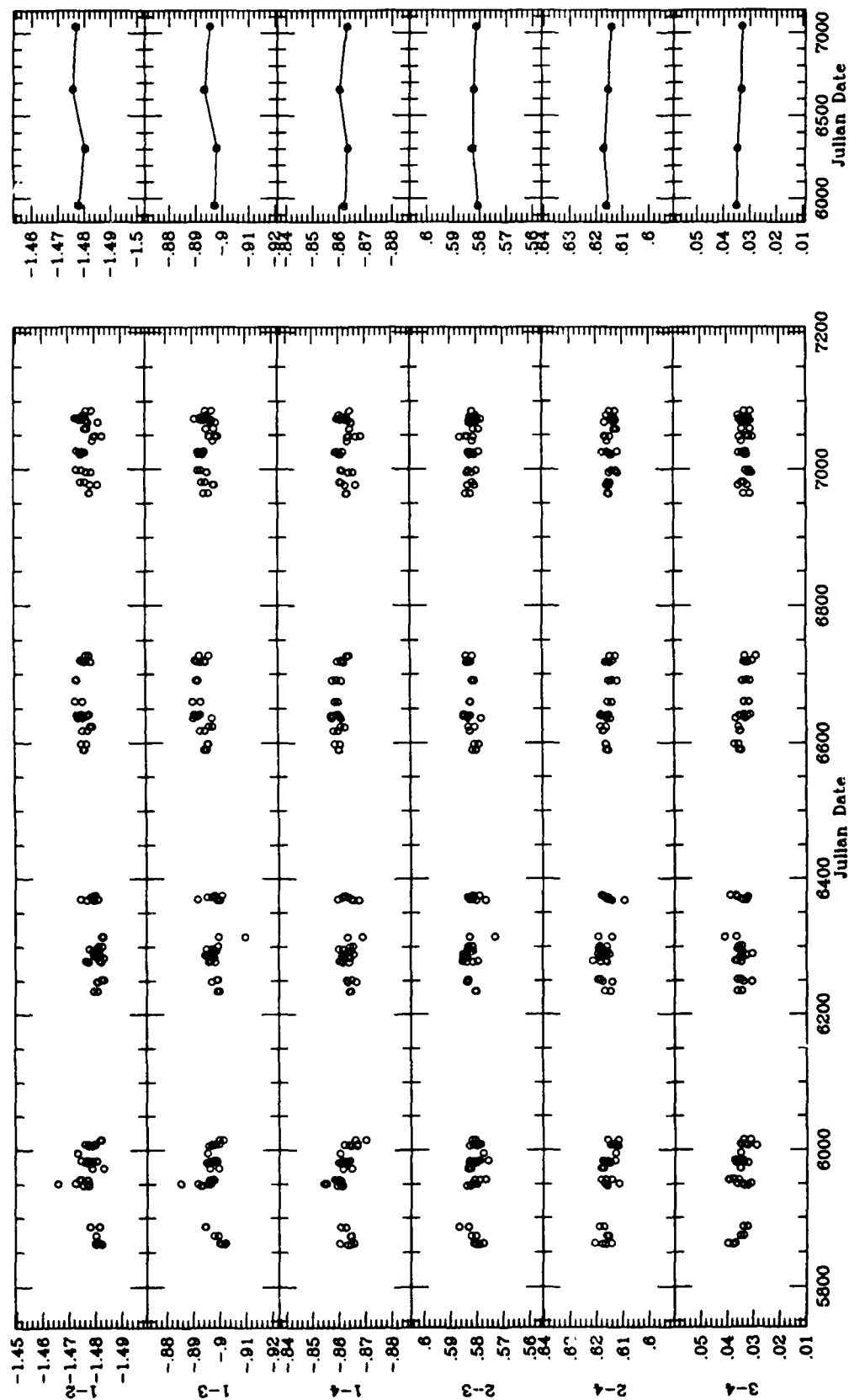


Figure 4.28. Light curves of the HD201091/HD201092 group. In this quiescent group, only star 1 = HD201091 (K5V), a *urby* and HK standard, is consistently variable each year. Its companion, star 3 = HD201092 may fluctuate slightly. Star 1 and star 4 may vary from season to season, but the light curves are confused.

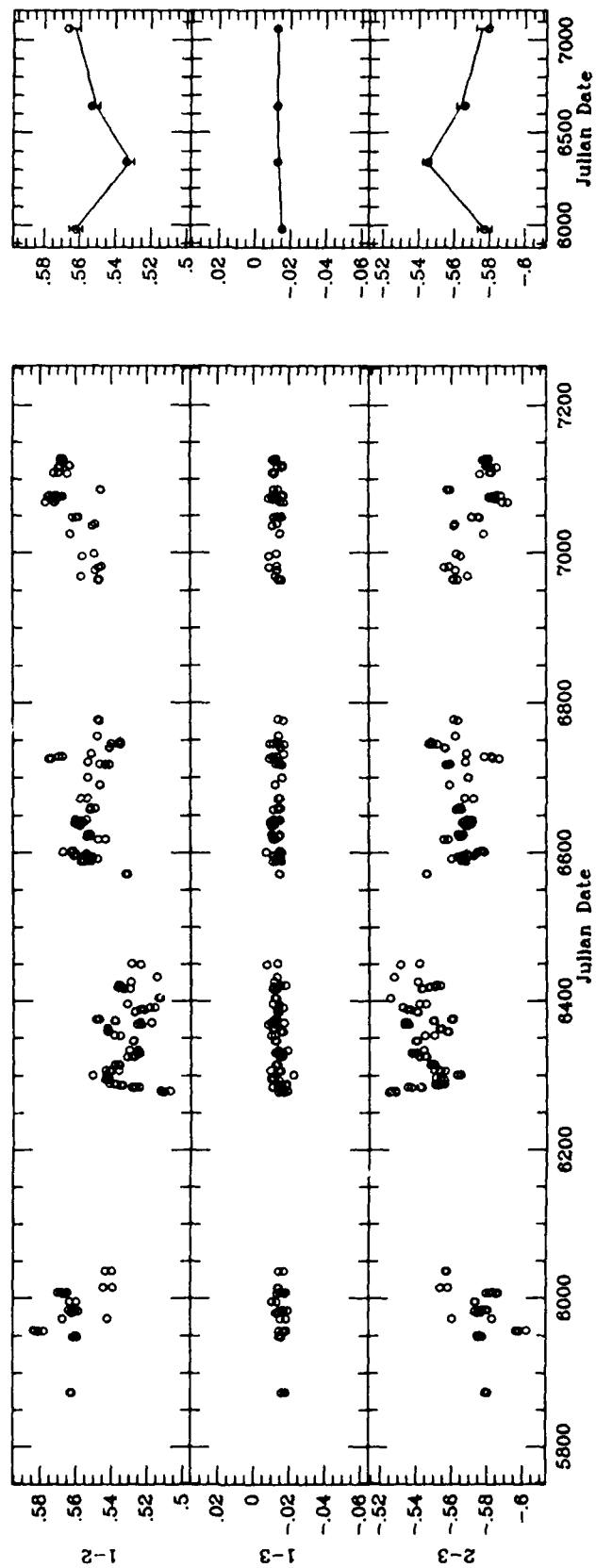


Figure 4.29. Light curves of the HD215704 group, compressed scale. Star 2 = HD215427 (K5) varies strongly.

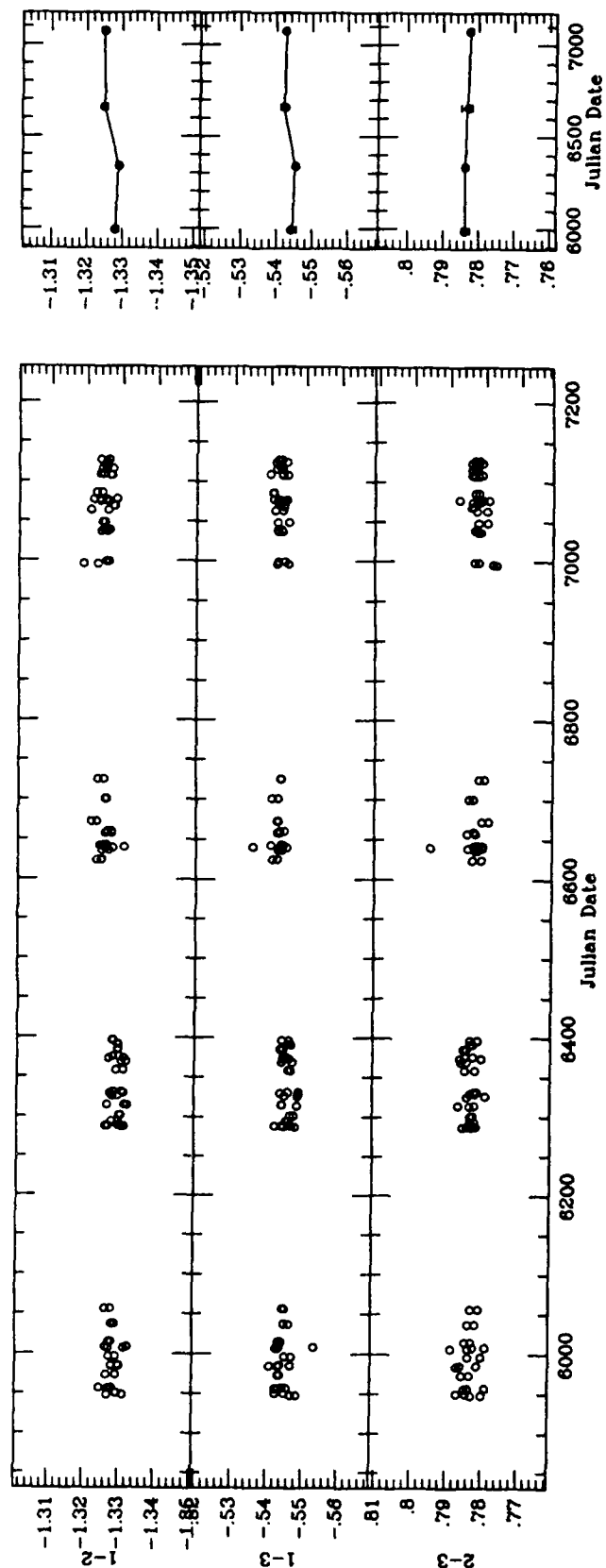


Figure 4.30. Light curves of the HD216385 group. Star 1 = HD216385 (F7IV) varies from season to season.

### 3.7.1 Cycle-to-cycle differences

Comparing the differential magnitudes of the same pair of stars observed in two separate cycles on the same night provides a useful measure of the precision actually attained on  $\sim 1/2$ -hour time scales, where the inconstancy of the atmospheric transparency and photometer response may be possible sources of noise. On this time scale, all the stars are assumed to be nonvariable.

Because the cycle order is always  $y, b, b, y$ , the comparison of cycles 2 and 3 (separated by less than 10 minutes) and cycles 1 and 4 (separated by about 20 minutes) provides a diagnostic of the stability of measurement over these intervals. We computed the absolute values of the differences [cycle 1–cycle 4] and [cycle 2–cycle 3] to investigate the repeatability of measurements independent of night-to-night intrinsic stellar variability and measurement error. Because this quantity is also independent of the actual differential magnitudes of the stars, it can be summed over all groups and all nights to provide global statistics pertaining to the entire program, not just small data subsets. Note that the absolute cycle-to-cycle differences are larger by a factor  $\sqrt{2}$  than the rms cycle-to-cycle dispersion of differential magnitudes.

The top panel of Figure 5 shows the observed distribution of the absolute values of cycle-to-cycle differences of differential magnitudes for a representative subset of all the observations. The observed error distributions are similar in shape, with medians of 0.0024 and 0.0022 and upper quartiles 0.0044 and 0.0039 mag for the absolute values [cycle 1–cycle 4] ( $y$ ) and [cycle 2–cycle 3] ( $b$ ), respectively. Higher count rates in  $b$  for all stars earlier than K3 probably accounts for the slight differences between the two histograms rather than the temporal proximity of the  $b$  cycles.

In the bottom panel of Figure 5, the predicted cycle-to-cycle photon-counting error distribution is shown, based on the actual  $B$  and  $V$  magnitudes—and the corresponding known count rate—of the 66 pairs of stars comprising the 22 original trio groups. (A distribution computed for quartet pairs should be essentially identical but was not computed.) Note that the variances contributing to this distribution are a factor of four larger than the photon count variance for a single star: computation of a differential magnitude doubles the variance, and subtracting one differential cycle from another doubles it again.

Comparing the two panels of Figure 5, we observe, with no surprise, that real observations (*top panel*) evidently include contributions to the total variance that greatly exceed the photon counting error (*bottom panel*). Some guidance to the relative importance of various sources of error is suggested in Table 2; but as the importance of the largest suspected variance source (i.e., centering) is basically just a guess, we must conclude tentatively that it is the small atmospheric transmission fluctuations on less-than-perfect photometric nights that contribute most to the tail of the histograms of Figure 5a.

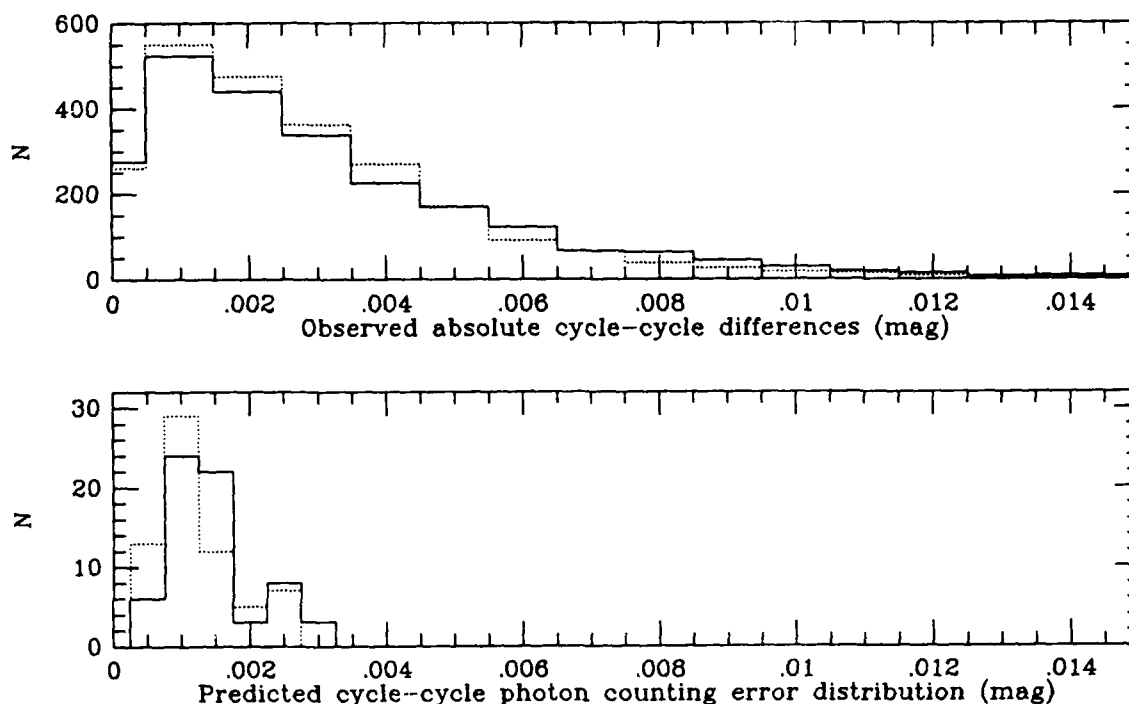


**Figure 5.** (*top*). Observed distribution of the absolute values of cycle-to-cycle differences obtained within the  $y, b, b, y$  sequence each night. A representative subset of the whole data set has been used. (*solid line*) –  $y$  data. (*dotted line*) –  $b$  data. (*bottom*). Predicted cycle-to-cycle error distribution due only to photon statistics, based on the  $V$  and  $B$  magnitudes of the pairwise combinations of stars in the 30 groups. (*solid line*) –  $V$ . (*dotted line*) –  $B$ .

### 3.7.2 Errors arising from differential extinction

Figure 6 shows the actual distribution of differential airmasses for the whole set of observations. The upper quartile of the distribution has the value 0.02 airmass. Assuming an uncertainty in the assumed seasonally adjusted mean extinction coefficient  $\sim 0.03 \text{ mag airmass}^{-1}$  (Lockwood and Thompson 1986*b*), the resulting differential magnitude error is  $\sim 0.0006 \text{ mag}$ , a negligible addition to the error budget contributing insignificantly to the night-to-night dispersion of nonvariable stars.

For those few groups having “large” ( $>0.02$ ) differential airmasses, averaging the nightly cycles will not reduce the systematic errors arising from incorrect assumed values of differential extinction. Figure 7 shows the relation between mean intraseason dispersion and differential airmass for a small group of stars presumed to be intrinsically nonvariable on the basis of their low chromospheric activity ( $\log R'_{\text{HK}}$ ) values. There is no tendency for the dispersion to increase at larger values of differential airmass, so we conclude that the use of mean extinction coefficients is not a significant source of systematic error.



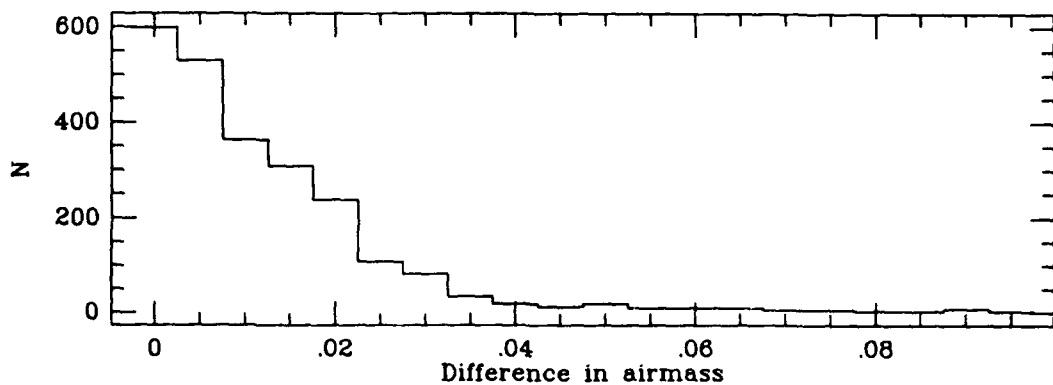


**Figure 6.** Distribution of differential airmasses for all of the observations. The third quartile of the distribution occurs at 0.02 airmass.

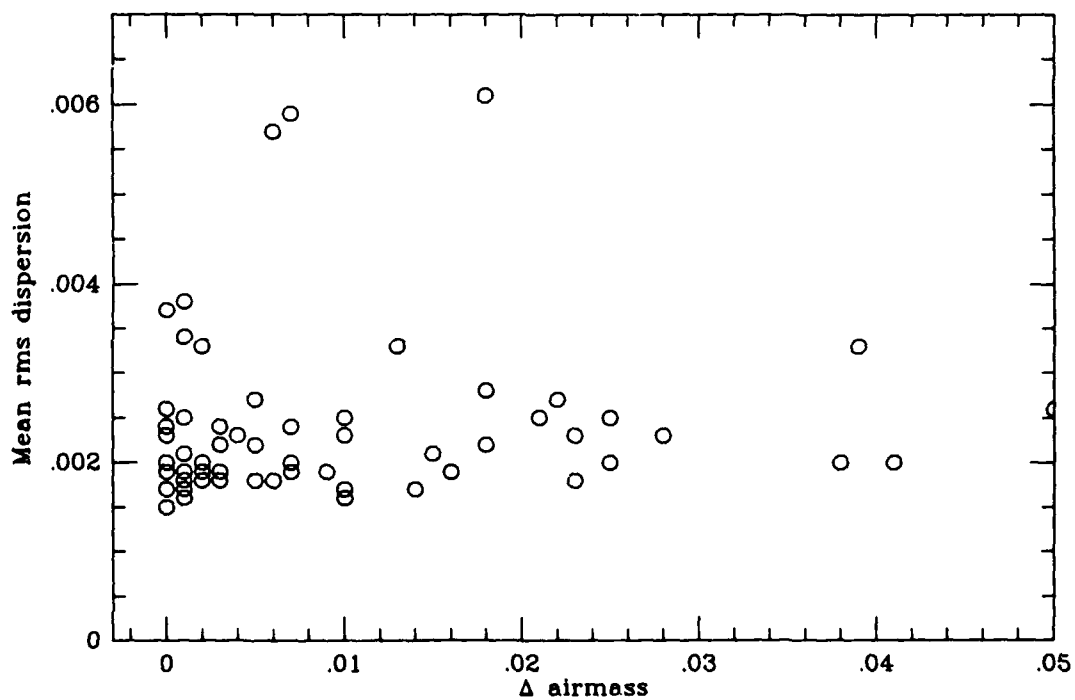


**Figure 7.** The relation between the seasonal rms dispersion of differential magnitudes and differential airmass for stars unlikely to be intrinsically variable.

### 3.8 Possible instrumental effects

#### 3.8.1 Color effects

Over the length of an observing season the conditions under which observations of a given group are made can change significantly. For example, between January and June the mean nighttime low temperature rises from  $-10^{\circ}\text{C}$  to  $+5^{\circ}\text{C}$  (NOAA Local Climatological Data for Flagstaff, Arizona). To test for seasonal temperature-related effects or temporal effects of unknown origin, we plotted on Figure 8 the cycle-to-cycle rms dispersion ( $b$  and  $y$  averaged) as a function of the difference in  $b - y$  color of the two stars of a pair for pairs that showed no evidence of intrinsic variability in any season. Temporal (perhaps temperature-related) changes in the transmission of either filter should cause the star pairs with large differences in  $b - y$  color to exhibit a larger dispersion. No effect is evident.

#### 3.8.2 Brightness and brightness difference effects

For the brighter stars, dead-time corrections are not insignificant, amounting to more than 0.5% at  $V = 5.0$ . Temporal—perhaps temperature-related—changes in the amplifier output pulse width could cause systematic effects. Changes in linearity of the pulse-counting electronics will be manifested as an increase in the dispersion as a function of the magnitude difference of the two stars of a pair and as a function of the magnitude of the brighter member of a pair. Using the same data as in §3.8.1 above, we plotted these relationships in Figures 9 and 10. No effects are evident.

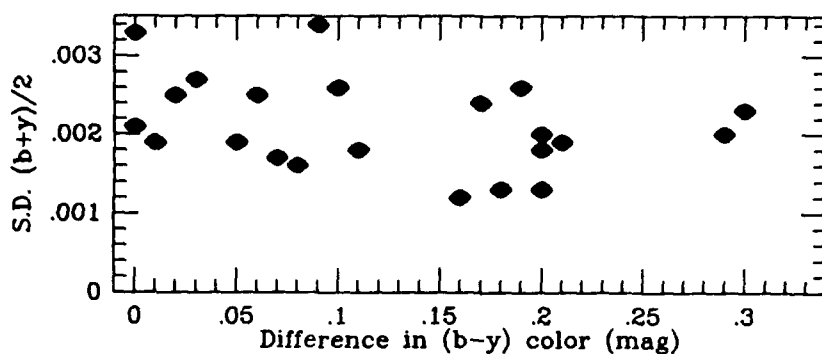
## 4. INTRINSIC STELLAR VARIABILITY ON INTRASEASON TIME SCALES

Observations in just one season provide information on the variability of stars on time scales of days to months and can reveal the modulation of disk-integrated brightness caused by the flux deficits as spotted regions rotate into view. On longer time scales, the evolution of spot groups may in principle be inferred by changes in the amplitude, phase, and period of rotational light curves. Having developed the tools needed to distinguish low-level intrinsic stellar variations from observational artifacts, we proceed to characterize the intrinsic variations.

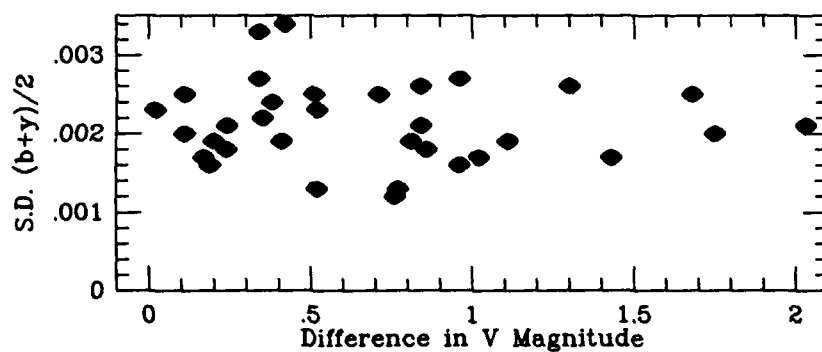
When a group contains only one varying star, as is ideally but not always the case, its identification is unambiguous: the two (three for a quartet) differential light curves for star pairs—each including the variable as one of its components—are correlated. Variability is thus quantitatively confirmed by the attained significance level of the correlation coefficients and is supported usually by an obvious pattern in the rms dispersions of the several differential magnitudes.

#### 4.1 Intraseason standard deviations

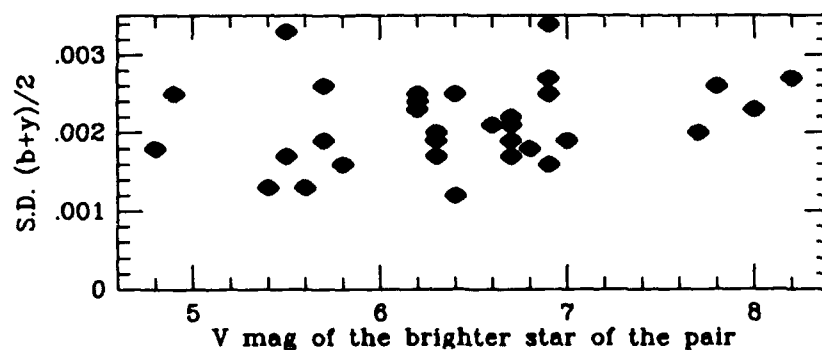
The rms dispersion of the seasonal mean differential magnitudes,  $s_b$  and  $s_y$ , based usually on two observations per night in each filter, can signal the presence of intrinsic stellar variability. For a given star pair,  $s_b \sim s_y$ ; so to reduce tabulation in this report, we shall use the standard deviations of the combined  $b$  and  $y$  magnitudes,  $s_{by}$ , formed by averaging the  $y$  magnitudes of cycle 1 with the  $b$  magnitudes of cycle 2, and the  $b$  magnitudes of cycle 3 with the  $y$  magnitudes of cycle 4, thus producing two nightly data points for each group observed.



**Figure 8.** Average intraseason standard deviations ( $b$  and  $y$  averaged) as a function of the difference in  $(b - y)$  color for pairs of stars showing no evidence of intrinsic variability.



**Figure 9.** Average intraseason standard deviations ( $b$  and  $y$  averaged) as a function of the difference in  $V$  magnitude for pairs of stars showing no evidence of intrinsic variability.



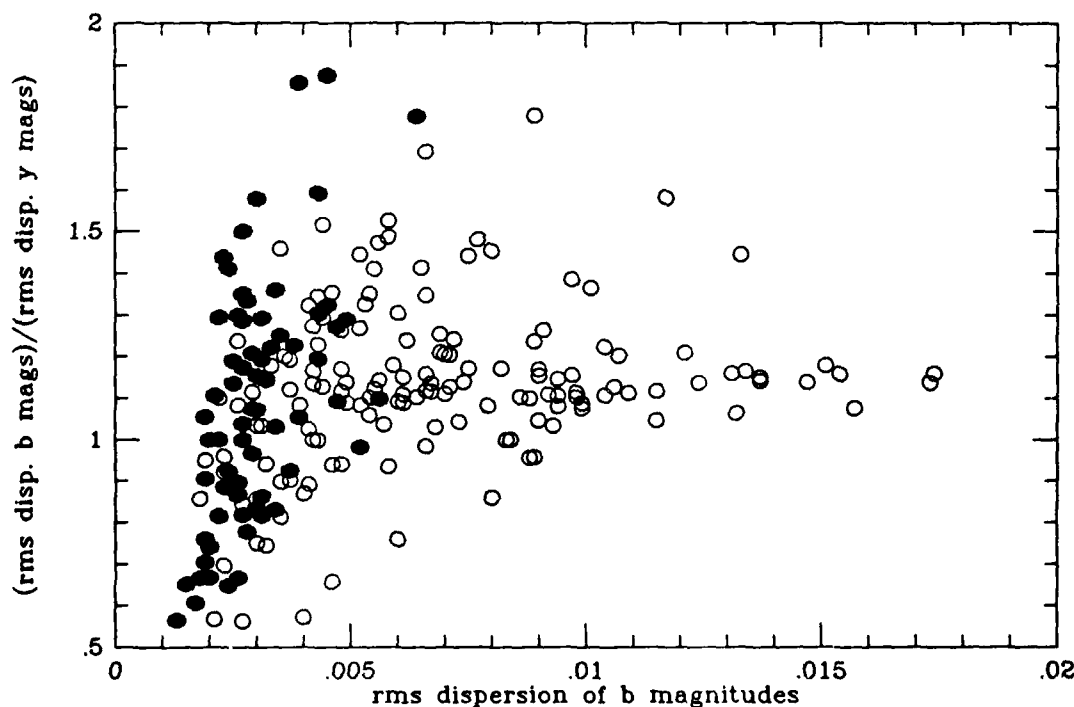
**Figure 10.** Average intraseason standard deviations ( $b$  and  $y$  averaged) as a function of the  $V$  magnitude of the brighter member of pairs of stars showing no evidence of intrinsic variability.

Table 4 gives  $s_{by}$  values for each observing season, the Julian Date range, and  $n$ , the number of averaged  $[(b + y)/2]$  data points. Except for the rare occasions when only one  $b$  and one  $y$  cycle were observed, the number of nights each season is therefore  $n/2$ . In each group, star 1 provides the group name and is the principal program star; the second program star in the group label for certain quartets is star 3 unless otherwise noted.

Following each  $s_{by}$  value in Table 4 is an indication of whether that particular star pair shows variability: V – definitely variable (99% confidence), v – possibly variable (95% confidence), or C – constant, according to the significance of correlation coefficients (§4.3). These designations are omitted when the identity of the variable star(s) is ambiguous.

#### 4.2 The relation between $s_b$ and $s_y$

Although  $s_b \sim s_y$ , the ratio  $s_b/s_y \sim 1.1$  for variables and  $\sim 1.0$  for constant stars, reflecting, at large values of  $s_b$  and  $s_y$ , mainly an aspect of intrinsic variability and, at small ( $<0.004$  mag) values of  $s_b$  and  $s_y$ , mainly observational noise. Figure 11 shows  $s_b/s_y$  plotted as a function of  $s_b$ . For stars whose consistent fluctuations every year verified their intrinsic variability, we find  $s_b \sim 1.15s_y$  and for consistently nonvariable stars,  $s_b \sim s_y$ .



**Figure 11.** The ratio of the intraseason standard deviation in  $b$  to the standard deviation in  $y$ ,  $s_b/s_y$  as a function of  $s_b$ . (filled circles) – consistently constant stars. (open circles) – consistently variable stars. The ratio is typically  $\sim 1.1$  for variable stars.

TABLE 4. Intra-season Dispersion and Inter-season Ranges in  $(b+y)/2$ 

Group	n	JD 2440000+	1-2 (mag)	1-3 (mag)	1-4 (mag)	2-3 (mag)	2-4 (mag)	3-4 (mag)	Variable
HD1835	28	5947.8-6077.6	0 <sup>m</sup> 0091 V	0 <sup>m</sup> 0087 V		0 <sup>m</sup> 0029 C			1
	53	6286.9-6432.6	0.0100 V	0.0105 V		0.0027 C			1
	38	6642.0-6777.6	0.0088 V	0.0088 V		0.0024 C			1
	28	7036.9-7136.6	0.0075 V	0.0075 V		0.0019 C			1
		Range	0.0135 V	0.0123 V		0.0013 C			1+
HD10476	30	5947.8-6068.6	0.0016 C	0.0017 C		0.0017 C			
	30	6293.9-6424.6	0.0017 C	0.0017 C		0.0022 C			
	28	6658.0-6807.6	0.0017 C	0.0017 C		0.0018 C			
	28	7038.9-7137.7	0.0019	0.0027 V		0.0030 V			3
		Range	0.0037 V	0.0046 V		0.0009 C			1
HD13421	24	5955.9-6065.7	0.0030 V	0.0023 V		0.0021 C			1
	18	6306.9-6450.6	0.0018 C	0.0018 C		0.0018 C			
	29	6678.9-6808.6	0.0019	0.0020		0.0022			2?, 3?
	14	7063.9-7127.7	0.0020 C	0.0024 C	0.0015 C	0.0018 C	0.0015 C	0.0018 C	
		Range	0.0159 V	0.0020 C		0.0179 V			2+
HD18256	18	5955.9-6082.6	0.0022 C	0.0021 C		0.0019 C			
	19	6307.0-6459.6	0.0011 C	0.0021 V		0.0021 V			3
	15	6679.9-6808.6	0.0018 C	0.0018 C		0.0017 C			
	11	7063.9-7127.7	0.0015 C	0.0021 C	0.0074 V	0.0019 C	0.0079 V	0.0073 V	4
		Range	0.0011 C	0.0037 V		0.0024 v			3?
HD23140	22	5955.9-6086.6	0.0037 V	0.0043 V		0.0020 C			1
	22	6307.0-6459.6	0.0036 V	0.0035 V		0.0018 C			1
	15	6680.0-6808.6	0.0027 v	0.0034 v		0.0021 C			1?
		Range	0.0027 C	0.0026 C		0.0019 v			
HD25998	16	5955.9-6086.6	0.0059 v	0.0063 v		0.0044 C			1?
	25	6331.0-6459.7	0.0057 V	0.0047 V		0.0036 C			1
	12	6679.0-6731.8*	0.0030 C	0.0043 C		0.0034 C			
	11	*6742.8-6827.9	0.0043 C	0.0059 C	0.0184 V	0.0043 C	0.0187 V	0.0195 V	4
		Range	0.0050 C	0.0048 C		0.0023 C			
HD35296/ HD35587	10	5760.7-5778.6	0.0054 C	0.0053 C	0.0041 C	0.0031 C	0.0042 C	0.0026 C	
	30	5956.0-6149.6	0.0086 V	0.0093	0.0065 V	0.0082 V	0.0051 C	0.0060 V	1,3
	63	6331.0-6512.6	0.0068 V	0.0074	0.0075 V	0.0056 V	0.0018 C	0.0061 V	1,3
	32	6705.0-6881.6	0.0055 V	0.0082	0.0060 V	0.0060 V	0.0019 C	0.0058 V	1,3
			0.0104 V	0.0115 V	0.0104 V	0.0144 V	0.0034 V	0.0146 V	1+, 3+

TABLE 4. Intra-season Dispersion and Inter-season Ranges in  $(b+g)/2$  (continued)

Group	n	JD 2440000+	1-2 (mag)	1-3 (mag)	1-4 (mag)	2-3 (mag)	2-4 (mag)	3-4 (mag)	Variable
HD76572, HD75332†	23	5760.7-5813.6	0.0028 v	0.0025 C		0.0032 v			2?
	27	6064.9-6158.7	0.0019 v	0.0017 C		0.0021 v			2?
	34	6363.0-6516.7	0.0017 v	0.0015 C	0.0048 V	0.0016 C	0.0050	0.0047 V	2?, 4
	29	6741.0-6905.6	0.0014 C	0.0018 C	0.0105 V	0.0017 C	0.0108 V	0.0101 V	4
		Range	0.0024 V	0.0020 V	0.0166 V	0.0007 C	0.0179 V	0.0180 V	1?, 4+
HD81809	19	5762.7-5814.6	0.0026 v	0.0024 v		0.0020 C			1?
	26	6064.9-6158.7	0.0024 v	0.0024 v		0.0020 C			1?
	14	6404.0-6511.7	0.0042 V	0.0017 C		0.0047 V			2
	28	6807.9-6907.6	0.0040 V	0.0034 V		0.0026 C			1
		Range	0.0037 V	0.0055 V		0.0086 V			3+
HD82885/ HD82635‡	19	5762.7-5814.7	0.0126 V	0.0066 C		0.0097 V			2
	54	6064.9-6196.7	0.0137	0.0127 V	0.0126 V	0.0051 V	0.0045 V	0.0023 C	1, 2
	55	6373.0-6570.7	0.0085	0.0057 V	0.0051 V	0.0056 V	0.0063 V	0.0019 C	1, 2
	41	6741.0-6920.7	0.0069	0.0035 V	0.0035 V	0.0051 V	0.0050 V	0.0016 C	1, 2
		Range	0.0155 V	0.0099 V	0.0067 V	0.0058 v	0.0044 V	0.0018 V	1+, 2+
HD103095	20	5762.8-5837.7	0.0016 v	0.0013 C		0.0016 v			2?
	28	6065.0-6164.7	0.0021 V	0.0011 C		0.0021 V			2
	21	6421.0-6539.7	0.0014	0.0014		0.0020			3?
	20	6808.9-6919.7	0.0021 C	0.0025 v		0.0024 v			3
		Range	0.0015 v	0.0028 V		0.0043 V			3
HD114710	18	5766.9-5814.8	0.0020 C	0.0036 V		0.0035 V			3
	18	6120.9-6224.7	0.0030 C	0.0057 V		0.0060 V			3
	27	6486.9-6570.7	0.0057 V	0.0048 C		0.0069 V			2
	12	6880.9-6965.7	0.0029 C	0.0088 V		0.0072 V			3
		Range	0.0049 V	0.0154 V		0.0110 V			3+
HD115383/ HD117176	12	5780.8-5839.7	0.0022 v	0.0017 v		0.0012 C			1?
	12	6103.9-6225.7	0.0046 V	0.0047 V		0.0014 C			1
	21	6486.9-6570.7	0.0026	0.0035		0.0028			1?, 3?
	9	6880.9-6964.7	0.0021 C	0.0026 C		0.0018 C			
		Range	0.0135 V	0.0171 V		0.0041 V			1+

† Star 4 = HD75332

‡ Star 2 = HD82635

TABLE 4. Intraseason Dispersion and Interseason Ranges in  $(b+y)/2$  (continued)

Group	n	JD 2440000+	1-2 (mag)	1-3 (mag)	1-4 (mag)	2-3 (mag)	2-4 (mag)	3-4 (mag)	Variable
HD115404	18	5780.9-5849.7	0.0052 V	0.0046 V		0.0025 C			1
	39	6104.0-6234.7	0.0062 V	0.0064 V		0.0014 C			1
	25	6486.9-6570.8	0.0086 V	0.0083 V		0.0019 C			1
	11	6880.9-6968.7	0.0082 V	0.0083 V		0.0021 C			1
		Range	0.0154 V	0.0109 V		0.0061 V			1+, (2? or 3? confused)
HD120136	24	5776.8-5864.7	0.0024	0.0033		0.0026			1?, 2
	16	6104.0-6237.7	0.0016 C	0.0017 C		0.0017 C			
	15	6486.9-6594.7	0.0042 C	0.0041 C		0.0038 C			
	16	6882.9-6969.7	0.0015 C	0.0016 C		0.0018 C			
		Range	0.0115 V	0.0099 V		0.0038 V			1+
HD124570	16	5776.9-5864.7	0.0016 C	0.0061 V		0.0053 V			3
	20	6144.9-6225.7	0.0015 C	0.0045 V		0.0045 V			3
	29	6486.9-6601.7	0.0015 C	0.0026 V		0.0027 V			3
	14	6882.9-6969.7	0.0021 C	0.0034 v		0.0035 v			3?
		Range	0.0025 V	0.0174 V		0.0195 V			3+
HD129333	14	5780.9-5873.7	0.0142 V	0.0150 V		0.0019 C			1
	53	6104.0-6251.7	0.0208 V	0.0218 V		0.0039 V			1
	52	6487.0-6639.7	0.0136 V	0.0137 V		0.0026 C			1
	26	6829.0-6982.7	0.0160 V	0.0161 V		0.0022 C			1
		Range	0.0471 V	0.0482 V		0.0014 C			1+
HD131156	28	5776.9-5873.7	0.0065 C	0.0075 v		0.0077 v			3?
	43	6104.0-6250.7	0.0056 V	0.0088	0.0061 V	0.0060 V	0.0015 C	0.0058 V	1, 3
	33	6487.0-6601.7	0.0081 V	0.0133	0.0068 V	0.0124 V	0.0026 C	0.0122 V	1, 3
	35	6882.0-6979.7	0.0075 V	0.0065	0.0075 V	0.0048 V	0.0015 C	0.0045 V	1, 3
		Range	0.0087 V	0.0027 v	0.0027 C	0.0139 V	0.0060 V	0.0079 V	2+, (3? or 4? confused)
HD143761	22	5782.9-5866.7	0.0021	0.0033		0.0026			1?, 3
	18	6145.0-6222.8	0.0011 C	0.0016 v		0.0014 v			3?
	18	6487.0-6601.8	0.0014 C	0.0014 v		0.0019 v			3?
	20	6885.0-6975.7	0.0015 C	0.0016 C		0.0018 C			
		Range	0.0022 V	0.0014 C		0.0029 V			2?

TABLE 4. Intraseason Dispersion and Intenseason Ranges in  $(b+g)/2$  (continued)

Group	n	JD 2440000+	1-2 (mag)	1-3 (mag)	1-4 (mag)	2-3 (mag)	2-4 (mag)	3-4 (mag)	Variable
HD19661/ HD152391	18 26 20 20	5781.0-5873.8 6145.0-6250.7 6566.8-6643.7 6908.9-6981.7	0.0042 V 0.0066 V 0.0041 C 0.0036 C	0.0066 V 0.0084 V 0.0070 V 0.0074 V	0.0084 0.0069 V 0.0077 V 0.0060 V	0.0040 C 0.0053 C 0.0064 C 0.0081 V	0.0084 v 0.0051 C 0.0063 V 0.0064 V	0.0052 v 0.0070 C 0.0079 0.0110	1,4? 1 3,4 1+,3+
		Range	0.0109 V	0.0247 V	0.0087 V	0.0228 V	0.0033 C	0.0218 V	
HD157856/ HD158614	14 14 12 18	5808.0-5873.8 6196.9-6244.7 6566.9-6624.7 6909.0-6982.7	0.0030 C 0.0020 C 0.0015 C 0.0020 C	0.0026 C 0.0021 C 0.0030 v 0.0017 C	0.0036 C 0.0023 C 0.0024 C 0.0018 C	0.0022 C 0.0021 C 0.0026 v 0.0021 C	0.0028 C 0.0025 C 0.0015 C 0.0019 C	0.0026 C 0.0018 C 0.0026 v 0.0019 C	1,3+
		Range	0.0034 V	0.0062 V	0.0025 v	0.0062 V	0.0015 C	0.0049 V	
HD160346	14 23 21 14	5781.0-5873.8 6190.9-6277.7 6547.9-6639.7 6922.0-6982.8	0.0045 V 0.0052 V 0.0033 0.0031 v	0.0015 C 0.0036 C 0.0027 0.0023 C		0.0041 V 0.0047 V 0.0050 0.0040 v			2 2 2,3 2?
		Range	0.0034 C	0.0040 V		0.0060 V			3+
HD161239	21 30 21 12	5807.9-5957.6 6192.9-6277.7 6516.9-6691.6 6907.9-6982.8	0.0016 C 0.0065 V 0.0042 V 0.0033 V	0.0021 v 0.0028 V 0.0037 V 0.0027 v	0.0023 C 0.0013 C 0.0013 C	0.0020 v 0.0059 0.0047 0.0032	0.0071 V 0.0044 V 0.0036 V	0.0032 V 0.0037 V 0.0030 v	3? 2,3 2,3 2,3?
		Range	0.0072 V	0.0036 V	0.0034 V	0.0056 V	0.0085 V	0.0048 V	1+,4+,(2? or 3? confused)
HD176095	22 31 22 23	5837.9-5986.6 6192.9-6325.6 6591.9-6720.6 6956.9-7059.6	0.0036 C 0.0020 C 0.0022 C 0.0012 C	0.0086 V 0.0092 V 0.0092 V 0.0081 V		0.0077 V 0.0093 V 0.0087 V 0.0085 V			3 3 3 3
		Range	0.0025 V	0.0043 C		0.0024 C			
HD182572	28 21 22 25	5861.9-5995.6 6218.9-6325.6 6591.9-6718.6 6956.9-7071.6	0.0020 v 0.0014 C 0.0017 C 0.0019 v	0.0019 v 0.0021 V 0.0016 C 0.0016 C		0.0018 C 0.0020 V 0.0018 C 0.0019 v			1? 3 2? 3
		Range	0.0017 v	0.0045 V		0.0053 V			



TABLE 4. Intra-season Dispersion and Inter-season Ranges in  $(b+y)/2$  (continued)

Group	n	JD 2440000+	1-2 (mag)	1-3 (mag)	1-4 (mag)	2-3 (mag)	2-4 (mag)	3-4 (mag)	Variable
HD185144	30	5861.9-5992.6	0.0028	0.0029		0.0023			2?,3?
	18	6224.9-6330.6	0.0015 C	0.0018 v		0.0021 v			3?
	14	6595.9-6717.6	0.0012 C	0.0015 v		0.0019 v			3?
	22	6962.9-7075.6	0.0026	0.0029		0.0040			2?,3
		Range	0.0054 V	0.0093 V		0.0052 V			1+, (2? or 3? confused)
HD190007	36	5861.9-6014.6	0.0085 V	0.0076 V		0.0024 C			1
	27	6218.9-6375.6	0.0038 V	0.0038 V		0.0024 C			1
	48	6587.9-6731.6	0.0064 V	0.0069 V		0.0026 C			1
	58	6956.9-7085.6	0.0094	0.0083		0.0026			1,2
		Range	0.0103 V	0.0102 V		0.0032 V			1+
HD201091/ HD201092	39	5862.0-6014.6	0.0032 V	0.0031 V	0.0031 V	0.0022 C	0.0021 C	0.0023 C	1
	34	6233.9-6375.6	0.0020 V	0.0028	0.0021 V	0.0025 V	0.0022 C	0.0020 V	1,3
	28	6589.9-6727.6	0.0018	0.0021	0.0017	0.0016	0.0016	0.0020	1,3,4?
	39	6964.9-7085.6	0.0026	0.0022 V	0.0023 V	0.0016 v	0.0015 v	0.0015 C	1,2?
		Range	0.0045 V	0.0033 V	0.0033 V	0.0015 V	0.0027 V	0.0021 V	1?,4? confused
HD215704	34	5874.0-6036.6	0.0109 V	0.0020 C		0.0113 V			2
	72	6277.8-6450.6	0.0097 V	0.0026 C		0.0097 V			2
	73	6570.9-6777.6	0.0091 V	0.0022 C		0.0086 V			2
	44	6963.9-7127.6	0.0100 V	0.0022 C		0.0102 V			2
		Range	0.0311 V	0.0026 V		0.0327 V			2+
HD216385	26	5947.8-6056.6	0.0018 C	0.0026 V		0.0025 V			3
	33	6286.9-6396.6	0.0016	0.0016		0.0017			2?,3?
	22	6623.9-6725.7	0.0019	0.0019		0.0032			2,3
	36	6995.9-7126.6	0.0019 V	0.0013 C		0.0019 V			2
		Range	0.0041 V	0.0032 V		0.0014 C			1

In addition to helping provide confirmation of intrinsic variability, the ratio  $s_b/s_y$  is astrophysically meaningful: it derives from the variation of the disk-averaged effective temperature of the star caused by the presence of cool dark spots. For stars of solar temperature, the  $b$  filter lies shortward of the blackbody maximum while the  $y$  filter is located near the peak, so that small temperature variations affect the two filters unequally:  $\Delta b > \Delta y$ .

As a simple illustration, at 6000 K, a 20 K decrease in disk-averaged blackbody temperature associated with a spotted hemisphere causes a 0.0185 mag drop in  $b$  and an 0.0164 mag drop in  $y$ , yielding the ratio  $\Delta b/\Delta y = 1.13$ . Similarly, a 20 K increase will increase  $b$  and  $y$  in the same ratio. Obviously, spotted regions of various temperatures, spatial distribution, and filling factors can produce similar indistinguishable effects.

#### 4.3 Correlations of light curves

The principal statistic used to confirm variability is the attained significance level of the correlation coefficient for light curves containing one star in common (e.g., [star 1–star 2] and [star 1–star 3]). In Table 4, the designation V (variable) and v (possibly variable) indicate, respectively, 99% and 95% significance of the correlation coefficient. Variable stars identified by this procedure are listed in the final column of Table 4. When it is impossible to determine uniquely from the array of correlation coefficients (three for trios, six for quartets) which stars are variable, as happens sometimes when more than one star is evidently varying, the variability designation is omitted even though the  $s_{by}$  values of individual differential light curves are large enough that variability is suspected.

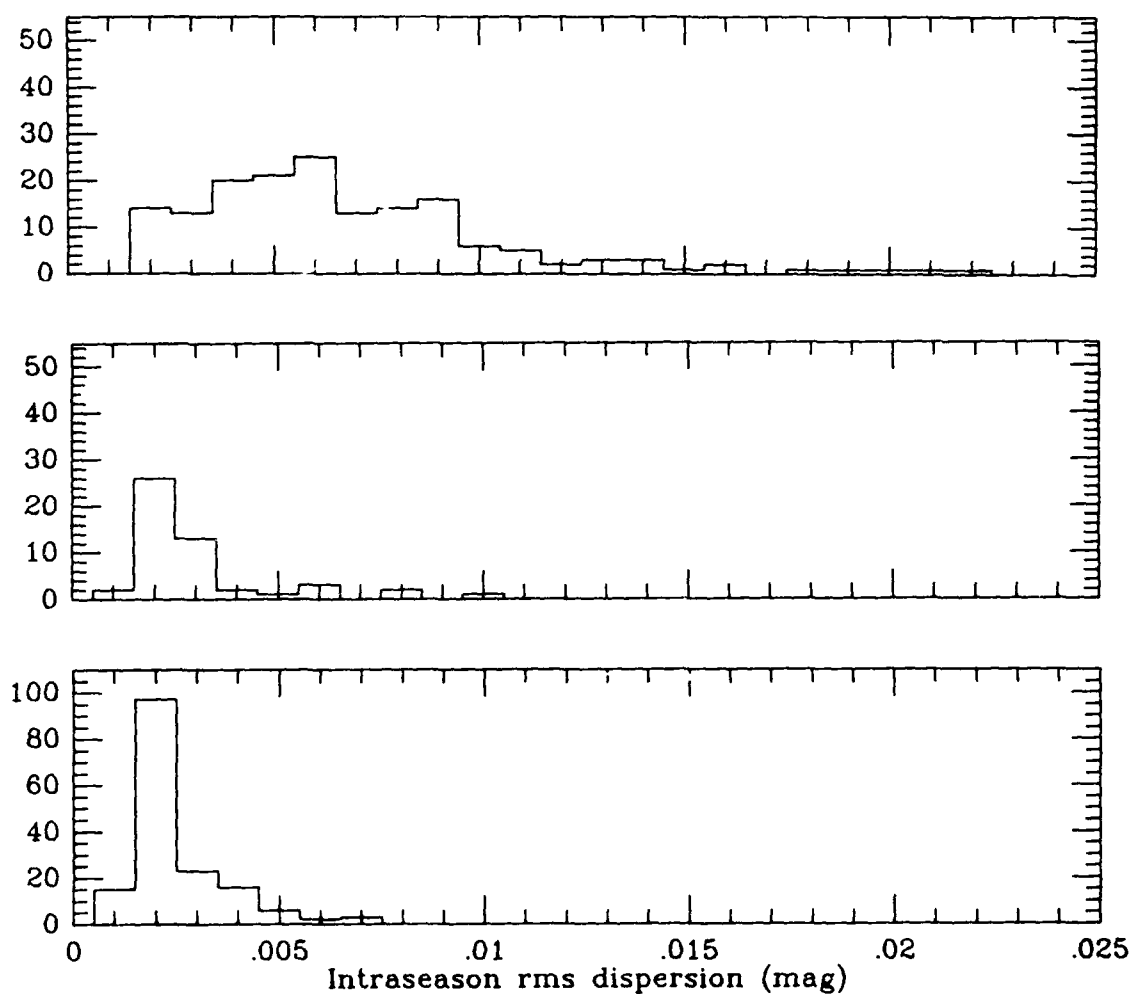
#### 4.4 Frequency histograms of intraseason variability

Figure 12 presents frequency histograms of the seasonal standard deviations,  $s_{by}$ , for constant pairs, possibly variable pairs, and variable pairs (Table 4). The data divide evenly between variable and constant pairs, with only ~15% falling in the possibly variable category. Pairs with both stars possibly or probably variable are omitted. Overlap between the histograms is small: the third quartile for constant pairs occurs at 0.0026 mag and the first quartile for variable pairs is located at 0.0041 mag. As a general rule, any pair with  $s_{by} > 0.0025$  mag is likely to include a variable star, since few of the constant pairs have dispersions this large.

According to Figure 12, half the star pairs include a variable star; but because of redundancy in pair membership, the fraction of variable stars is actually fewer than half. (One variable star in a trio produces two entries in the “variable” histogram and one in the “constant” histogram. One variable star in a quartet produces three “variable” pairs and three “constant” pairs; two variable stars in a quartet produce five “variable” pairs and one “constant” pair, etc.) According to the final column of Table 4, 35 stars were variable in two or more seasons, leading to the conclusion that field F, G, and K stars have a significant chance of being found perceptibly variable on short time scales. About half the program stars and one-fourth the comparison stars were variable.

TABLE 5. Intraseason Variability and Spectral Type

LUMINOSITY CLASS	SPECTRAL TYPE						TOTAL	
	F		G		K		Var.	Constant
	Var.	Constant	Var.	Constant	Var.	Constant		
I-III	1	2	3	9	5	2	9 (41%)	13
IV-V	7	17	6	9	7	4	20 (40%)	30
Unknown	1	11	1	6	3	3	5 (25%)	20
TOTAL	9	30	10	24	15	9	34	63
	(24%)		(29%)		(63%)		(34%)	



**Figure 12.** Frequency histograms for star pairs exhibiting definite variability at the 99% confidence level (*top*), at the 95% confidence level (*middle*), or nonvariability (*bottom*).

#### 4.5 Consistently variable stars

More than one-third of the program and comparison stars were found to be consistently variable in two or more seasons. Table 5 summarizes the number and percentage distribution of variable stars by spectral type and luminosity classification. About one-fourth the F and G stars and two-thirds the K stars were variable. Surprisingly, five of thirteen *uvby* photometric standard stars are variable. Variability at the  $<1\%$  level is therefore an extremely common phenomenon among cool stars regardless of luminosity type.

Figure 13 shows the relation between  $s_{by}$  (averaged over all seasons) and  $B - V$  color for consistently variable program and comparison stars. The scale of spectral types is from Fitzgerald (1970). Only one star (HD129333) fluctuated by more than 1%. The F and G variables were predominantly subgiants and dwarfs, while the K variables were mostly giants. Figure 13 includes seven *uvby* standards, but three (HD101606, HD201091, and HD201092) are marginal ( $\sim 0.002$  mag) detections. Two others (HD82885, HD82635), however, have recently derived photometric rotation periods based on light curves with amplitudes greater than 0.01 mag (Skiff and Lockwood 1986).

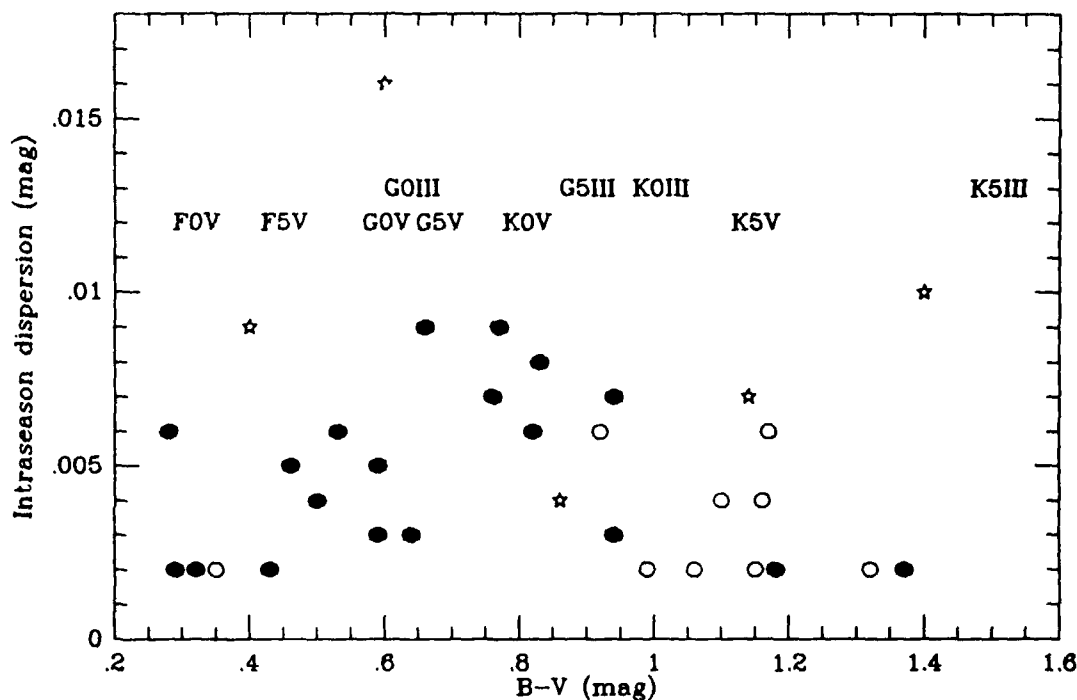


**Figure 13.** Average intraseason rms dispersion,  $s_{by}$ , for program and comparison stars that were variable in two or more seasons as a function of  $B - V$  color. (*filled circles*) - luminosity IV and V stars. (*open circles*) - luminosity class I, II, or III, (*stars*) - luminosity class unknown.

#### 4.6 Photometrically derived rotation periods

A number of the program stars have rotation periods determined earlier from their HK variations (Vaughan *et al.* 1981; Baliunas and Vaughan 1985). Because the relative variation in the HK index,  $S$ , is an order of magnitude greater than the photometric variation, it is much easier to measure—typically  $\Delta S/S$  is in the range 3–20%, while the rms  $b$  or  $y$  variation in the optical continuum rarely exceeds 1%.

Using an algorithm by Scargle (1982), we were nonetheless able to derive photometric rotation periods for nine stars, essentially confirming the HK periods for several, and obtaining original periods for three others. Table 6 summarizes the known HK and newly measured photometric rotation periods. Theoretical rotation periods,  $P_{\text{calc}}$ , derived from the convective turnover time and  $B - V$  color by Noyes *et al.* (1984) are included for comparison. To maximize the signal to noise ratio in this calculation, we first averaged together all the differential magnitudes having the program star in common; i.e.,  $[(\text{star 1} - \text{star 2}) + (\text{star 1} - \text{star 3}) + (\text{star 1} - \text{star 4})]/3$ . In Table 6, the quantity  $Z_{\text{max}}$  is a measure of the signal-to-noise ratio of the photometric rotation signal: if  $Z_{\text{max}} > 10$ , it was possible to derive photometric periods with some confidence.

#### 5. INTRINSIC STELLAR VARIABILITY ON INTERSEASON TIME SCALES

The detection of interseason variability is, in principle, straightforward and analogous to the procedure used to analyze intraseason variability: an analysis of variance is used to test the significance of the differences between seasonal mean magnitudes; and the correlation of seasonal mean light curves uniquely identifies the particular star that is varying. However, this task must be approached with caution because, on time scales of years, the risk of systematic errors is ever increasing.

Correlations, or the lack thereof, among pairs of seasonal mean magnitudes having a subject star in common were identified by simple inspection of the light curves—the number of annual data points is presently too small to justify formal statistics. Often, however, this method is completely sufficient. For example, in the light curves for the HD1835 group (Figure 4.1), it is obvious that the chromospherically active program star (star 1) is strongly variable from year to year: the total variation greatly exceeds the 95% seasonal confidence limits indicated by the error bars.

In other cases, more formal statistics must prevail. In the HD182572 group (Figure 4.25), for example, it appears from inspection that star 3 may be variable, though its light curves (star 1–star 3, star 2–star 3) show hardly more activity than the constant pair (star 1–star 2). An analysis of variance confirms the suspicion: the light curves for star 1–star 3 and star 2–star 3 both indicate variation at a confidence level  $>99.9\%$ . Variation of star 1–star 2 is significant at the 99% level.

In cases of low-range variation hardly distinguishable from noise, we must rely upon significance tests in a formal analysis of variance (AOV), using the consistency among pairs of light curves with a star in common to decide which star is actually varying. Some groups present insoluble complexity when more than one

TABLE 6. Summary of Rotation Determinations

HD	$\log R'_{\text{HK}}$	JD 2,440,000+	$n$	$s_{by}$	$P_{\text{photom}}$ (days)	$P_{\text{HK}}$ (days)	$P_{\text{calc}}^a$ (days)	$Z_{\text{max}}$
1835	-4.42	6287.0-6432.6	53	0.010	7.7	7.7	6.7	19.5
25998	-4.50					2.6		
35296	-4.38	6331.0-6512.6	63	0.007	2.3		3.3	10.4
39587	-4.40	6331.0-6512.6	63	0.007	4.9	5.2	5.9	11.4
82885	-4.58	6064.9-6196.7	54	0.013	18.2	18.1	18.4	23.1
		6373.0-6570.7	55	0.005	18.1	17.5		20.4
114710	-4.73	6486.9-6570.7	27	0.006	...	12.4	12.2	6.2
115383	-4.43			<0.005		3.4	4.9	
115404	-4.46	6104.0-6234.7	39	0.006	11.0	18.8	15.5	7.2
129333	-4.23	6104.0-6250.7	53	0.021	3.0	...	...	17.2
		6487.0-6639.7	52	0.014	2.7	...	...	11.7
131156 AB	-4.36	6104.0-6250.7	43	0.006	6.1	6.2 <sup>b</sup>	7.7	12.5
		6487.0-6601.7	33	0.007	6.4			12.6
		6882.0-6979.7	35	0.008	6.2			9.2
149661	-4.54			0.006		21.3	17.7	
160346	-4.71			<0.005		33.5	37.0	
176095	-4.68		31	0.009	2.8			10.4
190007	-4.59	5861.9-6014.6	6	0.008				
		6218.9-6375.6	37	0.004	35.0	29.3	25.2	11.6
		6587.9-6731.6	48	0.006	28.0			9.7
		5861.9-6998.4	147 <sup>c</sup>	0.008	26.3			14.8
201091	-4.80			0.003		37.9	40.6	9.1
201092	-4.91				...	48.0	50.0	

## NOTES:

<sup>a</sup>Noyes *et al.* 1984.<sup>b</sup>6.2-6.7 (Baliunas *et al.* 1985)<sup>c</sup>Four years combined.

star is evidently varying; e.g., HD161239 (Figure 4.23), HD201091/HD201092 (Figure 4.28).

On the bottom row of data for each group, Table 4 summarizes the results of the formal statistical tests for interseason variability. The peak-to-peak range ( $b$  and  $y$  averaged) for each star pair is listed along with the designation V, v, or C according to the outcome of the AOV for that pair: V means that the attained significance (via the  $F$  statistic) for variation in the annual mean values is 99% or greater; v indicates a significance greater than 95%, and C indicates no significant variability. By inspecting the decision for each pair, the identity of the variable star(s) is usually evident and is listed in the final column of Table 4. A "+" denotes variation in excess of 0.005 mag (0.5%) peak-to-peak—these are the most certain detections.

Figure 14 reports the outcome of the analysis of variance: the upper histogram pertains to pairs of stars that show evidence of variability at the 99% confidence level, the center histogram includes pairs in the 95–99% range, and the bottom histogram includes nonvariable pairs. According to this procedure, over half the pairs show evidence of some variability. As there remains some possibility of systematic error contributing to the observed variability, this statistic alone is insufficient; and we require further evidence before deciding that a particular star is variable, including correlation of the appropriate pairs of light curves, and the existence of a pair of stars in each group deemed "constant," regardless of the AOV.

In all groups, but especially in quartets, one pair of stars has to be chosen as "constant," regardless of the outcome of the formal AOV, to provide a basis for assessing the variations of the other stars. Sometimes this pair itself is suspect because the total amplitude of variation is clearly larger than that seen in some of the best-behaved groups. Most likely, this simply indicates that no pair of stars in that group is truly constant—or it could mean that a systematic error of unknown origin is contaminating the data for that particular group. We consider this problem further below.

Analogous to Figure 13 for intraseason variations, we show in Figure 15 the relation between peak-to-peak three- or four-year range of seasonal mean magnitudes ( $b$  and  $y$  averaged) and  $B - V$  color. The median range is 0.008 mag, and there are no trends with luminosity or spectral type. Ranges at the 0.002 mag level are marginally significant but may ultimately be confirmed by further observations.

#### 5.1. The least-variable stars

Having established (Table 5) that one-third of the entire sample and two-thirds of the K stars are consistently variable on intraseason time scales, we now consider the statistics of long-term variability. The least-variable stars are provisionally so designated and listed by differential pairs in Table 7 if they (1) show a total range of the averaged  $b$  and  $y$  seasonal mean magnitudes  $<0.003$  mag and (2) have an average intraseason rms dispersion  $<0.003$  mag. Twenty-six pairs of stars, including 40 individual stars (12 appear in two or more pairs) qualify for this list. Even with this

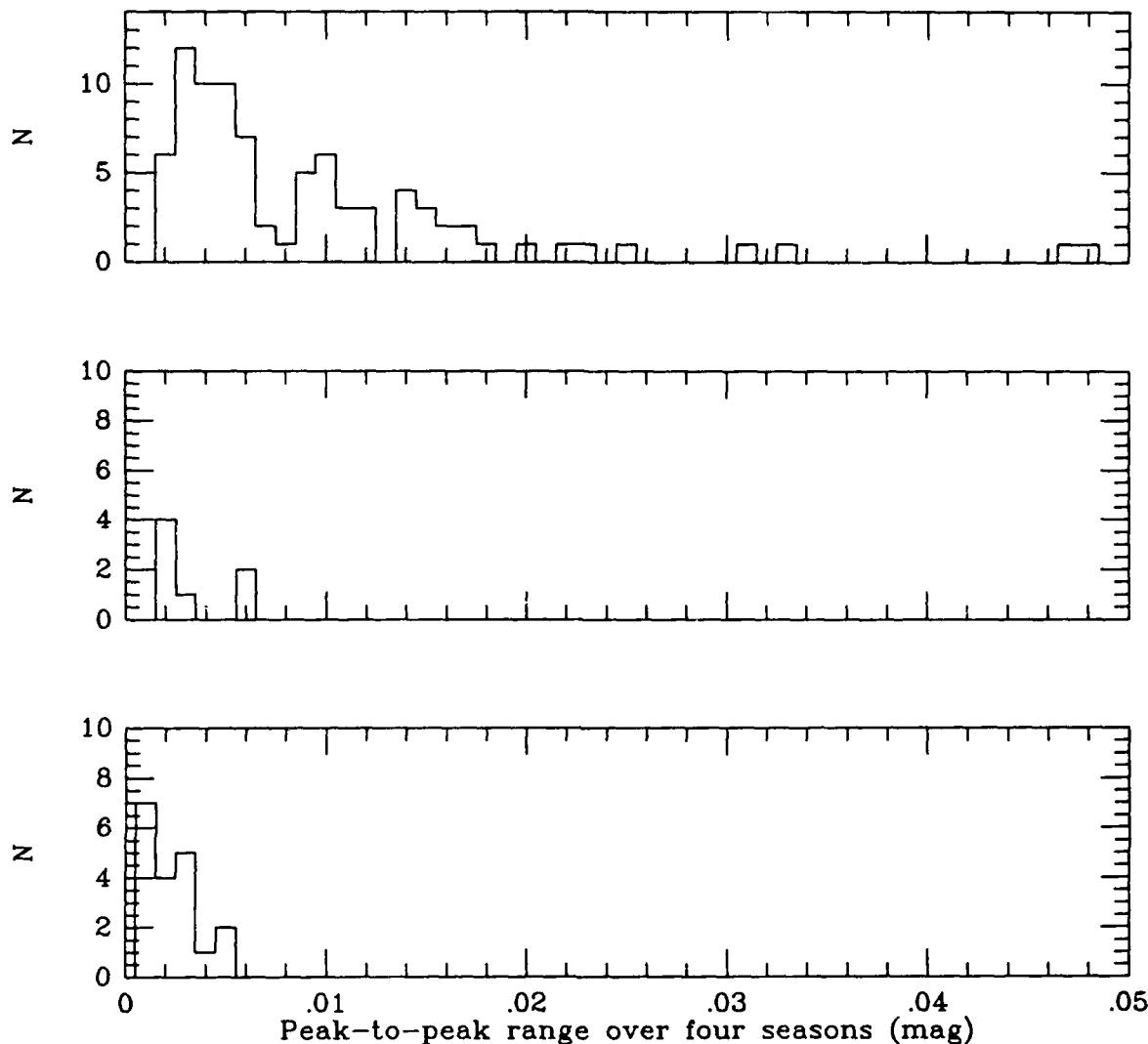


**Figure 14.** Frequency histograms of peak-to-peak range of seasonal mean magnitudes for pairs of stars judged variable at the 99% confidence level (*top panel*), possibly variable at the 95-99% confidence level (*middle panel*), or nonvariable (*bottom panel*).

severe restriction upon the total range of variability, 17 pairs of stars appear to be significantly ( $>95\%$  probable) variable according to the formal analysis of variance, leaving only 9 pairs showing no evidence whatsoever of long-term variability. These 18 "constant" stars are predominantly F stars; and the sole MK-classified giant in the list, HD73596 (F5III), may fluctuate slightly each year. Another likely giant, HD140716 (gG9), the coolest of the "constant" stars, is also suspected of varying slightly each year.



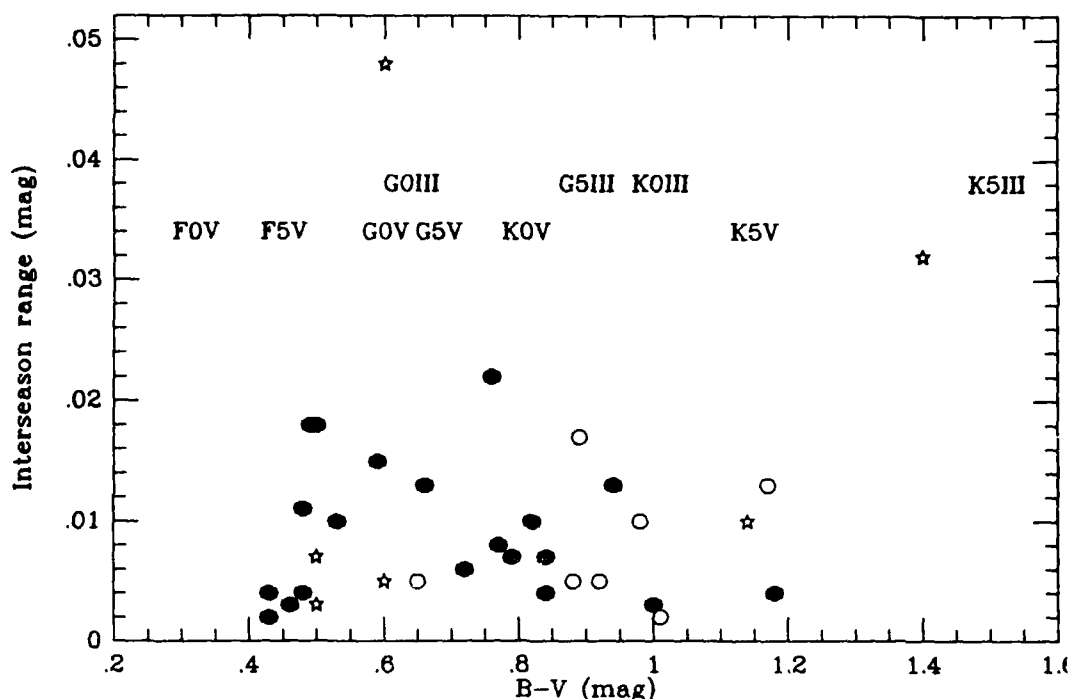


**Figure 15.** Interseason range for program and comparison stars that were judged variable according to the analysis of variance and correlated light curves. (*filled circles*) – luminosity class IV and V stars, (*open circles*) – luminosity class I, II, or III, (*stars*) – luminosity class unknown.

### 5.2 Possible long-term systematic effects

The most likely long-term systematic error source we could imagine has to do with the slowly changing color response of the photometer that might accompany the aging of the photomultiplier or the interference filters. Such an effect, if present, would be most easily seen as a drift in the differential magnitudes of two stars widely different in  $B - V$  color (cf. Figure 8). The group of least-variable stars (Table 7) contains pairs of stars whose  $B - V$  colors differ by up to 0.6 mag. On Figure 16 are plotted the colors of the hotter members of the various pairs as a function of color difference, using symbols whose size represents the range of variation (larger symbols for larger range, up to 0.003 mag). There is no tendency for the star pairs with the larger ranges of variability to cluster anywhere on this diagram; therefore we conclude that systematic color-related effects are absent.

### 5.3. The large-range variable stars: incipient cycles?

Stars exhibiting “large” variations (i.e.,  $>0.5\%$  peak-to-peak in the light curve of annual mean magnitudes) over the four-year course of this program (cf. Table 4) comprise about one-fourth of the total sample and are found predominantly among the program stars. These stars are listed in Table 8 along with an indication of their intraseason variability: a “V” signifies consistent variability in two or more seasons, and a “C” signifies nonvariability in most seasons. Typical values of the intraseason

TABLE 7. The Least-Variable Stars

HD	Spectral Type	Range (mag)	AOV	Average s.d.	Note
2488	F5	0.0013	C	0.0027	
1388	G0 V				
10697	G5 IV	0.0009	C	0.0022	
11326	G5				
13121	G0 V	0.0020	C	0.0021	<i>uvby</i> , HK std, $\log R'_{\text{HK}} = -5.21$
13683	F0				
18256	F6 V	0.0011	C	0.0017	$\log R'_{\text{HK}} = -4.79$
18404	F5 IV				
18404	F5 IV	0.0024	v	0.0019	
17659	F8				Variable?
23256	F2	0.0019	v	0.0020	Three seasons only
22679	G5				
76572	F6 V	0.0024	V	0.0020	HK std, $\log R'_{\text{HK}} = -4.94$ , variable
73596	F5 III				Var? each year
76572	F6 V	0.0020	V	0.0019	
78234	F2 V				
73596	F5 III	0.0007	C	0.0022	Var? each year
78234	F2 V				
83951	F3 V	0.0018	V	0.0019	Three seasons only
83525	F5				
103095	G8 VI	0.0015	v	0.0018	<i>uvby</i> std, $\log R'_{\text{HK}} = -4.87$
103520	K0 III				Var? in two seasons
103095	G8 VI	0.0028	V	0.0016	
101606	F4 V				<i>uvby</i> std, variable
124570	F6 IV	0.0025	V	0.0017	HK std, $\log R'_{\text{HK}} = -5.14$
125451	F5 IV				
129390	F2	0.0014	C	0.0027	
131330	F8				

dispersion (*b* and *y* averaged), and the interseason observed range are listed.

The sixteen program stars listed in Table 8 are for the most part consistently variable on intraseason time scales as well. Only four stars, those with the smallest

TABLE 7. The Least-Variable Stars continued.

HD	Spectral Type	Range (mag)	AOV	Average s.d.	Note
143761	G0 +Va	0.0022	V	0.0016	<i>uvby</i> , MK, HK std, $\log R'_{HK} = -5.02$ Variable
142091	K1 Va				
143761	G0 +Va	0.0014	C	0.0020	Slightly variable?
140716	gG9				
142091	K1 Va	0.0029	V	0.0017	Variable
140716	gG9				
157856	F3 V	0.0025	v	0.0025	$\log R'_{HK} = -4.70$ , variable?
157347	G5 IV				
156635	F8	0.0015	C	0.0022	
157347	G5 IV				
176095	F5 IV	0.0025	V	0.0023	$\log R'_{HK} = -4.68$
175515	K0 III				
182572	G8 IV	0.0017	v	0.0018	MK std, $\log R'_{HK} = -5.03$
180868	F0 IV				
200031	G5 III	0.0015	v	0.0020	<i>uvby</i> , MK std, $\log R'_{HK} = -4.91$
201092	K7 V				
200031	G5 III	0.0027	V	0.0019	
200577	G8 III				
201092	K7 V	0.0021	V	0.0020	
200577	G8 III				
215704	K0	0.0026	V	0.0023	$\langle S \rangle = 0.25$ .
216175	G5				
216048	F0 IV-V	0.0014	C	0.0023	Both slightly variable?
217232	A8 V				

(and most Sun-like)  $\log R'_{HK}$  values, failed to exhibit consistent intraseason variability. The eight comparison stars were evenly divided, with just half consistently varying within two or more seasons. Because the sample here is small, it seems imprudent to attempt to make a distinction between the statistics of the program and comparison stars in Table 8, even though the latter, by and large, is comprised of more-luminous stars.

Do the light curves of these stars contain clues to the nature of the variability? Can random variability be distinguished from segments of cycles? To consider these

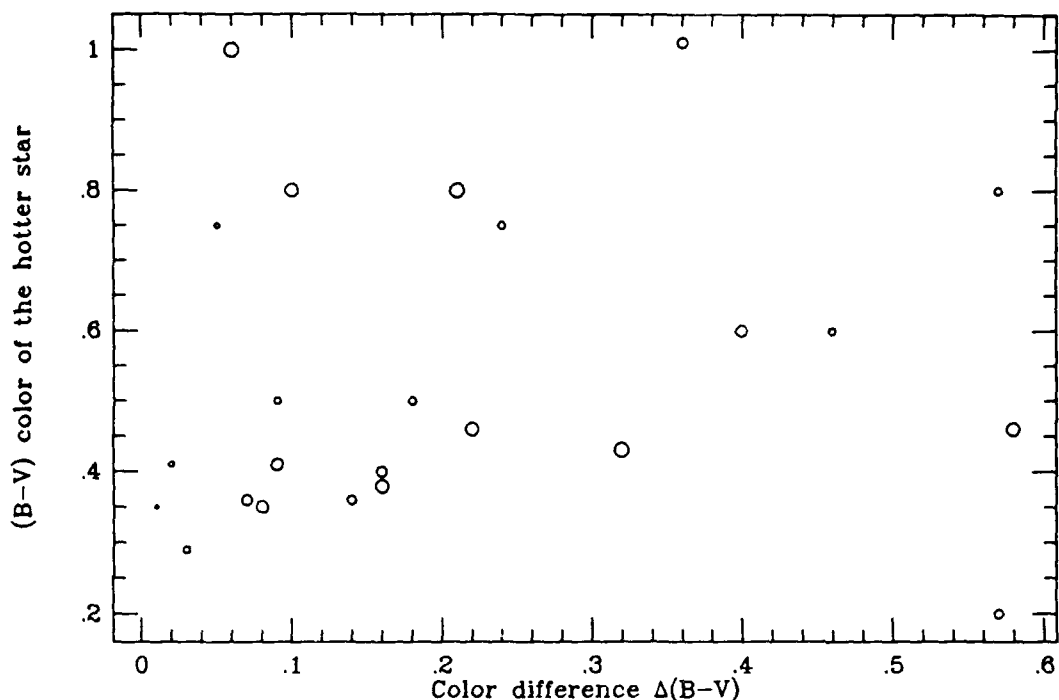


Figure 16.  $B - V$  colors of the hotter members of the pairs of least-variable stars from Table 7 as a function of color difference. The size of the symbols is related to the observed range of interseason variability, in the range 0.0007 mag–0.0029 mag.

questions, we examined the statistics of artificial “light curves” consisting of sets of four-point time series generated from normally distributed, consecutive random numbers. Fourteen percent of the artificial “light curves” thus generated were monotonic (steadily rising or falling), 52% contained a single maximum or minimum, and 34% contained two extrema—one maximum and one minimum. Thus 66% of the random-noise light curves had characteristics consistent with cycle segments where the periods are substantially longer than four years.

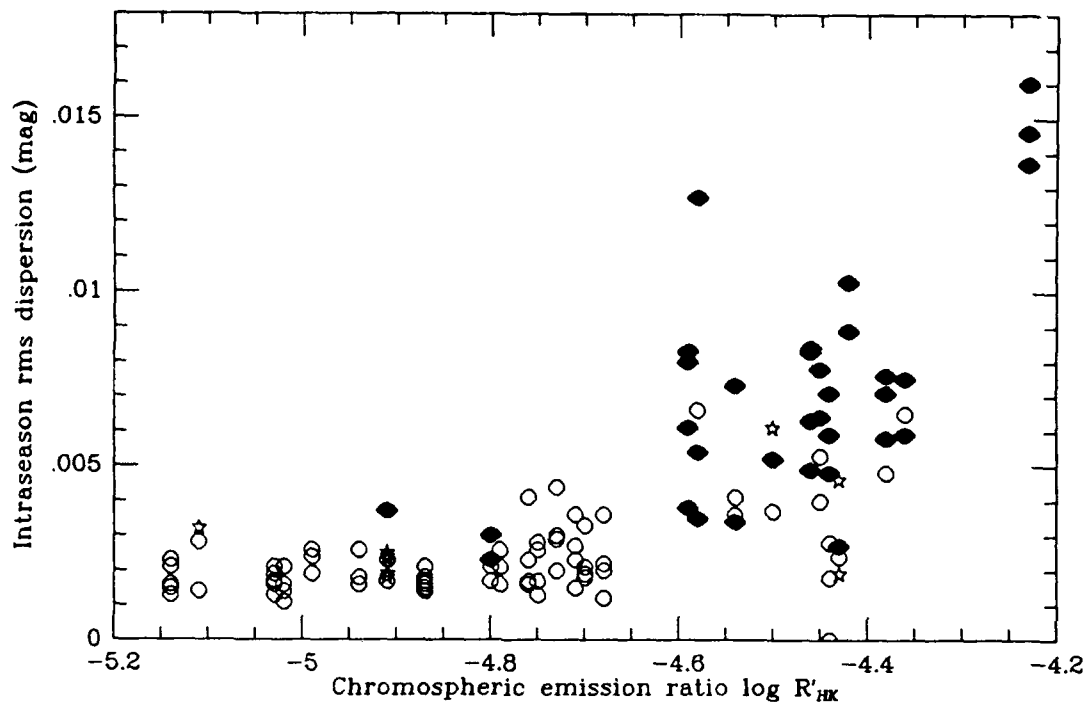
However, turning to the real data, only 13% of the observed light curves (Table 8) contained two extremes, 23% were monotonic, and 64% contained just a single maximum or minimum. Thus 86% were consistent with undersampled cyclic variation, compared with 66% of the artificial light curves, and the fraction of observed double-extrema light curves was less than half the fraction generated artificially. These statistics suggest that the observed light curves are slightly more consistent with short segments of some kind of cyclic phenomenon than with random noise on a one-year time scale. This conclusion is, of course, highly preliminary because of the short time base of available data; and it is prejudiced by the expectation that luminosity cycles, if detected, will be commensurate in length with the magnetic activity cycles.

TABLE 8. Strongly Varying Stars

HD	Spectral Type	Log $R'_{HK}$	Intra Season	Typ. rms Dispersion (mag)	Peak-Peak Range (mag)	Number of Extremes
<b>Program Stars</b>						
1835	G2V	-4.42	V	0.009	0.013	2
35296	F8V	-4.38	V	0.007	0.010	1
39587	G0V	-4.44	V	0.006	0.015	1
75332	F7Vn	-4.44	V	0.007	0.018	...
82885	G8IV-V	-4.58	V	0.007	0.008	1
82635	G8.5III	...	V	0.005	0.005	1
115383	G0Vs	-4.43	V(?)	0.003	0.015	1
115404	K1V+M1V	-4.46	V	0.007	0.013	1
120136	F6IV	-4.76	C	0.003	0.011	0
129333	G0	-4.23	V	0.017	0.048	0
149661	K2V	-4.54	V	0.006	0.010	1
152391	G7V	-4.45	V	0.007	0.022	1
158614	G9IV-V	-4.99	C	0.002	0.006	2
161239	G2IIb	-5.14	C	0.004	0.005	1
185144	K0V	-4.75	C	0.002	0.007	?
190007	K4	-4.59	V	0.007	0.010	1
<b>Comparison Stars</b>						
13611	G6II-III		C	0.002	0.017	0
112989	G9III		V	0.006	0.013	1
126426	F8V+G1V		V	0.004	0.018	1
129972	G8.5III		C	0.007	0.011	0
131511	K2V		V	0.003	?	0
160823	G0		C	0.004	0.005	2
160935	F5		C	0.003	0.007	1
215427	K5		V	0.010	0.032	1

## 6. PHOTOMETRIC VARIABILITY AND CHROMOSPHERIC ACTIVITY

Figure 17 shows the seasonal values of the dispersion,  $s_{by}$ , for each of the program stars as a function of the chromospheric emission ratio  $\log R'_{HK}$ . One symbol is plotted for each season's observations. Generally, the magnitude of variability each season is comparable, leading to the observed clustering of points on the diagram, and the conclusion that the amount of spot coverage may change only slowly with time. The G8IV-V program star HD82885 provides an example where the  $s_{by}$  values have showed a clear evolution: in four consecutive seasons,  $s_{by} = 0.0066$ , 0.0127 (with a rotational period determined), 0.0057, and 0.0035 mag. Obviously, it is important to determine if the changes in seasonal activity are in any way cyclic and if the intraseason variability can be related to the average brightness.



**Figure 17.** Intraseason standard deviation,  $s_{by}$ , as a function of the chromospheric emission ratio  $\log R'_{HK}$ . Each star is plotted once for each season in which a variability decision could be made. (*open circles*) – constant, (*star*) – possibly variable, (*filled circles*) – variable.

In Figure 17, the onset of consistent intraseason activity occurs rather suddenly at a value of  $\log R'_{HK} \sim -4.6$ , about twice (in linear units) the solar value of  $-4.94$ . In this regard, the data seem rather significantly grouped: there is only one program star with  $\log R'_{HK} > -4.6$  with an observed intraseason dispersion less than 0.003 mag. Below  $-4.6$ , the regime of the true solar analogs, the opposite holds: no star is more variable than about 0.004 mag. We note that the Sun itself, if observed in this manner, would be seen as quiescent, with a dispersion well under 0.001 mag.

Figure 18 shows the three- or four-year range of variation for the program stars as a function of the chromospheric emission ratio,  $\log R'_{HK}$ . The error bar tails indicate the 95% confidence interval: if the error bar lies fully above zero, the star is considered variable. By this criterion, most of the program stars seem to be variable. Note the position of the Sun on the diagram, based on an estimated cyclic amplitude of 0.1%.

Unlike intraseason variability, the ranges of interseason variation do not show a distinct grouping, except for the general rise with increasing  $\log R'_{HK}$ . In particular, among the "active" stars ( $\log R'_{HK} > -4.6$ ), some stars maintain a very small range of observed long-term variation.

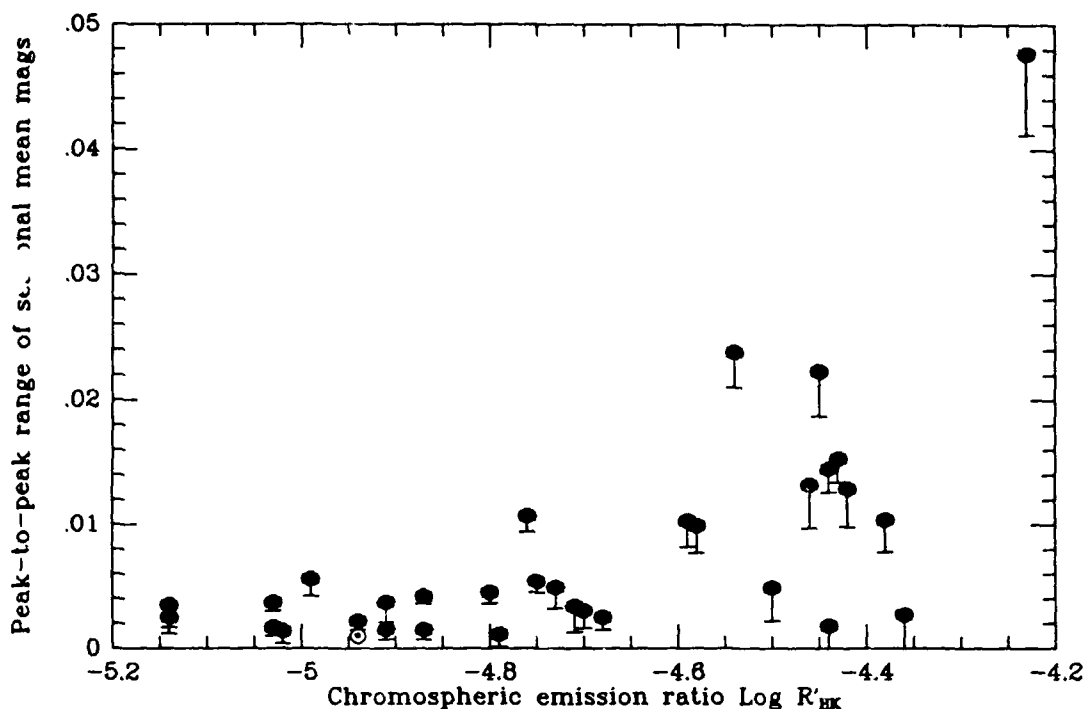


**Figure 18.** Interseason range of variation over four years plotted as a function of the chromospheric emission ratio  $\log R'_{HK}$ . The error bar "tails" indicate the 95% confidence interval for the range: if the bars lie above zero, the star is considered variable.

Intraseason and interseason variability are intimately related, at least among the program stars. Of the 16 program stars considered "strongly variable" because their four-year ranges exceed 0.005 mag, all but four have values of  $\log R'_{HK} > -4.6$ , and it is these four alone, those most like the Sun in terms of emission ratio, that fail to display intraseason variability as well. These four stars are HD120136 (F6IV), HD158614 (G9IV-V), HD161239 (G2IIIb—the sole giant), and HD190007 (K4).

## 7. SUMMARY AND CONCLUSIONS

To characterize the luminosity variations of stars similar to the Sun but covering a range of stellar age, we have obtained over 2,000 nightly observations of 36 program stars during the interval March 1984 through December 1987. Chromospheric activity in the program stars was previously monitored for a decade by O. C. Wilson, who discovered that many of the presumably old solar analog stars exhibited cycles of magnetic activity similar to that of the Sun. The program stars were selected to bracket the Sun in several observable quantities: (1) temperature, as suggested by  $B - V$  color and MK spectral type; (2) age, as suggested by atomic abundances and chromospheric activity; (3) rotation rate, as indicated by periodicities in the strength of chromospheric emission; (4) mass, as inferred from a variety of generally accepted astrophysical relationships; and (5) known cyclic behavior of magnetic activity.

The stars were measured differentially at 472 and 551 nm with respect to two or three nearby comparison stars of similar brightness and color, with the aim of obtaining the most precise observations possible. Accordingly, we have devoted considerable attention to "quality control": all observations were made using a standard time-tested procedure that has built-in checks of consistency and precision and which produces data sets of equal statistical weight, unbiased with regard to *a priori* assumptions about which star(s) within groups may be variable. Though not obtained using a fully randomized design, the observations seem to be free of temporal artifacts and the results demonstrate a precision that exceeds the expectations of the original experimental objective.

The principal conclusions of this study are:

1. About one-half the program stars and one-fourth the comparison stars are demonstrably variable on intraseason time scales, as indicated by (a) the magnitude of the night-to-night dispersion of differential magnitudes, (b) the correlation of pairs and trios of light curves having a variable star in common, (c) the repeated occurrence of large dispersions in two or more independent observing seasons, and (d) the ratio of dispersions in the two filter passbands, consistent with a "starspot" model of irradiance variation. The boundary between variable and nonvariable stars is about 0.003 mag (0.3%) rms in the cycle-to-cycle dispersion of averaged *b* and *y* differential magnitudes averaged together. The range of recorded variability is from 0.002–0.02 mag, with a median of 0.006 mag (compared with a median value of 0.002 mag for constant stars).

2. The incidence of intraseason variability is essentially independent of luminosity class—about 40% for classes I–III and IV–V alike—but is about twice as likely among K stars (63%) as among F and G stars, regardless of luminosity. However the amplitude of observed variation among the consistently variable stars is essentially independent of *B* – *V* color, even though it may arise from different physical phenomena, depending upon temperature and luminosity.

3. The determination of rotation periods is relatively more difficult from photometry than from the chromospheric HK index because the signal amplitudes are much smaller. Nonetheless, rotation periods were determined for nine stars, including three for which no HK rotation rates were available. For four stars, rotation periods were measured in at least two seasons, but the data are insufficient to tell if the season-to-season differences are significant.

4. Using principally an analysis of variance, most of the differential light curves exhibited statistically significant interseason variations with three- or four-year peak-to-peak ranges from 0.002–0.05 mag (0.2–5%). With only four data points per light curve, a formal correlation analysis is premature; however, in many cases, simple inspection of the ensemble of light curves is sufficient to identify variable stars unambiguously. Twenty-four stars (including 16 of the 36 program stars) exhibited large enough ranges (>0.005 mag) in two or more light curves to indicate variability beyond reasonable doubt. Such large-range variability was relatively uncommon among the comparison stars, occurring in only 8 out of a total of 61



stars observed in three or more seasons. By usual standards, therefore, a great majority of comparison stars are stable enough to be used as standard stars for conventional photometry, even though they may be demonstrably variable by small amounts. Nearly all the stars that vary strongly on interseason time scales are consistently variable on intraseason time scales, with the notable exception of four program stars with near-solar values of  $\log R'_{HK}$  (see below).

5. Variability of the program stars is a strong function of the chromospheric emission ratio  $R'_{HK}$ , and it tends to repeat at about the same level from year to year. Consistent intraseason variability is observed in stars with emission ratios about twice the solar value and greater ( $\log R'_{HK} > -4.6$ ). Interseason variability likewise is a strong function of emission ratio, but four stars with near-solar values of  $\log R'_{HK}$  have shown total ranges greater than 0.005 mag, even though intraseason variability was absent.

6. The identification of cyclic behavior is not yet possible for program stars because the time base is insufficient. However, it is significant that of the 16 program stars exhibiting total four-year ranges greater than 0.005 mag, twelve of the light curves are consistent with cyclic variation: either they rise or fall monotonically, or they exhibit at most one extremum—i.e., “flickering” is rarely seen. This strongly suggests that further observation will reveal cyclic variation.

## REFERENCES

- Abbott, C. 1963. *Smithsonian Misc. Collection* **146**, No. 3.  
 Abt, H. A. 1981. *Astrophys. J. Suppl. Ser.* **45**, 437.  
 Abt, H. A. 1986. *Astrophys. J.* **309**, 260.  
 Argue, A. N. 1966. *Mon. Not. R. Astron. Soc.* **133**, 475.  
 Baize, P. 1985. *Astron. Astrophys.. Suppl.* **60**, 333.  
 Baliunas, S. L., Horne, J. H., Porter, A., Duncan, D. K., Frazer, J., Lanning, H., Misch, A., Mueller, J., Noyes, R. W., Soyumer, D., Vaughan, A. H., and Woodard, L. 1985. *Astrophys. J.* **294**, 310.  
 Baliunas, S. L., and Vaughan, A. H. 1985. *Ann. Rev. Astron. Astrophys. J.* **23**, 379.  
 Baliunas, S. L., Vaughan, A. H., Hartmann, L. W., Middelkoop, F., Mihalas, D., Noyes, R. W., Preston, G. W., Frazer, J., and Lanning, H. 1983. *Astrophys. J.* **275**, 752.  
 Beavers, W. I., and Salzer, J. J. 1983. *Publ. Astron. Soc. Pac.* **95**, 79.  
 Bidelman, W. P. 1983. *Astron. J.* **88**, 1182.  
 Blanco, C., Catalano, S., and Marilli, E. 1979. *Astron. Astrophys. Suppl.* **36**, 297.  
 Blazit, A., Bonneau, D., and Foy, R. 1987. *Astron. Astrophys. Suppl.* **71**, 57.  
 Bohm-Vitense, E., and Johnson, H. R. 1985. *Astrophys. J.* **293**, 288.  
 Boyd, L. J., Genet, R. M., and Hall, D. S. 1984. *IAU Inf. Bull. Var. Stars* 2561, 2563.  
 Boyd, L. J., Genet, R. M., and Hall, D. S. 1985. *IAU Inf. Bull. Var. Stars* 2680.  
 Breger, M. 1969. *Astrophys. J. Suppl. Ser.* **19**, 79.  
 Campbell, B., and Cayrel, R. 1984. *Astrophys. J.* **283**, L17.  
 Cayrel de Strobel, G., Knowles, N., Hernandez, G., and Bentolila, C. 1981. *Astron.*

- Astrophys.* **94**, 1.
- Chugainov, P. F. 1976. *Izv. Krym. Astrofiz.* **54**, 89.
- Chugainov, P. F. 1980. *Izv. Krym. Astrofiz.* **61**, 121.
- Cowley, A. P., and Bidelman, W. P. 1979. *Publ. Astron. Soc. Pac.* **91**, 83.
- Dickinson, R. E. 1987. In *Solar Radiative Output Variations*, P. Foukal, ed. (National Center for Atmospheric Research, Boulder, Colorado), p. 49.
- Dorren, J. D., and Guinan, E. F. 1982. *Astron. J.* **87**, 1546.
- Duquennoy, A., and Mayor, M. 1988. *Astron. Astrophys.* **195**, 129.
- Eddy, J. A. 1976. *Science* **192**, 1189.
- Eggen, O. J. 1973. *Publ. Astron. Soc. Pac.* **85**, 289.
- Eggen, O. J. 1985. *Astron. J.* **90**, 1250.
- Fekel, F. C., Moffett, T. C., and Henry, G. W. 1986. *Astrophys. J. Suppl. Ser.* **60**, 551.
- Fernie, J. D. 1986. *Astrophys. J.* **306**, 642.
- Fitzgerald, M. P. 1970. *Astron. Astrophys.* **4**, 234.
- Foukal, P., and Lean, J. 1987. In *Solar Radiative Output Variations*, P. Foukal, ed. (National Center for Atmospheric Research, Boulder, Colorado), p. 323.
- Foukal, P., and Lean, J. 1988. *Astrophys. J.* **328**, 347.
- Gomez, A. E. and Abt, H. A. 1982. *Publ. Astron. Soc. Pac.* **94**, 650.
- Griffin, R. 1982. *Observatory* **102**, 82.
- Gutierrez-Moreno, H., Stock, J., Torres, C., and Wroblewski, H. 1966. *Publ. Cerro Calan* **11**, 1.
- Hardorp, J. 1978. *Astron. Astrophys.* **63**, 383.
- Hardorp, J. 1982. *Astron. Astrophys.* **105**, 120.
- Hartkopf, W. I., and McAlister, H. A. 1984. *Publ. Astron. Soc. Pac.* **96**, 105.
- Heintz, W. D. 1984. *Publ. Astron. Soc. Pac.* **96**, 557.
- Heintz, W. D. 1988. *Astron. Astrophys. Suppl.* **72**, 543.
- Hoyt, D. V., and Eddy, J. A. 1982. NCAR Tech Note TN-194+STR.
- Jerzykiewicz, M., and Serkowski, K. 1966. *Lowell Obs. Bull.* **6** (137), 295.
- Johnson, H. L., and Morgan, W. W. 1953. *Astrophys. J.* **117**, 313.
- Joy, A. H., and Abt, H. A. 1974. *Astrophys. J. Suppl. Ser.* **28**, 1.
- Kaitting, M. K. 1985. *J. Amer. Assoc. Var. Star Obs.* **14**, 15.
- Keenan, P. C., and Pitts, R. E. 1980. *Astrophys. J. Suppl. Ser.* **42**, 541.
- Khaliullin, K. H., Mironov, A. V., and Moshkalyov, V. G. 1985. *Ap. and Space Sci.* **111**, 291.
- Labitzke, K. 1987. *Geophys. Res. Lett.* **14**, 535.
- Lean J., and Foukal, P. 1988. *Science* **240**, 906.
- Lockwood, G. W. 1983. In *Solar System Photometry Handbook*, R. Genet, ed. (Willmann-Bell, Richmond), Chapter 2, pp. 2-1 to 2-19.
- Lockwood, G. W. 1984. In *Proceedings of the Workshop on Improvements to Photometry*, NASA Conference Publication 2350, W. A. Borucki and A. Young, eds. (NASA, Washington, D. C.), pp. 79-87.
- Lockwood, G. W., and Skiff, B. A. 1987. In *Proceedings of the Workshop on Improvements to Photometry*, NASA Conference Publication W. A. Borucki and A. Young, eds. (NASA, Washington, D. C.), in press.
- Lockwood, G. W., and Thompson, D. T. 1986a. *Science* **234**, 1543.

- Lockwood, G. W., and Thompson, D. T. 1986b. *Astron. J.* **92**, 976.
- Lockwood, G. W., Thompson, D. T., and Lumme, K. 1980. *Astron. J.* **85**, 961.
- Lockwood, G. W., Thompson, D. T., Radick, R. R., Osborn, W. H., Baggett, W. E., Duncan, D. K., and Hartmann, L. W. 1984. *Publ. Astron. Soc. Pac.* **96**, 714.
- McAlister, H. A., Hartkopf, W. L., Gaston, B. J., Hendry, E. M., Fekel, F. C. 1984. *Astrophys. J. Suppl. Ser.* **54**, 251.
- Middelkoop, F. 1982. *Astron. Astrophys.* **113**, 1.
- Morbey, C. L., and Griffin, R. F. 1987. *Astrophys. J.* **317**, 343.
- Neckel, H. 1986. *Astron. Astrophys.* **169**, 194.
- Neff, J. S. 1968. *Astron. J.* **73**, 75.
- Noyes, R. W., Hartmann, L. W., Baliunas, S. L., Duncan, D. K., and Vaughan, A. H. 1984. *Astrophys. J.* **279**, 763.
- Perry, C. L., Olsen, E. H., and Crawford, D. L. 1987. *Publ. Astron. Soc. Pacific* **99**, 1184.
- Radick, R. R., Thompson, D. T., Lockwood, G. W., Duncan, D. K., and Baggett, W. E. 1987. *Astrophys. J.* **321**, 459.
- Radick, R. R., Wilkerson, M. S., Worden, S. P., Africano, J. L., Klimke, A., Ruden, S., Rogers, W., Armandroff, T. E., and Giampapa, M. S. 1983. *Publ. Astron. Soc. Pac.* **95**, 300.
- Ramanathan, V. 1988. *Science* **240**, 293.
- Roach, F. E., and Gordon, J. L. 1973. *The Light of the Night Sky* (D. Reidel, Dordrecht), p. 11.
- Rufener, F. 1981. *Astron. Astrophys. Suppl.* **45**, 207.
- Rybka, E. 1979. *Astron. Acta* **29**, 177.
- Scargle, J. D. 1982. *Astrophys. J.* **263**, 835.
- Schild, R. E. 1973. *Astron. J.* **78**, 37.
- Simon, T. 1986. *Astron. J.* **91**, 1233.
- Skiff, B. A., and Lockwood, G. W. 1986. *Publ. Astron. Soc. Pac.* **98**, 338.
- Soderblom, D. B. 1985. *Astron. J.* **90**, 2103.
- Soderblom, D. B., and Clements, S. D. 1987. *Astron. J.* **93**, 920.
- Strassmeier, K., and Hall, D. S. 1988. *Astrophys. J. Suppl. Ser.* **67**, 439. 339
- Tinsley, B. A. 1988. *Geophys. Res. Lett.* **15**, 409.
- Vaughan, A. H. 1980. *Publ. Astron. Soc. Pac.* **92**, 392.
- Vaughan, A. H., Baliunas, S. L., Middelkoop, F., Hartmann, L. W., Mihalas, D., Noyes, R. W., and Preston, G. W. 1981. *Astrophys. J.* **250**, 276.
- White, N. M., and Feigerman, B. H. 1987. *Astron. J.* **94**, 751.
- Wilson, O. C. 1978. *Astrophys. J.* **226**, 379.
- Wilson, O. C. 1982. *Astrophys. J.* **257**, 179.
- Willson, R. C. 1982. *J. Geophys. Res.* **87**, 4319.
- Willson, R. C. 1987. In *Solar Radiative Output Variations*, P. Foukal, ed. (National Center for Atmospheric Research, Boulder, Colorado), p. 143.
- Willson, R. C., Gulkis, S., Janssen, M., Hudson, H. S., and Chapman, G. A. 1981. *Science* **211**, 700.
- Willson, R. C., Hudson, H. S., Frohlich, C., and Brusa, R. W. 1986. *Science* **234**, 1114.

- Wolff, S. C., Boesgaard, A. M., and Simon, T. 1986. *Astrophys. J.* **310**, 360.
- Young, A., Mielbrecht, R. A., and Abt, H. A. 1987. *Astrophys. J.* **317**, 787.
- Young, A. T. 1974. *Methods in Experimental Physics*, Vol. 12, Part A, N. Carleton, ed. (Academic Press, New York), Chapters 1 and 2.

### TYPICAL RAW DATA FILE AS RECORDED AT THE TELESCOPE

Entries to the right of the colons in the eight-line header are system defaults and information provided by the observer. Additionally, remarks may be inserted into the data stream at any point and are keyed by the time of entry (this file happens to have none).

One data line is produced for each 10-second integration. The columns, respectively, are UT month, day, year, hour, minute, second, star identification (in this case 2, 1, 4, or 3), filter number (2 =  $\text{Sr}^{90}$  source, 3 =  $y$ , 4 =  $b$ ), whether the observation is a "star" or a "sky" (ST or SK), a numerical code for the same information, and, finally, the number of counts recorded.

The order of integrations is the same as indicated in §2.3 (page 17): Dark, std source, std source, sky, sky, star, star, star .... Note at 04:51:51 the filter is changed from  $y$  to  $b$ , and at 05:06:10 from  $b$  back to  $y$ . The total elapsed time for four cycles,  $y, b, b, y$  is 31 minutes, yielding a data collection efficiency of 75% (a remarkable feat for a manually slewed telescope!).

OBSERVER: BAS ON LVS099, 870328.Q02  
 PROGRAM: LVSSS.HD 82885  
 WEATHER: CLEAR > WEAK TROUGH, CALM, DARK  
 COMMENTS: DIAPHRAGM 4, SEEING ~8"  
 TEMPERATURE: 24F, BOX @ 69F  
 TELESCOPE: 21 INCH  
 INTEG. TIME:10 SEC  
 S/N: 300 NPAUSS: 10 NPAUSB: 10

03 28 1987	04 43 06	2	2	SK	2	178
03 28 1987	04 43 19	2	2	ST	1	390983
03 28 1987	04 43 29	2	2	ST	1	389210
03 28 1987	04 43 41	2	3	SK	2	2098
03 28 1987	04 43 51	2	3	SK	2	2046
03 28 1987	04 44 08	2	3	ST	1	1706123
03 28 1987	04 44 18	2	3	ST	1	1702900
03 28 1987	04 44 28	2	3	ST	1	1699656
03 28 1987	04 44 55	1	3	ST	1	783740
03 28 1987	04 45 05	1	3	ST	1	784869
03 28 1987	04 45 15	1	3	ST	1	783002
03 28 1987	04 45 27	1	3	SK	2	2123
03 28 1987	04 45 37	1	3	SK	2	2102
03 28 1987	04 45 54	1	3	ST	1	784580
03 28 1987	04 46 04	1	3	ST	1	783807
03 28 1987	04 46 14	1	3	ST	1	781933
03 28 1987	04 46 44	4	3	ST	1	196831
03 28 1987	04 46 54	4	3	ST	1	198792
03 28 1987	04 47 04	4	3	ST	1	196888
03 28 1987	04 47 17	4	3	SK	2	1907
03 28 1987	04 47 27	4	3	SK	2	1895
03 28 1987	04 47 46	4	3	ST	1	198000
03 28 1987	04 47 56	4	3	ST	1	197245
03 28 1987	04 48 07	4	3	ST	1	197541
03 28 1987	04 48 34	3	3	ST	1	400397
03 28 1987	04 48 44	3	3	ST	1	399742
03 28 1987	04 48 54	3	3	ST	1	399286
03 28 1987	04 49 06	3	3	SK	2	2059
03 28 1987	04 49 17	3	3	SK	2	2048
03 28 1987	04 49 34	3	3	ST	1	401987
03 28 1987	04 49 44	3	3	ST	1	397263
03 28 1987	04 49 55	3	3	ST	1	398786

03 28 1987	04 50 21	2	3	ST	1	1696854
03 28 1987	04 50 31	2	3	ST	1	1702772
03 28 1987	04 50 41	2	3	ST	1	1701605
03 28 1987	04 50 55	2	3	SK	2	2041
03 28 1987	04 51 06	2	3	SK	2	2158
03 28 1987	04 51 19	2	4	SK	2	1487
03 28 1987	04 51 29	2	4	SK	2	1419
03 28 1987	04 51 48	2	4	ST	1	2103694
03 28 1987	04 51 59	2	4	ST	1	2114661
03 28 1987	04 52 09	2	4	ST	1	2114694
03 28 1987	04 52 34	1	4	ST	1	1040512
03 28 1987	04 52 44	1	4	ST	1	1044046
03 28 1987	04 52 54	1	4	ST	1	1038937
03 28 1987	04 53 06	1	4	SK	2	1354
03 28 1987	04 53 16	1	4	SK	2	1403
03 28 1987	04 53 37	1	4	ST	1	1039723
03 28 1987	04 53 47	1	4	ST	1	1040253
03 28 1987	04 53 57	1	4	ST	1	1041398
03 28 1987	04 54 24	4	4	ST	1	296813
03 28 1987	04 54 34	4	4	ST	1	298029
03 28 1987	04 54 44	4	4	ST	1	296944
03 28 1987	04 54 56	4	4	SK	2	1300
03 28 1987	04 55 06	4	4	SK	2	1322
03 28 1987	04 55 24	4	4	ST	1	296049
03 28 1987	04 55 34	4	4	ST	1	296342
03 28 1987	04 55 44	4	4	ST	1	297123
03 28 1987	04 56 09	3	4	ST	1	646679
03 28 1987	04 56 19	3	4	ST	1	647020
03 28 1987	04 56 30	3	4	ST	1	647352
03 28 1987	04 56 41	3	4	SK	2	1354
03 28 1987	04 56 51	3	4	SK	2	1365
03 28 1987	04 57 11	3	4	ST	1	647989
03 28 1987	04 57 21	3	4	ST	1	644257
03 28 1987	04 57 31	3	4	ST	1	644874
03 28 1987	04 58 03	2	4	ST	1	2111821
03 28 1987	04 58 13	2	4	ST	1	2117788
03 28 1987	04 58 23	2	4	ST	1	2110270
03 28 1987	04 58 35	2	4	SK	2	1538
03 28 1987	04 58 45	2	4	SK	2	1399
03 28 1987	04 59 05	2	4	ST	1	2104792
03 28 1987	04 59 15	2	4	ST	1	2104374
03 28 1987	04 59 25	2	4	ST	1	2107944

03 28 1987	04 59 53	1	4	ST	1	1043625
03 28 1987	05 00 03	1	4	ST	1	1050818
03 28 1987	05 00 13	1	4	ST	1	1037219
03 28 1987	05 00 25	1	4	SK	2	1361
03 28 1987	05 00 35	1	4	SK	2	1357
03 28 1987	05 00 51	1	4	ST	1	1045662
03 28 1987	05 01 01	1	4	ST	1	1041850
03 28 1987	05 01 11	1	4	ST	1	1042583
03 28 1987	05 01 38	4	4	ST	1	297718
03 28 1987	05 01 48	4	4	ST	1	296424
03 28 1987	05 01 58	4	4	ST	1	297957
03 28 1987	05 02 10	4	4	SK	2	1305
03 28 1987	05 02 20	4	4	SK	2	1262
03 28 1987	05 02 37	4	4	ST	1	296825
03 28 1987	05 02 47	4	4	ST	1	295665
03 28 1987	05 02 57	4	4	ST	1	295704
03 28 1987	05 03 24	3	4	ST	1	647121
03 28 1987	05 03 34	3	4	ST	1	645897
03 28 1987	05 03 44	3	4	ST	1	643341
03 28 1987	05 03 56	3	4	SK	2	1417
03 28 1987	05 04 06	3	4	SK	2	1388
03 28 1987	05 04 23	3	4	ST	1	646031
03 28 1987	05 04 33	3	4	ST	1	646196
03 28 1987	05 04 43	3	4	ST	1	644847
03 28 1987	05 05 13	2	4	ST	1	2102190
03 28 1987	05 05 23	2	4	ST	1	2113119
03 28 1987	05 05 33	2	4	ST	1	2112761
03 28 1987	05 05 46	2	4	SK	2	1485
03 28 1987	05 05 56	2	4	SK	2	1396
03 28 1987	05 06 10	2	3	SK	2	2065
03 28 1987	05 06 20	2	3	SK	2	2047
03 28 1987	05 06 39	2	3	ST	1	1699506
03 28 1987	05 06 49	2	3	ST	1	1703262
03 28 1987	05 06 59	2	3	ST	1	1704188
03 28 1987	05 07 24	1	3	ST	1	786593
03 28 1987	05 07 35	1	3	ST	1	790224
03 28 1987	05 07 45	1	3	ST	1	783932
03 28 1987	05 07 57	1	3	SK	2	2028
03 28 1987	05 08 07	1	3	SK	2	2000
03 28 1987	05 08 26	1	3	ST	1	782534
03 28 1987	05 08 36	1	3	ST	1	782951
03 28 1987	05 08 46	1	3	ST	1	782128



03 28 1987	05 09 13	4	3	ST	1	197812
03 28 1987	05 09 23	4	3	ST	1	198589
03 28 1987	05 09 33	4	3	ST	1	197407
03 28 1987	05 09 45	4	3	SK	2	1971
03 28 1987	05 09 55	4	3	SK	2	1923
03 28 1987	05 10 11	4	3	ST	1	197126
03 28 1987	05 10 21	4	3	ST	1	198257
03 28 1987	05 10 31	4	3	ST	1	195730
03 28 1987	05 11 02	3	3	ST	1	400082
03 28 1987	05 11 12	3	3	ST	1	399779
03 28 1987	05 11 22	3	3	ST	1	403006
03 28 1987	05 11 34	3	3	SK	2	2093
03 28 1987	05 11 44	3	3	SK	2	2173
03 28 1987	05 12 01	3	3	ST	1	401794
03 28 1987	05 12 11	3	3	ST	1	402532
03 28 1987	05 12 22	3	3	ST	1	400210
03 28 1987	05 12 51	2	3	ST	1	1700011
03 28 1987	05 13 01	2	3	ST	1	1701801
03 28 1987	05 13 11	2	3	ST	1	1700465
03 28 1987	05 13 23	2	3	SK	2	2092
03 28 1987	05 13 33	2	3	SK	2	2158
03 28 1987	05 13 47	2	2	ST	1	389807
03 28 1987	05 13 57	2	2	ST	1	391184
03 28 1987	05 14 13	2	2	SK	2	166

## REDUCED DATA OUTPUT, SAMPLE PRINTED FILE

On the first page, header information from the raw data file is repeated, amended to include input and output file names, the name of the file in which star positions are found, assumed value of extinction, and assumed positions of the stars in the group. The tabulation following gives the fractional time of day, an internal star identification number, filter number ( $S = \text{standard source}$ ,  $4 = y$ ,  $2 = b$ ), instrumental magnitudes for each sequence of three 10-second integrations (corrected for sky background, pulse pair dead time, and atmospheric extinction), and in the final column an indication of outlying data points (if any).

The second page includes in the upper section a tabulation of the differential magnitudes and differential air masses for each pairwise combination and for each cycle of observation. These values are reported, cycle by cycle, to the stored output file named in the header on the previous page, and are used for further analysis.

Finally, a summary at the bottom of the page provides averaged differential magnitudes for that particular data set.

PHOTOMETRY OF HD 82885

RAW DATA FILE: 870328.Q02      POSITION FILE: LVSSS.POS

INPUT FILE: 870328.S04      GROUP IDENT.= 4

OUTPUT FILE: 870328.T04      EXTINCTION: KB= 0.230 KV= 0.360 KY= 0.170

OBSERVER: BAS ON LVS099, 870328.Q02

PROGRAM: LVSSS.HD 82885

WEATHER: CLEAR > WEAK TROUGH, CALM, DARK

COMMENTS: DIAPHRAGM 4, SEEING ~8"

TEMPERATURE: 24F, BOX @ 69F

TELESCOPE: 21 INCH

INTLG. TIME: 10 SEC

S/N:300

NPAUSS:10

NPAUSB:10

COORDINATES OF OBJECT 1      9 35.7 35 49

COORDINATES OF OBJECT 2      9 34.2 36 24

COORDINATES OF OBJECT 3      9 42.7 35 6

COORDINATES OF OBJECT 4      9 40.0 35 20

DATE (U.T.)

1987 3 28

STAR- SKY

FRAC. DAY   \*   F      D      A.M.   N   COUNT > 2 SIGMA FROM MEAN

--      S   -   6.0204   --

0.1974      2   4   4.2140   1.0003   3

0.1980      1   4   5.0930   1.0001   3

0.1987      1   4   5.0936   1.0002   3

0.1992      4   4   6.6005   1.0000   3

0.2000      4   4   6.6000   1.0000   3

0.2005      3   4   5.8288   1.0000   3

0.2012      3   4   5.8300   1.0000   3

0.2017      2   4   4.2155   1.0008   3

0.2028      2   2   3.9478   1.0010   3

0.2033      1   2   4.7218   1.0008   3

0.2040      1   2   4.7225   1.0009   3

0.2046      4   2   6.0902   1.0004   3

0.2053      4   2   6.0930   1.0005   3

0.2058      3   2   5.2414   1.0003   3

0.2065      3   2   5.2436   1.0004   3

0.2071      2   2   3.9463   1.0022   3

0.2078	2	2	3.9502	1.0024	3
0.2084	1	2	4.7186	1.0021	3
0.2090	1	2	4.7191	1.0023	3
0.2096	4	2	6.0895	1.0015	3
0.2103	4	2	6.0942	1.0017	3
0.2108	3	2	5.2439	1.0014	3
0.2115	3	2	5.2434	1.0015	3
0.2121	2	2	3.9479	1.0041	3
0.2131	2	4	4.2436	1.0046	3
0.2136	1	4	5.0880	1.0042	3
0.2143	1	4	5.0940	1.0045	3
0.2148	4	4	6.5978	1.0034	3
0.2155	4	4	6.6527	1.0037	3
0.2161	3	4	5.8253	1.0031	3
0.2168	3	4	5.8238	1.0034	3
0.2174	2	4	4.2443	1.0069	3

-- S - 6.0193 --

DEADTIME CORRECTION: MAX.= -0.0116 MIN.= -0.0011 MAG.

#### DIFFERENTIAL MAGNITUDES FOR OUTPUT FILE 870328.T04

CYCLE= 1	FILTER= 4	-2	-3	-4
STAR 1-	DAY= 28.1983	DMAG= 0.8486	-0.7361	-1.5069
		DAIR= -0.0004	0.0001	0.0001
STAR 2-	DAY= 28.1996	DMAG=	-1.5846	-2.3555
		DAIR=	0.0006	0.0006
STAR 3-	DAY= 28.2009	DMAG=		-0.7708
		DAIR=		0.0000
CYCLE= 2	FILTER= 2	-2	-3	-4
STAR 1-	DAY= 28.2037	DMAG= 0.7751	-0.5203	-1.3695
		DAIR= -0.0008	0.0005	0.0004
STAR 2-	DAY= 28.2049	DMAG=	-1.2955	-2.1446
		DAIR=	0.0012	0.0011
STAR 3-	DAY= 28.2061	DMAG=		-0.8491
		DAIR=		-0.0001

CYCLE= 3	FILTER= 2	-2	-3	-4
STAR 1- , DAY= 28.2087	DMAG=	0.7698	-0.5248	-1.3730
	DAIR=	-0.0010	0.0008	0.0006
STAR 2- , DAY= 28.2099	DMAG=		-1.2946	-2.1428
	DAIR=		0.0018	0.0016
STAR 3- , DAY= 28.2112	DMAG=			-0.8482
	DAIR=			-0.0002

CYCLE= 4	FILTER= 4	-2	-3	-4
STAR 1- , DAY= 28.2140	DMAG=	0.8470	-0.7336	-1.5093
	DAIR=	-0.0014	0.0011	0.0008
STAR 2- , DAY= 28.2152	DMAG=		-1.5806	-2.3563
	DAIR=		0.0024	0.0022
STAR 3- , DAY= 28.2165	DMAG=			-0.7757
	DAIR=			-0.0002

#### AVERAGED DIFFERENTIAL MAGNITUDES

	FILTER= 4	-2	-3	-4
STAR 1- , DAY= 28.2061	DMAG=	0.8478	-0.7348	-1.5081
STAR 2- , DAY= 28.2074	DMAG=		-1.5826	-2.3559
STAR 3- , DAY= 28.2087	DMAG=			-0.7733

#### AVERAGED DIFFERENTIAL MAGNITUDES

	FILTER= 2	-2	-3	-4
STAR 1- , DAY= 28.2062	DMAG=	0.7725	-0.5226	-1.3712
STAR 2- , DAY= 28.2074	DMAG=		-1.2950	-2.1437
STAR 3- , DAY= 28.2086	DMAG=			-0.8487

MIDTIME OF OBSERVATIONS WAS 1987 3 28.20746